Nylon-6/Agricultural Filler Composites

by

Yasaman Amintowlieh

A thesis

presented to the University of Waterloo

in fulfillment of the

thesis requirement for the degree of

Master of Applied Science

in

Chemical Engineering

Waterloo, Ontario, Canada, 2010

AUTHOR'S DECLARATION

I hereby declare that I am the sole author of this thesis. This is a true copy of the thesis, including any required final revisions, as accepted by my examiners.

I understand that my thesis may be made electronically available to the public.

ABSTRACT

Preparation of thermoplastics composites using engineering thermoplastics and plant fibers or fillers is a technical challenge because the processing temperature of the thermoplastics is generally above the temperature of degradation of plant fibers of fillers. There have been numerous attempts for processing high melting point engineering thermoplastics like Nylon-6 with plant natural fibers and fillers. Low temperature processing methods, fiber modification or addition of additives which drops polymer melting point are some of proposed solutions for this problem.

The objective of this thesis was to develop a formulation using wheat straw (WS) as a reinforcing fiber for Nylon-6. The concentration of WS was 15 wt-%. The thermoplastic composites were prepared by mixing grinded wheat straw and Nylon-6 using a laboratory scale twin-screw extruder; follow by preparation of samples using injection moulding. The strategy investigated in this thesis was utilization of additives to lower the melting point or to decrease the viscosity of Nylon-6. Lithium chloride salt (LiCl) and N-Butyl benzene Sulfon amide plasticizer (N-BBSA) were used as process additives to decrease melting point and to reduce the processing temperature and time.

The addition of the wheat straw (15 wt-%) to the Nylon-6 increased modulus by 26.9 % but decreased the strength by 9.9 %. Effect of different level of these two additives on mechanical, thermal, physical properties and processability of the composite runs were studied. Addition of 4 wt-% LiCl was found to decrease the melting point from 222 °C to 191 °C, to increase modulus by 14 % in comparison to Nylon-6/wheat straw (15 wt-%). However, it decreased the processability and strength by 12.7 %.

Plasticizer was investigated to easing processability and decreasing the degradation by reducing the residence time in the extruder, it does not affect the melting point of Nylon-6. The addition of 4 wt-% of plasticizer (N-BBSA) increased modulus and strength only by 2.6 % and 3 %, respectively, in comparison to Nylon-6/wheat straw (15 wt-%) composites. The results of mechanical properties were used as a benchmark for comparisons among samples with different formulations (levels of additives) to find out levels of LiCl and N-

BBSA for the best mechanical properties. It was found that samples with 2 wt-% LiCl and 2 wt-% of N-BBSA had 29.3 % higher tensile modulus than neat Nylon-6, while its strength was almost same as neat Nylon-6 and 6.3 % higher than Nylon-6/WS (15 wt-%). These results were used to correlate the mechanical properties as a function of percentage of salt and plasticizer in the formulation.

Differential scanning calorimetry (DSC) was used to evaluate the percentage of crystallinity and the melting point of the thermoplastic phase and thermal gravimetric analysis (TGA) was used to measure the thermal stability of different formulation. The kinetics of crystallization and degradation were evaluated using results from DSC and TGA, respectively. The activation energy for thermal degradation and the percentage of crystallinity of the thermoplastic composites were correlated to mechanical properties using linear regression. It was found that fiber degradation had a significant effect on strength but the effects of percentage of crystallinity on composites strength were insignificant. On the other hand, the percentage of crystallinity affects stiffness and impact strength. The ductility was a function of both crystallinity and thermal stability.

ACKNOWLEDGEMENTS

DEDICATION

I like to dedicate this thesis to my mother for all her love and support.

TABLE OF CONTENTS

LIST OF FIGURES

LIST OF TABLES

LIST OF EQUATIONS

LIST OF ABBREVIATIONS

°

°C

A

A

ANOVA

C

C

cm

CMC

CO2

D

D

df

DMTA

DSC

E

F

H

I

J

K

L

M

N

O

P

R

M

1   INTRODUCTION

In the early ages of automotive industry, most of the components were made of metals. The introduction of plastics to the automotive industry changed the way cars were manufacture and provided great opportunity for new designs and improved performance. Nylon-6 is a thermoplastic that finds many applications as a versatile, flexible, mouldable material with resistance through physical abrasion and chemical solutions (Carlson, Nelson 2003). It is known to be an easy to process polymer with high impact resistance (Jacobson, Ferrante et al. 2009). Its flexibility to fill unusual moulds and its high thermal and chemical resistance was the key properties that define its usage for advanced applications (Lozano-González, Rodriguez-Hernandez et al. 2000).

Nylon application in automotive industry is wide ranged, from less important pieces like: mirror housing brackets, clutch pedals, clutch master cylinders, steering wheels, levers, auto seat frames, door handles and door lock mechanisms, valve stems, wiring clips, gears, bearing, bushings, switch housing and wind shield wiper to more engineering pieces like under the hood applications (i.e. engine cooling flex fans, transmission thrust washer and air cleaner support brackets) which need high resistance to temperature and pressure (Jacobson, Caulfield et al. 2001). In the year of 2000 the mount of Nylon which was consumed in applications for under the hood of the car was approximately 11.06 lb per vehicle, this amount increased to 14.4 lb per vehicle in 2005.

Nylon-6 reinforced with glass fibers and mineral fillers is used in engineering applications due to its better performance in comparison to the neat polymer. For example, reinforcing Nylon-6 with glass fiber increases its modulus, strength at breaks and heat deflection temperature.

1.1 MOTIVATION

Nylon-6 composites reinforced with glass fiber and mineral fillers have numerous applications in different industries, especially automotive industry. Parts used in under the hoods applications of cars can be manufactured with Nylon-6 reinforced glass fiber composites. The advantage of this material is the balance of mechanical properties and weight, but the key property that allows the utilization of glass fiber reinforced Nylon-6 composites is the high heat deflection temperature.

However, adding glass fiber as reinforcement in Nylon-6 having its own disadvantages. These disadvantages can be summarized under the following list (Zhang, Zhou et al. 2008):

- high density which leads to composites that are heavier;

- abrasive nature of glass fibers cause unsafe handling, health issues for human labor;

- abrasion of equipment during processing; and

- difficulties associated with recycling.

There is a need for alternative reinforcement with:

- low density;

- acceptable specific properties;

- low cost;

- easy processing with no hazards for working environment

- renewable resource, not competing with food supply chain;

- recyclable at the end of product life (Panthapulakkal, Zereshkian et al. 2006)(Panthapulakkal, Sain 2006); and

- low overall emissions with decreased negative impact on the environment.

Therefore, applying plant natural fibers and fillers in automotive industry is beneficial for the environment. It decreases CO_2 emission and energy consumption. The reduction of 1

kilogram (kg) in weight of each diesel car due to substitution of glass fibers with natural fibers is equal to saving energy of production and burning of 7 litres of gasoline per automobile over the destination of 175,000 km (Joshi, Drzal et al. 2004).

According to studies which have been done in 2002, natural fibers including wood fiber composites demand in market was approximately 1.3 billion lb per year, which is about 900 million dollar. This is equal to 20 % increase in market demand compare to year 2000 (Cleveland, Spiegelhalter et al. 2008). Motivation for this increase was attributed to environmental reasons. Demand for these materials in North America and Europe continued to increase to 1 billion dollars by 2007. The automotive industry contributed to such increase.

The reduction in weight by changing filler from short glass fiber to plant natural fibers or filler is due to the density, from 2.8 gr/cm^3 for glass to 1.2-1.5 gr/cm^3 for cellulose bases fibers or fillers. The weight reduction leads to more fuel efficient vehicles (Joshi, Drzal et al. 2004).

Using agricultural residues as reinforcement in thermoplastics is a novel application of crop derived materials and it has numerous advantages for the environment. Mishra et al. have investigated the potential of wheat straw to become a commercial alternative for wood fiber or in applications that strength is not a critical factor (Mishra, Sain 2009). The authors reported that for non structural applications wheat straw filled composites are economical alternatives for wood fibers.

However, applying natural fiber and fillers as a reinforcement in polymer plastics has the following disadvantages:

- the mechanical properties are non-homogenous and the product is seasonal;

- low thermal stability of these fibers had confined their application to commercial thermoplastics with low melting point (mostly polyolefins); and

- high moisture absorbance due to hydrophilic nature of these fillers causes reduction in mechanical properties of the composites over time.

Wheat straw application for reinforcement in common thermoplastics has been proven. These materials were shown an increase in tensile and flexural properties (modulus and strength) of polyolefins like polypropylene (Panthapulakkal, Zereshkian et al. 2006). However, Nylon-6 is an engineering thermoplastic with high melting point and high heat distortion temperature (HDT) due to its crystalline structure. The high melting point of Nylon-6 makes it a technical challenge for preparation of composites with wheat straw and other plant natural fibers or fillers because the melting point of Nylon-6 is above the temperature for thermal degradation of plant natural fibers or fillers.

Despite all these possible potential and advantages of plant natural fibers in reinforced thermoplastic composites, including wheat straw fibers, it is generally accepted that natural fiber reinforced Nylon-6 composites cannot be made due to high melting point of the Nylon-6 (Misra M., K. et al. 2004).

1.2 OBJECTIVES

The objectives of this research are:

1) to identify additives which allow processing Nylon-6 and wheat straw by decreasing the thermal degradation and improving processing;

2) to identify the temperature for processing

3) to characterize physical and mechanical properties of Nylon-6/wheat straw composites; and

4) to correlate level of additives based on mechanical and physical.

1.3 OUTLINE OF THE THESIS

The literature review section of this thesis explains physical and mechanical properties of matrix and WS filler individually. The methods which are presented in the literature for

4

processing Nylon/ WS are categorize and explained in three categories of modifying processing condition, fiber/filler treatments, and matrix modification.

The material and method chapter contains information about processing and data analysing tools, materials and the steps which were followed for manufacturing composites. The mechanical physical and thermal tests procedure are also presented.

Composites thermal, mechanical, physical and morphological properties are the data in the result section of this thesis. The processability of the composites is summarized in melt flow index (MFI) section. Thermal properties are measured with DSC and TGA tools. From the analysis which was performed on Isothermal and non-isothermal DSC test results, melting and crystallization temperature, crystallization percentage and kinetics were found. Degradation temperature and kinetic were analysed and results are presented in TGA section. Mechanical properties are measured by tensile, flexural and impact test. Interfacial bonding between WS and Nylon-6 is monitored by scanning electron microscopy (SEM) images. The mechanical properties are correlated to additives level or physical proprieties like percentage of crystallinity and degradation energy by statistical methods.

2 LITERATURE REVIEW

2.1 PHYSICAL PROPERTIES OF NYLON-6

Polymorphic materials are those that have more than one stable crystalline structure. That's due to ability of chains which can take more than one favourable morphology in crystalline structure. Nylon-6 is polymorphic semicrystalline material with two different chain conformations inside the polymer. The structure which is more stable and is more commercially important is alpha structure. Alpha structure made of planar sheets which are made of fully extended chains with zigzag conformation. These chains are locating antiparallel to each other (Figure 2-1). This arrangement ease the formation of hydrogen bonding and H bonds and it can be formed without any force (Jacobson, Caulfield et al. 2001).
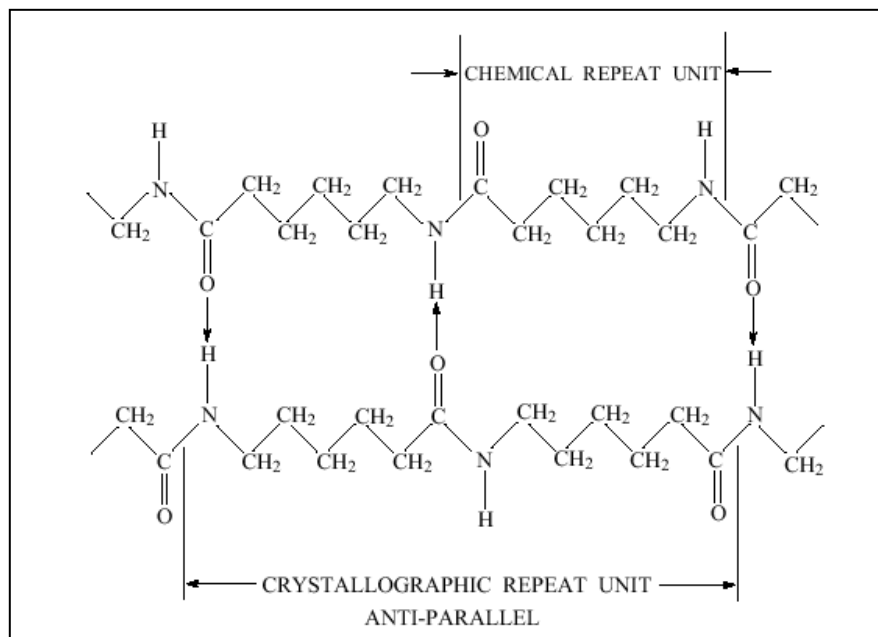
Figure 2-1: Alpha morphology in Nylon-6 crystalline structure copied from reference: (Xu, Sun et al. 2000)

Due to low symmetry and anti-parallel chain placement, the unit cells are monoclinic which means not only all dimensions of unit cells are not equal with each other, but also one of the angles is unequal to the other two. The crystalline parameters in α structure of Nylon-6 monoclinic unit cells are: a=0.956 nm, b=1.724 nm, c=0.801 nm and β= 67.5° (Zhou, Wang et al. 2009).

If adjacent chains locate parallel to each other, then amount of hydrogen bonds formed should be half of the time that chains locate anti-parallel to each other; however, hydrogen bonded chains stagger up and down to form more bandings (Figure 2-2). The resultant unitcell structure in this case is monoclinic or pseudo hexagonal. The unit cell dimensions are: a=0.933 nm, b=1.688 nm, c=0.478 nm and β=121°. Structure is called gamma and it is mesostable. Gamma crystalline structure can be made while quenching the Nylon-6 and it can be transformed to more stable alpha structure. This transition is preferred due to perfect structure of alpha form which leads to better mechanical properties. Annealing is a way to induce this transition in the polymer (Ramazani S.A, Mousavi S 2005).

It worth to note that due to higher crystalline stability melting point and enthalpy of alpha structure in Nylon-6 is 226.42 °C and 48.33 J/g respectively, while it is 221.1° and 38.56 J/g for gamma form (Zhao, Zheng et al. 2004).
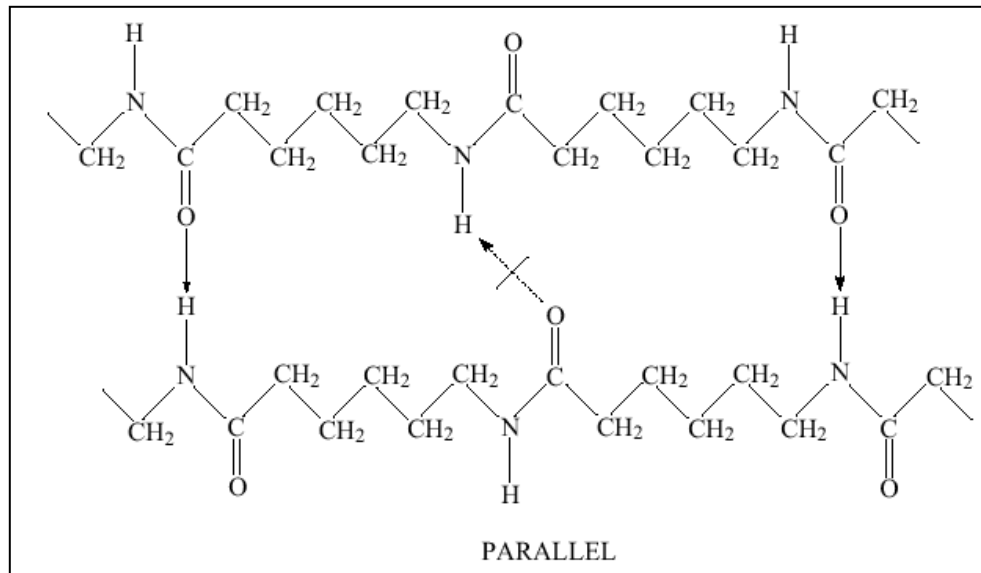
Figure 2-2: Gamma morphology in Nylon-6 crystalline structure; copied from reference: (Xu, Sun et al. 2000)

According to Russel et al. both structures are present in injection moulded bars of Nylon-6 (Russell, Beaumont 1980). Pseudo hexagonal gamma phase is reported on the surface of the mould while alpha is reported to be in the core of the moulded bars (Ho, Wei 2000). Percentage of crystallinity on the surface is lower than the core of the bars; however, by annealing or exposure to boiling water the transition to alpha and increase in the percentage of crystallinity is expected. Higher gamma phase on the surface of the mould is due to high cooling rate and by increase in mould temperature and decrease in cooling rate the percentage of crystallinity and transformation from alpha to gamma were observed. Size of the spherulites is 7 μm and this is independent of the mould temperature. In terms of chain orientation for the case of pure Nylon-6, no specific chain orientation is present in neat Nylon-6 bars even after the injection moulding (Keating, Gardner et al. 1999).

2.2 PHYSICAL AND MECHANICAL PROPERTIES OF WHEAT STRAW

Natural fibers and fillers are known with the terms like lignocellulosic material, vegal fiber/fillers, and green material. These materials are considered to be ecologically green (Santos, Spinace et al. 2007).

Natural fibers have been extensively used for reinforcement of thermoplastic and thermoset materials. Hemp, flax, jute, sisal, bagasse, ramie and kapok are some of these fibers. These fibers have higher amount of cellulose in compare to agricultural products such as wheat straw, rice straw, corn cobs and corn stalks. In shortage of fibers that need forestry recourses, agricultural residues can be used for reinforcement. Wheat straw has been added mostly in grounded form rather than fibrous form and its application in different pieces leads to improvement of agricultural based products.

Pathapulakkal et al. investigated the potential of wheat straw fibers for reinforcement in polypropylene and conclude that it can be used as effective filler for reinforcement of polypropylene. They characterize thermal, structural, physical and mechanical properties of wheat straw fibers (Panthapulakkal, Zereshkian et al. 2006).

The properties of wheat straw like any other natural product depend on its components and percentage of each component in its structure. However, these two factors in the structure of wheat straw depend on cultivation place, season and preparation process (GOLBABAIE 2008). Table 2-1 shows how different preparation methods for wheat straw can affect its chemical content (Panthapulakkal, Zereshkian et al. 2006).

Wheat straw contains of cellulose of hemicelluloses and of lignin. Lignin is amorphous cross linked polymer network. The chemical structure of lignin is $C_1H_{1.08}O_{0.37}$. Lignin is known as the glue between cellulose fibers and its polarity is lower than cellulose fibers. It has lowest onset of degradation among all wheat straw components but it has highest thermal stability. Hemicellulose is another low thermal stable component in wheat straw. It is a branched and low molecular weight polymer. Cellulose is the most thermal stable component with structure of $C_6H_{12}O_5$ (Clemons, Sanadi 2007). Its structure in natural

fibers/fillers is in the form of microfibrils that bind together with lignin and hemicelluloses in the cell wall (Panthapulakkal, Zereshkian et al. 2006). The higher the cellulose content is the higher crystalline structure, thermal and structural stability will become. Summarize the composition of wheat straw which is provided by chemical and mechanical method.

Table 2-1: Chemical composition of wheat straw provided by two methods of chemical alkali treatment and mechanical grinding; copied from reference: (Panthapulakkal, Zereshkian et al. 2006)

Wheat straw fiber	Cellulose (%)	Hemicellulose (%)	Lignin (%)
Mechanical processing	47.55	31.89	18.59
Chemical processing	63.14	11.90	5.57

Sardashti stated that wheat straw has a composite like structure where highly crystalline microfibrils of cellulose are bounded together with amorphous lignin and hemicelluloses (Sardashti 2009).
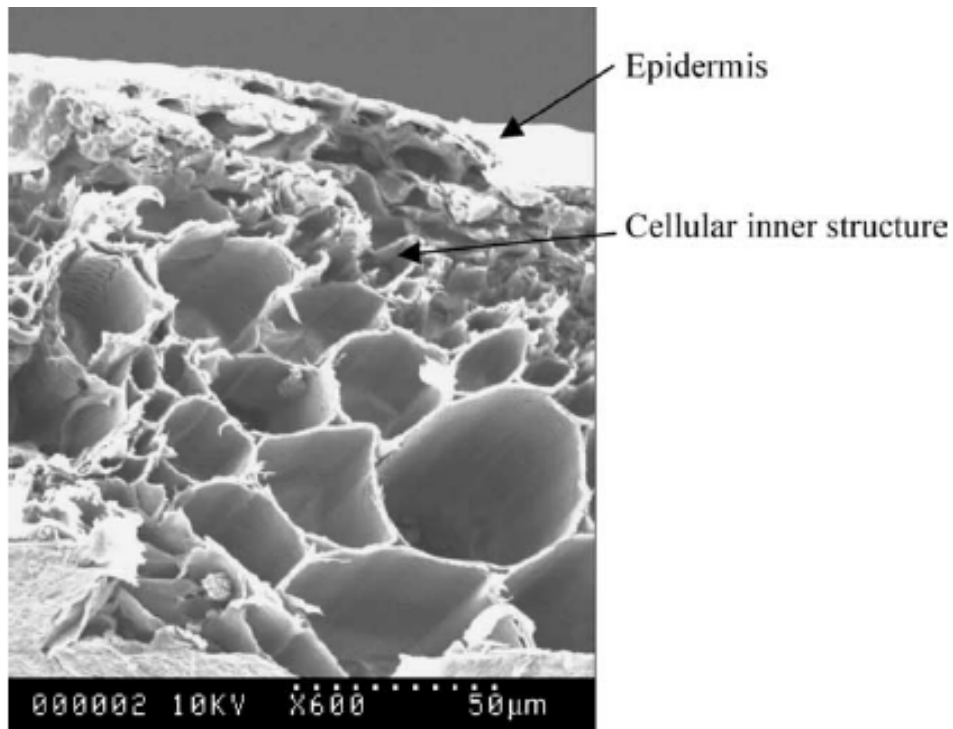
Figure 2-3: Different parts of wheat straw structure ; copied from reference: (Panthapulakkal, Zereshkian et al. 2006)

Pathapulakkal et al. also measure the size and the module of the wheat straw fibers provided by chemical and mechanical methods and concludes that mechanically prepared wheat straw fibers yield higher length; however, chemically treated wheat straw shows higher modulus, strength and even higher onset of degradation (Table 2-2) (Panthapulakkal, Zereshkian et al. 2006). It worth to note that the high standard deviation in the strength and modulus of the wheat straw fibers in Table 2-2 is due to wide size and property distribution of this natural product.

Table 2-2: Mechanical and physical properties of wheat straw obtained with mechanical and chemical methods ; copied from reference: (Panthapulakkal, Zereshkian et al. 2006)

Property	Avg. diameter (mm)	Avg. length (mm)	Tensile strength (MPa)	E-modulus (GPa)	Onset of degradation (°C)
Mechanically processed	0.094±0.03	1.87±0.66	58.7±51	2.8±2	217
Chemically processed	0.076±0.03	2.70±0.74	146.3±53	7.9±3.7	242

E-modulus: Tensile modulus, Avg: Average.

They attribute this superior behaviour of chemically prepared wheat straw to higher cellulose percentage due to removal of hemicelluloses and lignin. Despite better mechanical properties of chemically treated fibres in compare mechanically prepared ones, polypropylene composite filled with 30 wt-% of mechanically prepared wheat straw show better mechanical properties (Table 2-3). They attribute this to lower interaction between chemically prepare wheat straw fibres and the polypropylene due high amount of cellulose which cause agglomeration and weak dispersion in hydrophobic matrix.

Table 2-3: Mechanical properties of polypropylene filled with mechanically and chemically prepared wheat straw ; copied from reference: (Panthapulakkal, Zereshkian et al. 2006)

Property	Polypropylene	Wheat straw	
		Mechanical processed	Chemically processed
Tensile strength (MPa)	31.60±0.03	40.80±0.5	35.50±0.80
Tensile modulus (GPa)	1.21±0.03	2.99±0.04	2.44±0.03
Flexural strength (MPa)	50.00±0.50	74.60±1.20	74.50±0.60
Flexural strength (GPa)	1.41±0.04	3.45±0.04	2.98±0.06

It worth to note that fiber length and length to wide ratio will not remain the same after severe processing conditions: shear and thermal degradation, and this is one of the factors that lowers reinforcement potential. Panthapulakkal et al. have been reported that fibers length decrease to half after processing with high intensity thermokinetic internal mixer (Panthapulakkal, Zereshkian et al. 2006).

2.3 ATTEMPTS FOR PROCESSING NYLON AND NATURAL FIBRES

According to plastic technology website Nylon-6 filled with 20 wt-% of Curaua fibers were extruded and injection moulded without addition of any additives. Curaua give rise to modulus, strength and it is lighter than glass fiber. It has been claimed that Nylon-6 with 20 wt-% of this fiber has been used in frame of the sun visor in the car. Table 2-4 compared mechanical properties of neat Nylon-6 with Nylon-6 filled with 20 wt-% of Curaua, Glass and Talc (PLASTIC TECHNOLOG. 2009).

Table 2-4: Comparison between mechanical properties of Nylon-6 filled with Curaua fiber, Talc and glass fiber; copied from reference: (PLASTIC TECHNOLOGY. 2009)

Property	Nylon-6 unfilled	20 % Curaua	20 % Glass fiber	20 % Talc
Density (g/cm^3)	1.14	1.18	1.27	1.27
Tensile strength (MPa)	63	83.00	101	73
Flexural strength (MPa)	95	115.00	160	115
Tensile modulus (GPa)	1.4	55	6.5	6.5
Elongation at break (%)	>60	3	3	3
Notched Izod impact (kJ/m^2)	10	9	9	9
HDT °C at 1.82 (MPa)	57	186	194	110

The other fibers which were blended with Nylon-6 are sugarcane bagasse. Dweiri and Azhari prepare sugarcane bagasse fiber blend with Nylon-6 in twin screw extruder in temperature of 210 °C and 60 rpm (Dweiri, Azhari 2004). They make the composites in three weight percentages of 2, 5 and 10 wt-% and three length ranges of L_1, L_2, L_3. These lengths are correspond to the sizes of <100 μm, <250 μm and <500 μm, respectively. They measure thermal and rheological properties of the composites using DSC and capillary

rheometry. It was found that melting point decreases by addition of fibers. They attributed this to the partial miscibility of amorphous region of the Bagasse fiber in Nylon-6 and the probability that the Bagasse fiber changed the Nylon-6 crystalline size and structure or the presence of strong interfacial interaction between fiber and matrix. The authors also found a dependency between glass transition temperature (T_g) of the matrix (Nylon-6) and the fiber loading and length. Increasing fiber loading and decreasing the fiber length decreased the T_g. This behaviour was attributed to the diffusion of contents from the fiber to the matrix; such components may have behaved like plasticizer in the matrix. From thermal gravimetric analysis (TGA) data the authors concluded that addition of fibers decreased the thermal stability and that increasing fiber loading imposed more weight loss due to degradation of the fibers.

The rheological analysis of sugarcane bagasse fiber/Nylon-6 composites showed an increase in viscosity with an increase in the fiber loading and length. The same authors reported pseudo plastic behaviour for the composite; the melt flow index did not correlate with fiber loading or length (Dweiri, Azhari 2004).

In order to obtain composites with better mechanical properties several modifications were suggested in the literature. These suggestions are in aspect of

- Treating natural fiber to reduce degradation (Jacobson, Caulfield et al. 2001, Santos, Spinace et al. 2007)

- Modifying the process condition to impose less degradation on fibers (Jacobson, Caulfield et al. 2001, Sears, Jacobson et al. 2001)

- Adding additives to Nylon which decrease its melting point or ease its processing and consequently drop its processing temperature (Misra M., K. et al. 2004, Xu 2008)

In the following sections, each of these suggested solutions for obtaining Nylon-6/natural filler reinforced composites is summarized from the literature and the properties of the composites made with each of these methods is explained.

2.3.1 FIBER TREATMENT

Santos et al. used fiber modification as a treatment to make Nylon-6 natural fiber composites with better mechanical properties. Treatments like mercerization with NaOH followed by washing with water and oven drying or N_2 cold plasma exposure were applied on Curaua fibers prior to mixing with Nylon-6 (Santos, Spinace et al. 2007).

Moreover, they have investigated the effect of fiber size and percentages on mechanical properties of the resulted composites which were made by run mixer and concluded that shorter fibers produce composites with higher modulus and strength. Generally, a high percentage of fiber can lead to low strength and higher modulus. However, these results for fibers length were not consistence for all processing methods. According to their results, 20 wt-% of fiber produced optimum strength and modulus. Using a twin screw extruder, long fibers provided a better reinforcing effect than short fibers. Using different extruders with different shearing elements resulted in composites with different mechanical properties. Thus, the processing equipment can also greatly affect the mechanical properties of final composite bars.

Those authors also concluded that drying the raw fiber and the polymer did not affect mechanical properties (Santos, Spinace et al. 2007). Moreover, they observed very good bonding between fiber and matrices which were not oven dried and concluded that the water in the fiber was compatible with Nylon-6. They attributed this to possible hydroxylation of Nylon-6 carboxylic groups in high processing temperatures under reaction shown in Figure 2-4:
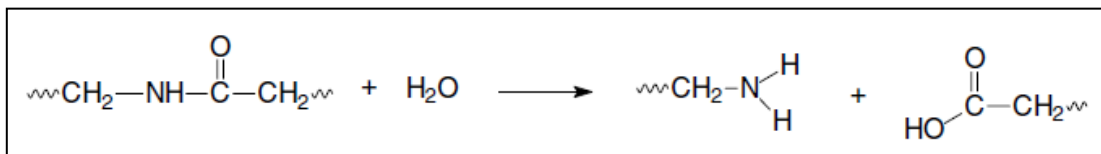
Figure 2-4: Hydrolyzing Nylon-6 in presence of water; copied from reference: (Santos, Spinace et al. 2007)

Excessive Water absorption can affect the mechanical properties of in Nylon-6/Curaua fibber composites and Nylon-6/glass fiber composites. Typically water absorption

decreases the tensile and other mechanical properties, except the impact resistance of the composites. Water works as a plasticizer in Nylon-6.

Comparing the mechanical properties of composites which were obtained from fibers treated with two methods i) plasma and ii) NaOH treatments, the authors found out that plasma treated fibers had a higher tensile properties than neat Nylon-6, while NaOH treatments on fibers produced higher tensile and flexural properties. Thus, NaOH treatment is known to be more effective than N_2 plasma exposure (Santos, Spinace et al. 2007).

Jacobson et al. introduced pelletization and mercerization as effective ways to decrease fiber degradation or biological growth (Jacobson, Caulfield et al. 2001). They present mercerization, prehydrolization and pelletization was used as the effective fibber treatments prior to compounding.

Sears et al. reported that pelletization not only helped to keep the original fibber length but also facilitated processing. For example, using pelletized fibers for feeding the extruder kept the feeding rate constant (Jacobson, Caulfield et al. 2001, Sears, Jacobson et al. 2001). It worth noting that in order to have a good dispersion, consistency in loading the level of fibers and processing stability (torque and shear rate consistency), it is essential to have control over feeding rate (Jacobson, Caulfield et al. 2001). In bulkier fibers, like wood fibers, the following method is used for pelletizing fibers:

1) cold room storage (36 °F, 50 % relative humidity);

2) mixing fibers with additives like carboxyl methyl cellulose (CMC) in run mixer; this material acts as viscosity modifier and it is added to fibers to prevent dewatering and modify rheological properties of the fibers;

3) vacuum conveying fibers out of mixer; and

4) metering and pelletizing with dual rotating roll-mills that provide downward horizontal forces (Sears, Jacobson et al. 2001).

2.3.2 PROCESS MODIFICATION

The first attempts for processing Nylon-6 and cellulose fibers goes back to 1984 were resulted composites have lower mechanical properties than pure Nylon. Thus, the first treatments consider process modification in a way that degradation in fibers decreases (Xu 2008).

Clemons stated that mechanical properties of the wood fiber reinforced polypropylene composites depend largely on fiber length, orientation, dispersion and degradation of the fibers (Clemons 2000). These factors change by processing conditions. Shear rate is the most critical factor that affects length of glass fiber during blending of Nylon-6 with glass fiber. Thus, increase in screw speed reduces length of the glass fiber during processing. High temperature has dual effect on properties on glass fibers during processing; from one side it increases thermal degradation and from the other side it reduces shear rate by dropping the viscosity. Cellulosic fibers and natural fillers are different from glass fibers in different aspects like: higher fiber flexibility and more sensitivity through thermal degradation. To acquire reinforcing effect from these fibers, mixing time and temperature profile are more important factors in compare to glass fiber composites (Jacobson, Caulfield et al. 2001, Sears, Jacobson et al. 2001).

Thus, screw speed, feeding rate, residence time in extruder, processing temperature and shearing elements are important processing factors that affect mechanical properties of the composites. For example, Santos et al found that even extruder size influences fiber properties. Larger extruder and introduction of fibers from the second feeder cause better mechanical properties in the composites. The effect of bigger extruder with more effective shearing elements on boosting mechanical properties of the composites is explained by better dispersion and distribution of the fibers in the molten matrix (Santos, Spinace et al. 2007).

The following section describes methods that were introduced in literature for processing Nylon-6 with natural fibers to achieve lower levels of degradation.

2.3.2.1   USING MULTIPLE HEATING ZONE EXTRUDER FOR PROCESSING

From the early research stages, it was noticed that compounding cellulosic fiber with pure Nylon was not an easy task and it took extensive work, trial and error and well planned experiments to find a processing window which was suitable for low degradation temperature of cellulosic fibers.

Low temperature compounding (LTC) were proposed by Jacobson and his group (Jacobson, Caulfield et al. 2001, Sears, Jacobson et al. 2001). The inventors of this processing method claim that by controlling temperature, screw speed and cooling rates of various extruder zones, it was possible to make Nylon-cellulose fiber composites in temperature lower than Nylons' melting points. This idea was coupled with minimum exposure of fibers to high temperatures by inputting fibers through a second feeder. These fibers were introduced to molten polymer in the middle zones of a twin screw extruder. The extruder used for this method has seven heating zones and compounding method has three stages:

1) Start-up condition: all heat zones were set on 10 degree higher than Nylon-6 melting point. Fibers introduced with the rate which was adjusted for specific percentage of fibers. By increasing melt viscosity due to addition of filler, the rate of filler addition was increased to compensate for the melting pressure in the extruder. During this stage, heat was generated from shear viscosity. These heats are plotted against time in the graph below Figure 2-5:
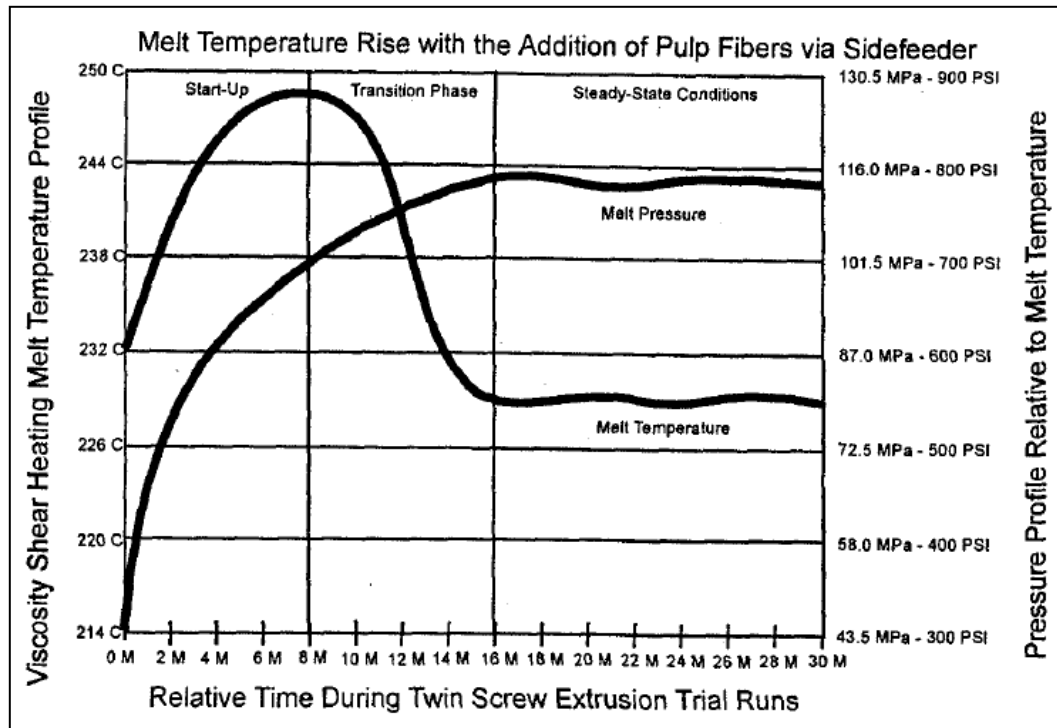
Figure 2-5: Temperature and pressure profile of the extruder during three stages of low temperature processing; copied from reference: (Jacobson, Caulfield et al. 2001)

2) Transition condition: due to addition of fillers and generation of shear viscose heats, the real temperature of extruder can reach 260 °C. The brown color and scorching in strands coming out of die was an indication of this stage. At this point, the temperature was lowered in the last zones after addition of the fibers. Thus, the color changed from dark brown to light brown and finally cream (note that color change was associated with fiber thermal degradation).

3) Steady state condition: from the first feeder to the second feeder, the temperature was set 10 °C higher than Nylon-6 melting point, while after the addition of fibers the temperature was set at 149 °C. This temperature depended on screw configuration, rpm and die face condition.

By reaching the end of the process, the temperature was increased to the start up condition. For injection moulding of these compounds with the same approach, the barrel temperature

was set at 232 °C and the nozzle temperature was set at 227 °C (this narrow configuration was a result more shear viscose heat generation) (Jacobson, Caulfield et al. 2001).

Other authors have adopted this approach of lowering the processing temperature as well. Xu reported better mechanical properties in Nylon-6 and Nylon-6,6 bars which are made with this low temperature processing technique in comparison to normal high temperature processing techniques (Xu 2008).

2.3.2.2 COMPRESSION MOULDING AND HOT PRESS

McHenry and Stachursk made Nylon-6/wood fiber composites using hot press at the temperature of 230 °C and under pressure of 50 kN with time intervals of 2.5 min. This temperature was above the melting point of Nylon-6 but just below the wood fiber degradation temperature. In order to prepare these composites, they sieved wood fiber on Nylon-6 and then mixed them completely in a container prior to placing the mixture in the mould (McHenry, Stachurski 2003). The authors observed improvement in tensile properties of recycled Nylon-6/wood fiber composites. The composites were made by addition of four different weight percentages of 2.5, 5.0, 7.0, 10 wt-% of wood fiber to Nylon-6. There was a significant correlation between weight percentage of wood fiber and strength of the composites. The maximum amount of strength reported was at 2.5 wt-% of fiber; addition of more fiber decreased the strength of the composites. The authors also compared those results of Nylon-6/wood fiber with polypropylene/wood fiber. A decrease in mechanical properties was observed for polypropylene (PP), which was attributed to weak interfacial bonding. The modulus of polypropylene/ wood fiber composites did not change significantly, while for Nylon-6/wood fiber composites the modulus increased significantly. Xu also used compression moulding method for making composites of Nylon-6 and Nylon-6,6 reinforced with cellulose fibers. In this study, the mechanical and physical properties of the composites made from injection and compression moulding were compared with each other. In the same percentage of the fiber, bars made from compression moulding had lower density when the same fiber percentage was used. This was attributed to fewer voids during injection moulding of the bars. It was also found that fibers were

submitted to less thermal and mechanical degradation during compression moulding (the color of the bars were brighter and fibers were longer after composite analysis) (Xu 2008).

2.3.3   POLYMER MATRIX MODIFICATIONS

2.3.3.1   USING LITHIUM CHLORIDE SALT TO DECREASE NYLON MELTING POINT

Addition of halide salts to polyamides (Nylon) is a common way to modify performance due to formation of ionic interactions (Xu, Sun et al. 2000). The anion and its cation counterpart can be ranked based on the attraction of the cation to polar groups in Nylon. Acierno et al. investigated the effect of addition of different halide salts to Nylon-6. It was found that among different salts like KCl, LiCl and LiBr, potassium chloride showed absolutely no interaction with Nylon-6, but lithium chloride showed intermediate interaction and lithium bromide show the best interaction with Nylon-6 (Acierno, La Mantia et al. 1979). Balasubramanian et al. ranked salts based on their activity against Nylon with the following order: NaCl<LiCl<LiBr<LiI (Acierno, La Mantia et al. 1979, Balasubramanian, Shaikh 1973).

In order to explain the interaction between salt and amide, Zhang et al. proposed explanation based on size and charge of the ions. Lithium is a small atom. Its ion (Li^+) has high charge density and it has strong electron withdrawing capacity. After addition of LiCl to Nylon-6, the ion Li^+ can coordinate with N-H groups in Nylon-6; as a result, hydrogen bonds between amide groups of Nylon-6 will be eliminated. One ion Li^+ can coordinate with four N-H group and form an intermolecular ionic crosslink between the Nylon-6 chains. Although this pseudo-cross linked structure is not as strong as the well-known cross linking based on covalent bonding and it can be eliminated by increase in temperature, it can cause an increase in polymer viscosity and modulus and it decreases polymer chains mobility considerably (Zhang, Zhou et al. 2008).

For explaining this bonding interaction between the ion and the N-H groups, which can explain the properties of polymer after addition of salt, Balasubramanian et al. proposed the

structures shown in Figure 2.7 for lithium attack to polyamide. These mechanisms were based on Fourier Transform Infrared (FTIR) and Nuclear Magnetic Resonance (NMR) (Figure 2-6) (Balasubramanian, Shaikh 1973). Using FTIR, they confirmed that lithium attacks the oxygen group rather than N-H and consequently, structure [I] will be formed.
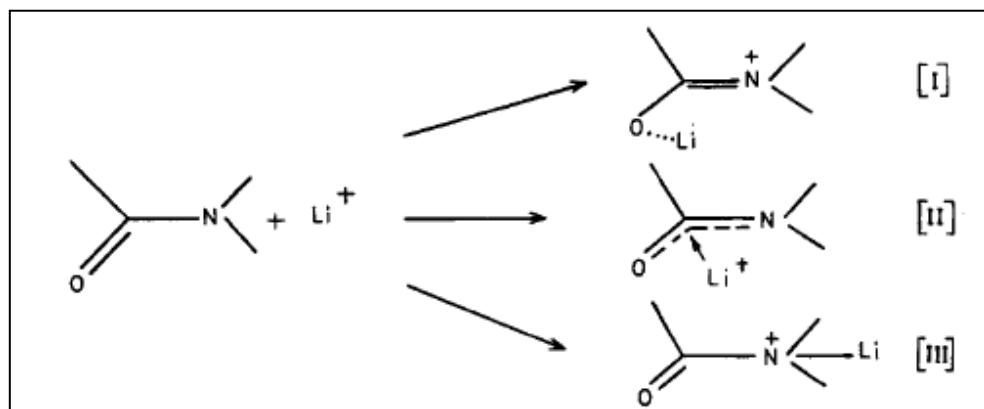
Figure 2-6: Proposed modes that Lithium halide salt can attack amide group; copied from reference: (Balasubramanian, Shaikh 1973)

By increasing in the level of LiCl the degree of crystallization decreases, this depression continues to the point in which no crystalline structure in Nylon-6 remains. In lower levels of salt, crystallization rate decreases but still limited degree of crystallinity is present in samples (Table 2-5) (Xu, Sun et al. 2000; Zhang, Huang et al. 2007). In this case, small crystals nuclei form on the junctions of polymer chains and ions and give rise to higher orientation in amorphous regions of salted Nylon-6 in comparison to pure Nylon-6. Hence, salt can control the level of orientation of Nylon-6 chains.

Table 2-5: Effect of salt percentage on melting temperature and heat fusion of melting; copied from reference: (Xu, Sun et al. 2000)

Material	Cooling condition			
	High cooling rate		**Low cooling rate**	
	$T_m(°C)$	$\Delta H(J/g)$	$T_m(°C)$	$\Delta H(J/g)$
Nylon-6	221.10	38.56	226.42	48.33
LiCl/Nylon-6=5/95	183.06	3.37	195.75	9.58
LiCl/Nylon-6=5/95	-	-	-	-

At higher salt concentrations, all crystalline structures are transformed to amorphous. The cooling rate does not affect the morphology of the polymer, so no peak in DSC or no diffraction in X-ray diffraction (XRD) is observed. Figure 2-7 shows DSC thermogram and Figure 2-8 shows X-ray pattern (Xu, Sun et al. 2000). The DSC results reveal that addition of 5 wt-% salt decreased the melting enthalpy considerably and the addition of 10 wt-% salt to Nylon-6 eliminated the endothermic peak completely (meaning no crystallinity) (Figure 2-7) (Xu, Sun et al. 2000). It was reported that halide salts can increase the stiffness (Youngs' modulus) after annealing and drawing (Xu, Sun et al. 2000).
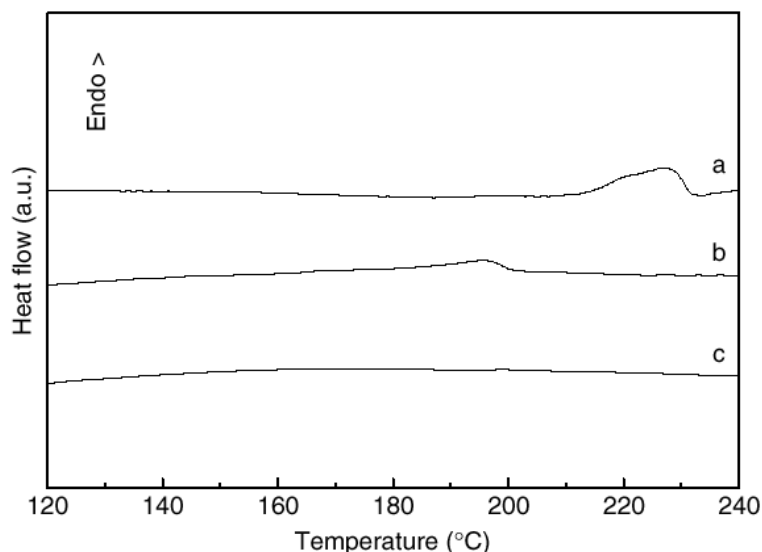
Figure 2-7: a)Pure Nylon-6, b) Nylon-6/LiCl (95/5), c) Nylon-6/LiCl (90/10) copied from reference: (Zhang, Huang et al. 2007)
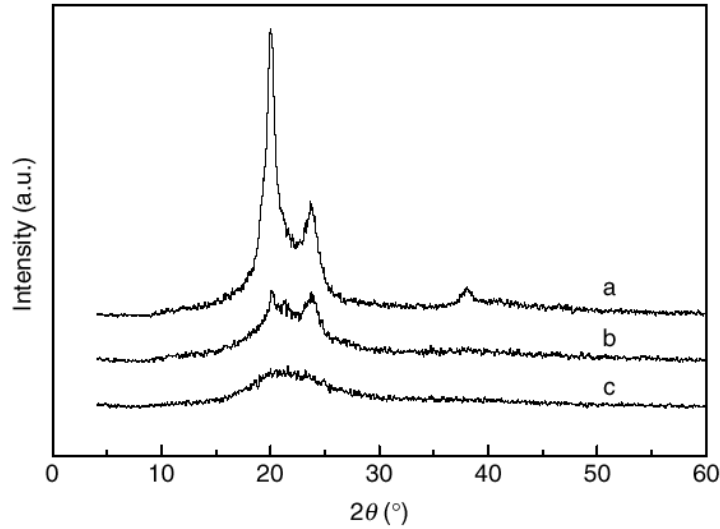
Figure 2-8: X-ray patterns of : a) pure Nylon-6, b) Nylon-6/LiCl (95/5), c) Nylon-6/LiCl (90/10); copied from copied from reference: (Zhang, Huang et al. 2007)

Knowing these effects, Misra et al. used lithium chloride as a tool to decrease Nylon-6 processing temperature and added hemp fiber to Nylon-6. They observed that addition of 3 wt-% lithium chloride cause 44 °C decrease in heat distortion temperature (HDT) of the blend in comparison with pure Nylon-6; however, addition of hemp fiber increased the HDT and compensated the negative effects of adding salt. The increase in HDT after addition of hemp fiber was not only due to increase in stiffness, but also due to increase in degree of crystallinity. Misra et al. suggested keeping the level of salt at lower percentages mainly due to its negative effect on HDT. This group also suggested some solutions for the low impact resistance of such composites. They suggested a) using a combination of fibers, that is, natural fibers and manmade fibers (glass fiber) composite, b) modifying the surface of the fibers, or c) using natural fibers with specific reinforcement effect (Misra M., K. et al. 2004). Figure 2-9 shows the effect of addition of salt and fiber on tensile properties. The addition of salt did not affect stiffness or strength, but addition 30 to 40 wt-% of fibers to Nylon-6 blended with 3 wt-% salt increased stiffness and strength significantly (Misra M., K. et al. 2004).

24
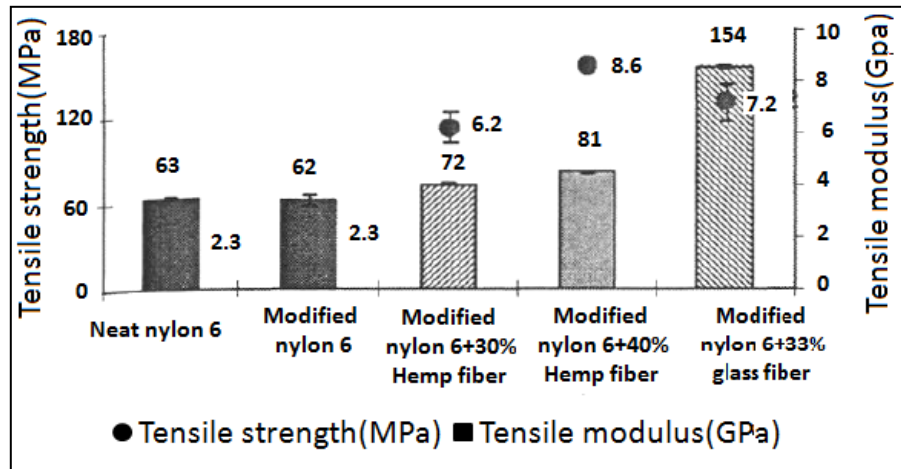
Figure 2-9: Tensile property of Nylon-6 blend with salt and Nylon-6 composite in compare to pure Nylon-6; copied from reference: (Misra M., K. et al. 2004)

Xu reported the addition of lithium chloride to Nylon-6 and Nylon-6, 6 prior to blending with cellulose fibers. Lithium chloride had the most significant effect on melting point of Nylon-6 and Nylon-6, 6 in comparison to other chloride metal salts. Nylon-6 was compounded with lithium chloride in a twin screw extruder and the mechanical properties of the resulted bars were tested prior to addition of the fibers. In the case of Nylon-6, addition of 3 wt-% LiCl decreased the tensile modulus but it increased the tensile strength of the samples. However, in the case of Nylon-6, 6, the addition of 4 wt-% of salt caused a 1.4 time increase in the tensile modulus (Table 2-6 and Table 2-7) (Xu 2008).

Table 2-6: Effect of addition of 3 wt-% LiCl or 3 wt-% N-BBA on mechanical properties of the Nylon-6; copied from reference: (Xu 2008)

	Nylon-6	3% LiCl	3% NBBSA
Tensile modulus(GPa)	1.92	1.47	1.62
Tensile stress(MPa)	44.20	52	31.70
Tensile strain (%)	26.30	19.80	4.09
Flexural modulus(GPa)	1.37	1.59	1.06
Flexural stress(GPa)	69.80	70.90	45.10
Flexural strain (%)	7.36	7.87	8.17

In Nylon-6,6 the tensile strength of the matrix after addition of 4 wt-% of salt decreased (Table 2-7). Addition of 10 wt-% of salt caused drop in modulus, consequently a low level

of salt was suggested for optimum mechanical properties. It is worth noting that a transparent appearance of bars with high level of salt was an indication for amorphous morphology due to the elimination of the crystals.

Table 2-7: Effect of addition of level of LiCl or 4 wt-% NBBA on mechanical properties of the Nylon-6, 6; copied from reference: (Xu 2008)

	Nylon-6, 6	10 % LiCl	4 % LiCl	4 % NBBSA
Tensile modulus(GPa)	1.54	0.21	3.69	2.73
Tensile stress(MPa)	66.2	19.2	41.4	65.8
Tensile strain (%)	23.5	47.4	1.26	7.4
Flexural modulus(GPa)	1.88	0.59	2.62	2.15
Flexural stress(GPa)	77.8	29.1	125.5	92.1
Flexural strain (%)	7.56	8.4	6.85	7.43

According to Xu, a very low amount of salt increased the torque in the extruder considerably, even in high processing temperature condition. Moreover, in constant shear rate, after addition of fibers from the second feeder to the mixture, the extruder reached its torque limitation due to increase in viscosity, thus Nylon with 4 wt-% of salt cannot be mixed with fibers. Figure 2-10 illustrates the effect of addition of LiCl on viscosity and consequently extruder performance.
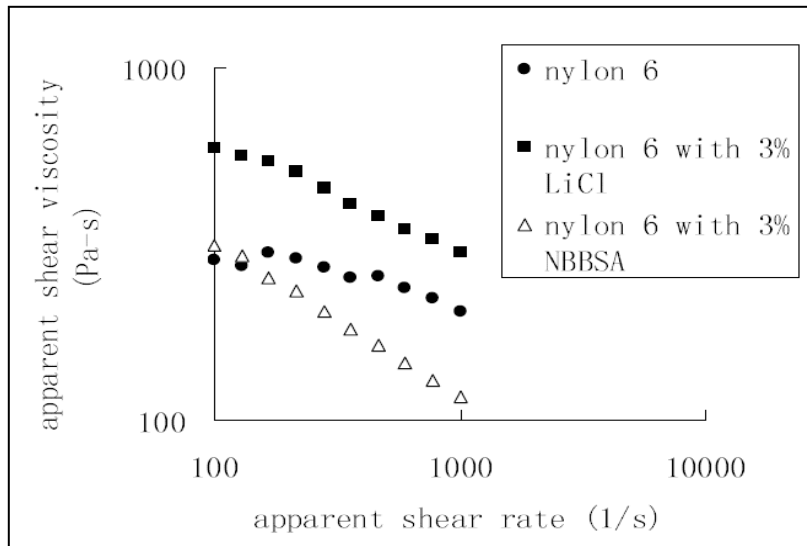
Figure 2-10: Effect of addition of salt on the viscosity versus shear rate; copied from reference: (Xu 2008)

2.3.3.2 USING PLASTICIZERS TO DECREASE RESIDENCE TIME AND MELTING POINT

Xu introduces plasticizers that can decrease melting point of Nylon-6 and Nylon-6,6. N-butylbenzenesulfonamide (N-BBSA) is generally used as a plasticizer to decrease melting point of Nylons (Xu 2008). According to their DSC results, N-BBSA had no effect on decreasing T_m of the Nylon-6 and only decreased the T_m of Nylon-6,6.

Figure 2-10 shows that addition of plasticizer decreased both modulus and viscosity of Nylon-6. Xu suggested a combination of LiCl and N-BBSA together for processing Nylon-6 with cellulose fibers (Xu 2008).

2.3.3.3 USING INTEC

INTEC is a commercial product which is designed to give fast injection cycles in injection moulding of automotive parts. The manufacturer, International Technical Polymer System Inc. (ITPS), claims easier processing and faster mould filling and ejection of parts from the mould with no negative effect on mechanical properties of the parts. ITPS claims, after addition of INTEC, lower rpm and drag forces are needed during processing and extrusion of Nylons (RHD Polymer and Chemical LLC).

Xu used INTEC as additive to Nylon-6 and Nylon-6,6. The objective was to facilitate blending of these two Nylons with cellulose fiber. ITPS reported that INTEC is composed of metallic oxides and that it has the capability to lower the viscosity and cause fast and uniform heat transfer (heating and cooling cycles in plastics). Xu found that INTEC did not change the melting point but it increased the solidification temperature, which is opposite to what was claimed by ITPS; therefore INTEC increased the viscosity of Nylon-6 in the presence of cellulose fibers. However, processing Nylon-6 with 3 wt-% INTEC could be done at lower temperatures. Table 2-8 and Table 2-9 summarize the mechanical properties of Nylon-6 and 3 wt-% of INTEC with different levels of fibers. The drastic decrease in strength and strain of composites containing cellulose fibers in comparison to neat Nylon-6 is an indication that of changes in the composite behaviour from ductile to brittle. The effect of INTEC was not the same in enhancing stiffness (modulus) and strength with different fibber percentages (Xu 2008).

Table 2-8: Flexural properties of Nylon-6/3 wt-% Intec and different level of cellulose wood fibers; copied from reference: (Xu 2008)

	Strain at yield (%)	Stress at yield (MPa)	Modulus (GPa)
Injection Moulding			
Nylon-6	7.36	69.8	1.37
Flexural property of Nylon-6/cellulose fiber			
Nylon-6/10% CF(13.3%)	7.06	71.6	1.57
Nylon-6/20% CF(25.0%)	6.79	85.6	2.00
Nylon-6/30% CF(33.3%)	5.11	95.7	2.60
Flexural property of Nylon-6/3 % INTEC cellulose fiber			
Nylon-6/10% CF(16.3%)	6.13	97.8	2.91
Nylon-6/20% CF(22.6%)	5.3	95.3	3.09
Nylon-6/30% CF(28.4%)	4.32	99.8	3.74

Table 2-9: Tensile properties of Nylon-6/3 wt-% Intec and different level of cellulose wood fibers (CF); copied from reference: (Xu 2008)

	Strain at yield (%)	Stress at yield (MPa)	Modulus (Gpa)
Injection Moulding			
Nylon-6	26.3	44.2	1.92
Tensile property of Nylon-6/cellulose fiber			
Nylon-6/10% CF(13.3%)	3.29	47.90	3.12
Nylon-6/20% CF (25.0%)	2.15	54.20	4.32
Nylon-6/30% CF(33.3%)	1.63	53.3	5.15
Tensile property of Nylon-6/3 % INTEC cellulose fiber			
Nylon-6/10% CF(16.3%)	3.24	56.10	3.47
Nylon-6/20% CF(22.6%)	2.35	62.00	4.05
Nylon-6/30% CF(28.4%)	1.99	67.70	4.96

In order to compensate for unwanted effects of INTEC, Xu mixed INTEC with plasticizer, lithium chloride salt and a combination of salt-plasticizer together. It was stated that although the modulus improved after any of these treatments, the strength decreased because of degradation (Xu 2008).

2.3.3.4   USING REACTIVE POLYMERS

Gardner et al. claimed finding a novel method for processing thermoplastics with high melting point with natural fibers. They suggested addition of another reactive polymer with lower viscosity and melting point, like cyclic anhydrides or maleic anhydride structures, to the high melting point polymer. Also they suggested coating lignocellulosic fibers with heat stabilizing agents or lubricants. The reactive polymer can react with the fibers surface and cause better interaction between fiber and matrix (Gardner, West et al. 2009). The authors measured dynamic mechanical thermal properties (storage and loss modulus) and monitored changes on glass transition (T_g). By measuring the storage and loss module and the mechanical damping (tan δ) in temperature range of -40 to 140 °C, the authors found the T_g of the composites of Nylon-6 with about 40 wt-% of wood fibers to be lower than pure Nylon-6 (Gardner, West et al. 2009). The addition of glass and wood fiber caused an increase in storage and loss module with temperature; the effect of glass fiber was more

pronounced, which was consistent with tan δ behaviour (Figure 2-11). They suggest that this lower T_g might be due to several reasons:

1) Additive and reactive polymers can cause a drop in T_g;

2) Additive and fibers cause excessive moisture uptake in the composites this excessive water cause T_g to depress.

It is known that viscosity of highly glass fiber filled Nylon-6 composites is lower in comparison to wood fiber filled composites. This property can also be seen in lower reduction of storage and loss modulus with temperature in wood fiber reinforced composites in comparison to glass fiber filled composites (Gardner, West et al. 2009).
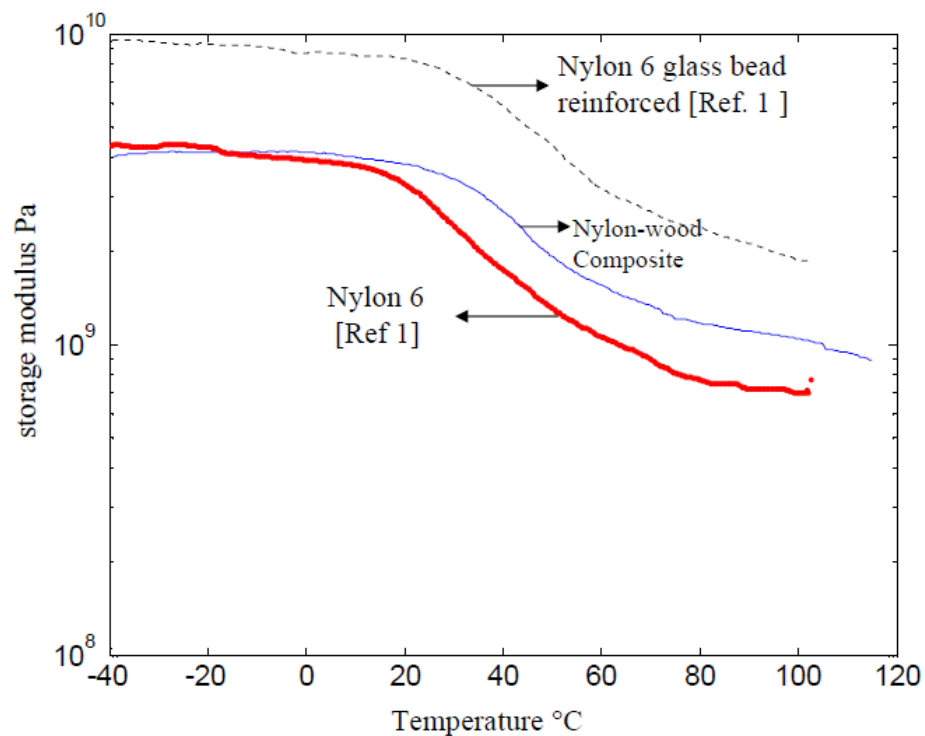
Figure 2-11: Storage modulus vs. temperature for Nylon-6; copied from reference: (Gardner, West et al. 2009)

2.3.4 BLENDING WITH LOWER MELTING POINT POLYMERS

The drawback of high processing temperature of Nylons can be mitigated by blending these polymers with polyolefins, like polypropylene for example. Dagli et al. reported blending 85 wt-% of Nylon-6 and 15 wt-% of polypropylene using polypropylene modified with acrylic acid as a compatibilizer. The compatibilizer can react with N-H group and decrease some of the hydrogen banding among the Nylon-6 chain, thus causing a possible decrease in the crystallinity of Nylon-6 (Dagli 1994).

Liu et al. studied the mechanical properties, the crystallization behaviour, the thermal stability and the water absorption on blends of Nylon-6 and high density polyethylene reinforced with banana fiber. The authors used different compatibilizers to increase the interfacial bonding between fiber and matrix. The amount of Nylon-6 in the blend was kept at 20 wt-% and the effect of different percentage of styrene/ethylene-butadiene/styrene triblock copolymer as compatibilizer was investigated. The compatibilizer was meant to affect the interface between banana fiber and the polyolefin part of the blend (Liu, Wu et al. 2009).

2.4 NYLON-6/NATURAL FIBER/FILLER MECHANICAL AND INTERFACIAL PROPERTIES

Addition of plant or mineral fillers can result in composites with better physical properties, such as higher tensile and flexural properties (except for elongation at break), but in general it decreases impact resistance of the composites in compare to pure Nylon-6 (Santos, Spinace et al. 2007). It was reported that the mechanical properties of Nylon-6 reinforced with cellulose fiber were higher than those reinforced with wollastonite but lower than those reinforced with glass fiber , except the impact resistance and HDT which were the same as in the glass fiber counterparts (Jacobson, Caulfield et al. 2001, Sears, Jacobson et al. 2001).

A comparison between the interfacial bonding of Nylon-6 and polypropylene reinforced with wood fiber showed that the interfacial bonding between wood fiber and Nylon-6 was strong, while the weak interfacial bonding between wood fiber and polypropylene caused fiber pull out from the matrix during deformation. The author concluded that the interaction between Nylon-6 and cellulose fibers was strong enough and there was no need for coupling agent (Xu 2008). However, Chen et al. suggested that the addition of coupling agents with carboxyl group can improve the interfacial bonding, thus which leading to better mechanical properties of the composites of Nylon-6 reinforced with wood pulp (Chen, Gardner 2008).

Sears et al. investigated the effect of addition of compatibilizer on the properties of wood fiber reinforced with Nylon-6. They stated that the addition of compatibilizer not only enhanced the mechanical properties, but also it facilitated the processing of composites. They used 2 wt-% of titanate compatibilizer (with the trade name of L-44-N) along with 30 wt-% of fiber. The properties of Nylon-6 filled with wood fiber composites increased in a way that the specific properties reached the same levels of those obtained with Nylon-6 filled with 30 wt% glass fiber composites Nylon-6/wood fiber composite is 10 % lighter than Nylon-6/glass fiber composite in 30 wt-% of fiber) (Sears, Jacobson et al. 2001).

Xu added 2 wt-% of polyurethane as a binder between Nylon-6 and Nylon-6,6 and cellulose fibers. They predicted the following reaction between cellulose fiber modified with polyurethane and polyamide (Nylon-6) (Figure 2-12).
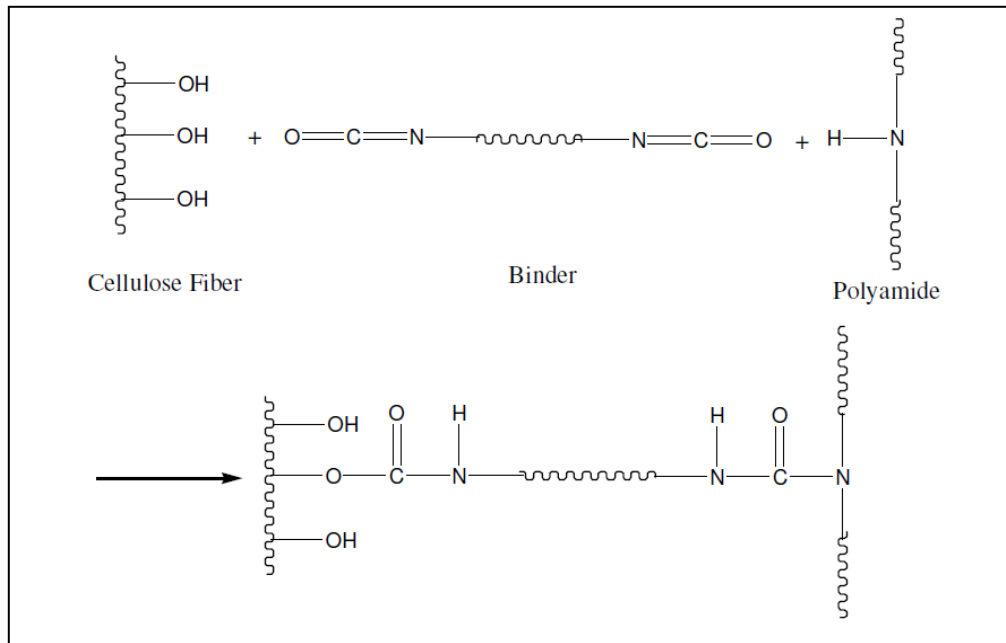
Figure 2-12: The reaction between polyurethane on cellulose fibers and Nylon-6; copied from reference: (Xu 2008)

It was reported that addition of 2 wt-% of binder did not change the mechanical properties (tensile or flexural strength and modulus).

In this research, between three proposed solutions of modifying processing condition, filler or polymer, the later (polymer modification) were used for dropping processing time and temperature. In another word, in order to overcome challenges of making Nylon-6/wheat straw composites, LiCl and N-BBSA were used as additives. Lithium chloride was used to drop Nylon-6 processing temperature and N-BBSA was used to reduce mechanical shear and residence time during processing. The Objective is finding a level of LiCl and N-BBSA mixture that optimized mechanical properties. This is one of the objectives as the effect of salt in increasing the viscosity and process time is in contrast with plasticizer effect in reducing the viscosity and decrease in processing time.

Low temperature processing techniques cannot be used in this study as there was limitation in our lab equipments and Fiber treatment is not intended to be use as a solution for this project.

Effects of compatibilizer on interface and mechanical properties were beyond the scope of this research and are suggested to be done in next studies.

The mechanical, thermal and morphological analysis were done on runs with different levels of LiCl salt and N-BBSA plasticizer.

3 MATERIALS AND METHODS

3.1 MATERIALS AND INSTRUMENTS

Materials that were used in this project and their supplier are listed in Table 3-1.

Table 3-1: List of materials which were used in the experiments

Materials	Supplier	Comments
Nylon-6	A. Schuman Inc.	MFI=31
Irganox 1098	Ciba	Nylon antioxidant
Lithium Chloride	Sigma-Aldrich	Anhydrous Grade
Formic Acid	Sigma-Aldrich	99%
N-Butylbenzenesulfonamide	Sigma-Aldrich	N-BBSA
Wheat straw	Omtec Inc.	Agricultural filler

Table 3-2 presents instruments that were used in this project, their model and manufacturer.

Table 3-2: List of instrument used for processing and testing experiments

Equipment	Manufacturer
DSC Q2000	TA Instruments
TGA Q500	TA Instruments
MiniLab Extruder Haake	Thermo Electron Corporation
Injection Moulding Apparatus RR/TSMP	Ray-Ran, UK
FESEM gold coating unit Desk II with Argon	Denton Vacuum, USA
Field Emission Scanning Electron Microscope (FESEM) Leo 1530 with EDX/OIM PV9715/69 ME	Leo Gemini (Carl Zeiss AG, Germany); EDAX (AMETEK Inc.)
Testing machine4467	Instron corp
Flexural testing machine 4465	Instron
Izod Impact machine43-02-01-0001	TMI(Testing Machines Inc.)
Specimen Notch XQZ-I, Travel: 24 mm	Chengde JinJian Testing Instrument Co., Ltd
Grinder5890A GC	IKA® Werke
Oven 5890A GC	Hewlett Packard
MFI Dynisco Polymer Test D4001DE	Alpha Technologies
Analytical balance AB304-S	Mettler Toledo
Tzero Hermetic low-mass pan and lid (DSC)	TA Instruments
XRD Instrument, 30 kV, 30 mA, with Cu Kα radiation	Bruker Instrument Inc.
Hot press, Model 3853-0, S/N 12000-937	CARVER, INC.
FTIR Tensor 27	Bruker Optik GmbH

3.1.1 POLYMER: NYLON-6

Nylon-6 (AE GIS H8202 NLB) was provided by A. Schuman Inc. The melt flow index of this product is 31 g/10-min and its melting point is 221 °C due to its highly crystalline structure. The percentage of crystallinity was found to be 20 % for this grade of Nylon-6.

3.1.2   ANTIOXIDANT: IRGANOX 1098

This Irganox is a phenolic antioxidant used for increasing the thermal stability of Nylons at high processing temperatures. Concentrations of 0.05-1 wt-% are recommended when using this antioxidant (CIBA SPECIALTY CHEMICALS INC. 2005). Irganox 1098 has special compatibility with Nylons due to its polar nature and presence of functional groups like carboxyls, amides and hydroxyls that are similar to Nylons backbone (Figure 3-1).
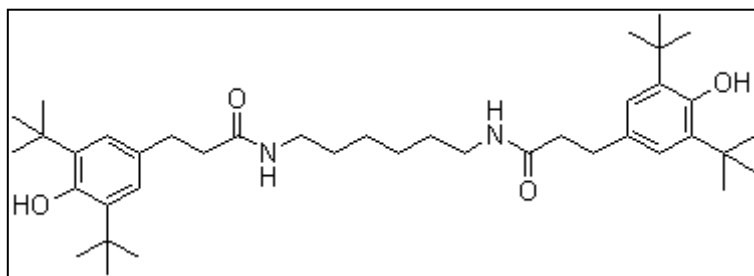
Figure 3-1: Irganox 1098 chemical structure; copied from reference: (LOOKCHEM)

3.1.3   LITHIUM CHLORIDE

LiCl is an inorganic salt with high reactivity and high water absorbency so anhydrous grade were chosen to have low water content in the raw material in first place.

3.1.4   FORMIC ACID

Formic acid is a good solvent for Nylon- 6. It is also able to dissolve lithium chloride salt. In this project it was used for removing Nylon-6 and Nylon-6/LiCl compounds from the processing tools surface. It also can be used for fiber extraction.

3.1.5   N-BUTYLBENZENESULFONAMIDE

N-Butylbenzenesulfonamide is an oily liquid lubricant with the chemical structure is presented in Figure 3-2.
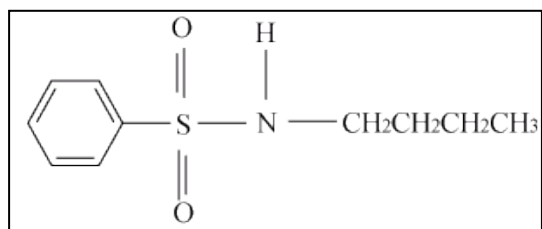
Figure 3-2: N-Butylbenzenesulfonamide chemical structure; copied from reference: (JIANGSU KANGXIANG GROUP COMPANY)

This chemical is a special lubricant for Nylons with recommended usage for Nylon-11 and Nylon-12 (CHEMICALLAND21).

3.1.6   FILLER: WHEAT STRAW FILLER

The wheat straw filler was supplied by Omtec Inc. located in Mississauga, ON, Canada. The sieve mesh used for fractionation of grinded wheat straw was size of 16 to 35. This size of wheat straw consists of particles that passed the sieve with mesh size of 16 (1.19 mm opening) but was retained in the sieve with the mesh size of 35 (0.5 mm opening). The wheat straw fractionated with these sieves is classified as "mid size" by Sardashti in a previous research work in our laboratory in collaboration with Omtec Inc (Sardashti 2009). Sardashti had conducted Thermal gravimetric analysis (TGA) tests on different size range of wheat straw fibers. The wheat straw known as mid size have the highest thermal stability (Sardashti 2009).

3.2   PROCESSING PROCEDURE

3.2.1   EXTRUSION

Nylon-6 and antioxidant were dry blended with different amount of salt and plasticizer as listed in Table 3-3. The mixture was melt mixed in the laboratory-scale extruder with the co-rotating conical twin screw extruder [Haake, Thermo Electron Corporation] (Figure 3-3).
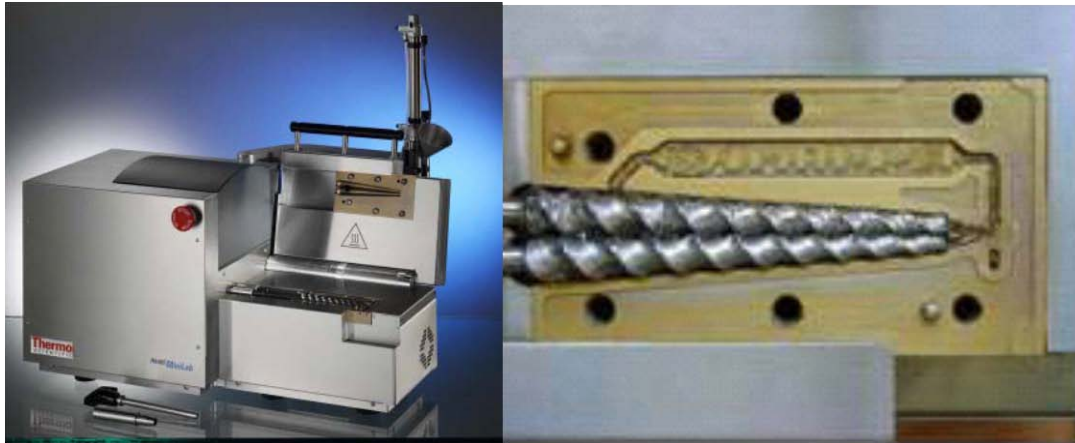
Figure 3-3: Thermo Haake minilab extruder (left), co-rotating conical twin screws (right)

The processing conditions for compounding Nylon-6 with additives (without wheat straw) was 225 °C and 30 rpm for all runs. This step took place prior to addition of the straw filler. This initial step of pre-compounding Nylon-6 and additives before adding the straw filler was carried out to obtain uniform mixture between the polymer and the additives. The role of the additive is to depress the melting temperature of the polymer before adding wheat straw filler. The resulted compound was granulated using a grinder [5890A GC IKA-Werke] and then the granules were fed again to the extruder with the straw filler. The pre-compounded Nylon-6/additive blend and the wheat straw were then mixed in the same Minilab extruder at 60 rpm. The increase in the screw speed (rpm) was adopted to decrease the residence time in the extruder during the compounding with wheat straw and to add more shear viscose heat to the blend. Figure 3-4 shows a schematic picture from process step.
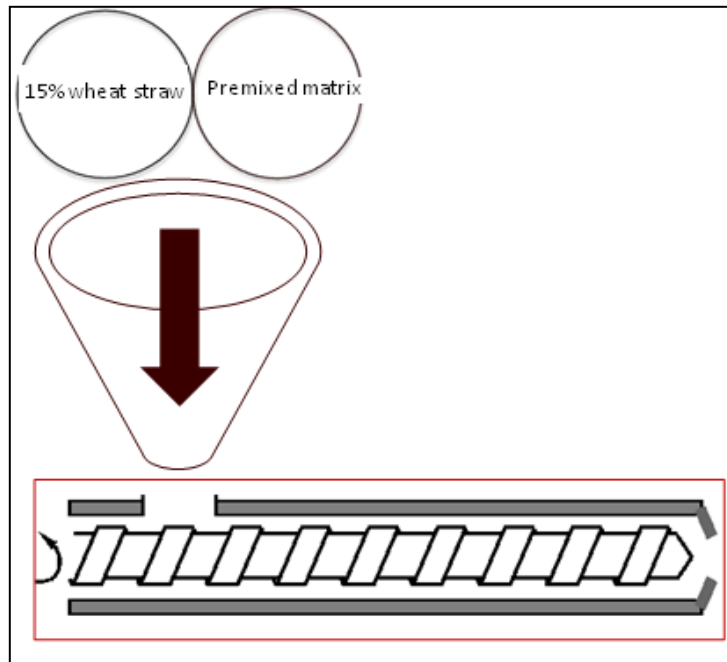
Figure 3-4: Schematic picture of the extrusion process

The compounding temperatures were differed from run to run depending on the different amounts of salt and plasticizer. The extruder temperatures for runs 1 to 4 was kept at 225 °C, while for run 5 the temperature was 235 °C due to absence of salt. The screw speed (rpm) was kept stable at 60 rpm to reduce the residence time in the extruder. After compounding in the extruder, the material was granulated using a grinder [5890A GC IKA-Werke]. Figure 3-5 shows the obtained granules after extrusion. As it was expected, the addition of salt and plasticizer caused a drastic decrease in the processing temperature; however, this was not possible to implement this condition in the laboratory extruder because of limitation associated to design of the extruder. The extrusion temperature could not be reduced because the extrudate was clogging at the die and blocking the discharge.

Figure 3-5: Granulated composite of Nylon-6/ wheat straw filler 15 wt- %

3.2.2   INJECTION MOULDING

The used lab scale Ray Ran injection moulding device [Ray Ran, RR/TSMP] had a static heating chamber for loading the granules (Figure 3-6). The granules were heated at 250 °C from 15 to 25 min to melt the material before injecting it inside the mould. Rectangular bars were made for impact and flexural test according to ASTM 790.07E (ASTM International 2008a). Dumbbell (dog bone shape) samples were made based on ASTM D638 (ASTM International 2008c) for tensile test. Injection moulding was performed under a pressure of 90 to 100 psi. This packing pressure was hold for 30-35 s for each bar. Although salt was added to lower the processing temperature of the composites, no significant improvement in flow properties was observed at the low processing temperature. High viscosity of the melting along with low packing pressure of the moulding machine resulted in scrap samples. Hence, using higher temperatures (250 °C) was inevitable for making sample bars without defect. The main degradation of the fibers occurred during this processing step when the samples stayed for 15 to 25 min inside the injection moulding chamber. The composite blends were exposed to the temperature of 250 °C until the viscosity decreased and the molten composite could easily be purged

41

inside the mould. The residence time inside the chamber increased to 35-50 min when the processing temperature decreased to 235 °C. The injection moulding was not possible at temperatures lower than 235 °C. This means, that adding salt and plasticizer effectively decreased the melting point of Nylon-6; however, the processing temperature could not been decreased due to equipment limitations.

Figure 3-6: Lab scale Ray Ran injection moulding

3.3 RUN FORMULATIONS

Different formulations were chosen based on the aim of the project. The objective was the identification of key parameters in the formulation that can affect the processability and the mechanical properties. These formulations were chosen using the Design Expert Statistical software for a set of experiments based on mixture design. The highest and the lowest level

of additives were 4 and 0 wt-%, respectively. These formulations are summarized in Table 3-3. Replications for the compounding experiments were not performed because of time limitations; in each compounding experiment approximately 100 g of sample were prepared.

Table 3-3: Summary of runs formulations

Run #	Label	Irganox (wt-%)	Salt (wt-%)	Plasticizer (wt-%)	Wheat straw (wt-%)
1	15WS-4s-0p	0.1	4	0	15
2	15WS-3s-1p	0.1	3	1	15
3	15WS-2s-2p	0.1	2	2	15
4	15WS-1s-3p	0.1	1	3	15
5	15WS-0s-4p	0.1	0	4	15
6	15WS-0s-0p	0.1	0	0	15
7	Neat Nylon-6	0.1	0	0	0

Run 7 and 6 are made to compare between properties of neat Nylon-6 and Nylon-6/15 wt-% WS with properties of composites that have different level of additives (run 1 to 5).

3.3.1   MIXTURE DESIGN

Design-Expert (v.7) software was used to minimize the number of experiments while keeping the ability to find correlations for the amounts of salt and plasticizer the mechanical properties. Statistical analysis of the experimental data was done using Excell Statistics tools.

3.4 PROCESSABILITY

3.4.1   MELT FLOW INDEX (MFI)

The melt flow index (MFI) is a simple experiment; it reflects the viscosity of the blend. It shows how fast a polymer material can flow through the extruder and how fast it can fill the mould. The MFI was carried out according to the ASTM D 1238–04c (ASTM International

2008a). The MFI instrument chamber was loaded with 5-6 g of sample. The test was done at 235 °C and with the piston weight 2.16 kg. After 360 sec, the molten samples were cut within time intervals of 10sec. At least 5 measurements were carried out for each sample. The MFI is reported in unit of gram of material that transfers within 10 min through the die with diameter of 8 mm. It has an inverse relation with the viscosity and flow-ability during processing.

3.5 MECHANICAL TESTING

3.5.1 ANNEALING

Sample bars were kept in vacuum oven under gauge pressure of -10 psi g (10 psi lower than the atmospheric pressure), and temperature of 100 °C for 48 hours for thermal stabilization (also known as annealing) (Ramazani S.A, Mousavi S 2005) . This temperature is above the T_g but below the melting temperature of Nylon-6 and it is reasonable for large injection moulded samples in the industry (Xie, Zhang et al. 2005). In most of the polymers the annealing step is necessary to erase the thermal history of the samples. This thermal history is due to different processing and cooling conditions. The reasons for this procedure are:

1) Nylons have hydrophilic structure, thus making them susceptible for absorption of the moisture. Heating Nylon-6 in vacuum conditions removes moisture. This effect is critical to the final properties because water can act as plasticizer or increase the free volume between chains, consequently, increasing chain mobility.

2) The second reason for annealing is to prevent the effect that water have on crystalline morphologies. The gamma crystalline structure will transform to a more stable alpha crystalline structure in the absence of water and improve the mechanical properties.

3.5.2 CONDITIONING

Conditionings were based on ASTM D618-08 (ASTM INTERNATIONAL 2008). Samples were located in an environmental chamber for 48 hours. The temperature was 23 °C and the

relative humidity was 50 %. This temperature and humidity were also the laboratory environmental conditions during the tests.

3.5.3   FLEXURAL TEST

The flexural was done based on ASTM D790-07 (ASTM International 2008b). Rectangular bars with the size of 2.98 cm X 12.4595567 cm X 62.71cm were prepared by injection moulding. At least 5 injection moulded bars were tested for this test. Analysis was done by Instron testing machine. The cross head speed is 0.18 (mm/s) which according to ASTM is calculated using Equation 3-1:

$$R = \frac{Z * L^2}{6d}$$

Equation 3-1

Z [mm/mm/min]: strain rate which have been kept on 0.01

L[mm]: length of sample

D[mm]: depth of the sample

3.5.4   TENSILE TEST

Tensile test were done based on ASTM D 638 – 08 (ASTM International 2008c). The dumbbell (dog bone) shape samples were made under category of type II size range. Testing speed was 5 mm per min. At least 5 specimens were tested and properties were averaged.

3.5.5   IZOD IMPACT TEST

Test bars with the dimensions of 2.98 cm X 12.4595567 cm X 62.71cm were made and notched based on ASTM D 256-06 (ASTM International 2008b). 5 notched bars were tested and the reported impact resistance in this document is the averaged value.

3.6 THERMAL PROPERTY CHARACTERIZATION

Thermal properties are measured with differential scanning calorimetry (DSC) and thermal gravimetric analysis (TGA). The DSC was used to measure crystallization temperature, kinetics and melting behaviour of the runs, while the TGA was used to study the degradation temperature and degradation kinetics of the runs.

3.6.1 DIFFERENTIAL SCANNING CALORIMETRY

The DSC is an instrument that measures heat flow, thus it can be used to identify and measure the enthalpy of phase transition in polymers. The temperature which corresponds to endothermic peak is melting point (T_m) and the temperature corresponds to exothermic peak is crystallization point (T_c). The percentage of crystallinity can also be found by integrating area of the melting peak and normalize it to heat fusion of the pure polymer with 100 % crystallinity (Equation 3-2):

$$X_c = \frac{\Delta H}{\Delta H_0 (1-w)}$$
Equation 3-2

where ΔH is the Area under melting peak, ΔH_0 is the Heat fusion of the polymer with 100 % crystallinity which is found to be equal to 190 W/g and w is the weight percentage of matrix in the composites (Lincoln, Vaia et al. 2001).

Extruded and pelletized samples were prepared in the shape of films using hot press. The films were made at 220 °C and pressure 3000 lb-ft. Granules was kept under this temperature for 1 min, then the pressure were released and then again the pressure of 3000 lb-ft was forced on films for 2 min (in 220 °C) so that air bubbles were eliminated. The films were cooled fast to room temperature. Approximately 3 to 5 mg of the resulted films was used for DSC analysis. The DSC was done under two conditions of isothermal and non-isothermal. In non-isothermal condition, samples were heated with high rate to 250 °C and kept at that temperature for 15 min to erase the thermal history. Then the

samples were cooled with the rate of 10 °C/min to 35 °C, this step was followed by heating with same rate (10°C/min) to 250°C .

3.6.2   THERMAL GRAVIMETRIC ANALYSIS

The stability was investigated by measuring the onset and kinetics of thermal degradation. The onset of thermal degradation was measured as the temperature corresponding to 1 wt-% of mass loss. Approximately 5 mg of sample was obtained after extrusion was grinded and used for this investigation. The temperature was increase from room temperature to 800°C and percentage of weight loss with time and temperature were monitored. The TGA procedures were done under nitrogen purge with the flow rate of 50 mL/min.

3.7 MORPHOLOGY ANALYSIS

The morphology of the composites was investigated with scanning electron microscopy to better understanding the interfacial interactions between fiber (wheat straw) and matrix (Nylon-6).

3.7.1   SCANNING ELECTRON MICROSCOPY

Injection moulded samples (bars) were submerged in liquid nitrogen for 15 min so that the entire went under its glass transition temperature (T_g) and became brittle (Valenza, Spadaro et al. 1993). Then, the bars were taken out of the liquid nitrogen and broken with sudden impact (hammered). The cold fractured surfaces were used for SEM analysis. The samples were mounted on the SEM stub with a conductive double-face adhesive tape. Gold coating was applied with thickness of about 10 nm before taking SEM image. Argon was used as inert gas during the gold coating.

4 RESULTS AND DISCUSSIONS

4.1 SPECIMENS COLOR

It is obvious that addition of fibers to Nylon-6 matrix gives a brown color to the composites. Figure 4-1 shows granules of Nylon-6/wheat straw (15 wt-%) after extrusion, and the injection moulded test bar. It can be seen from black color of the bar that injection moulding process severely degraded the material. Extend of degradation of WS is higher in injection moulding process due to high residence time and temperature of the processing stage.

Figure 4-1: Nylon-6 with 15 wt-% of wheat straw: extruded pellets and innjection moulded test bar

Figure 4-2 compares the degree of degradation between run 1 and 5 based on their apparent color. The darker color in the specimens is an indication of higher degradation in WS fiber. Run 1 had both the highest level of salt (4 wt-%) and residence time during processing. This caused the specimens to have darker colors along with burn smell. However, run 5 with 4 wt-% plasticizer was easier to process and had shorter exposure to heat. Therefore, specimens formulated at 4 wt-% plasticizer had relatively brighter colors.

Figure 4-2: Comparison between color of sample with 4 wt-% salt(left) and sample with 4 wt-% of plasticizer(right)

Comparison between samples in Figure 4-2 further provides information with respect to processing behaviour of the composites. Samples with 4 wt-% salt have lower melting point (192 °C) compared to sample with 4 wt-% plasticizer (220 °C) and hence should be processed at a lower temperature. However, due to an increase in viscosity of the melt during processing upon addition of salt, a higher processing temperature was needed. Also an increase in the viscosity of the melt can induced higher heat generation in the melt during processing. This in return caused higher extent of degradation in the composite and resulted in samples with darker colors. Rauwendall reported that the heat generation is related to viscosity; the higher viscosity results the higher heat generation (Rauwendaal 2001).

4.2 MELTING AND CRYSTALLIZATION TEMPERATURE

In order to find the effect of addition of WS, salt, and the plasticizer on the processing temperature and also to determine the lowest processing temperature, the measurement of melting and crystallization temperatures were performed. Figure 4-3 shows the DSC graph for the pure Nylon-6. It can be seen that Nylon-6 melting peak is sharp with a shoulder at

lower temperature. The shoulder is reported to be due to two crystalline structure of Nylon-6 (Wei, Davis et al. 2002). The sharp peak can be attributed to alpha crystalline forms as alpha crystals have higher thermal stability. The shoulder in lower temperature is reported to be attributed to gamma crystals with lower thermal stability (Ho, Wei 2000, Keating, Gardner et al. 1999). Similarly, Wu and Liao who studied crystallization of Nylon-6 filled with nanoclay reported that these peaks are attributed to melting point of alpha and gamma structure respectively (Wu, Liao 2000).
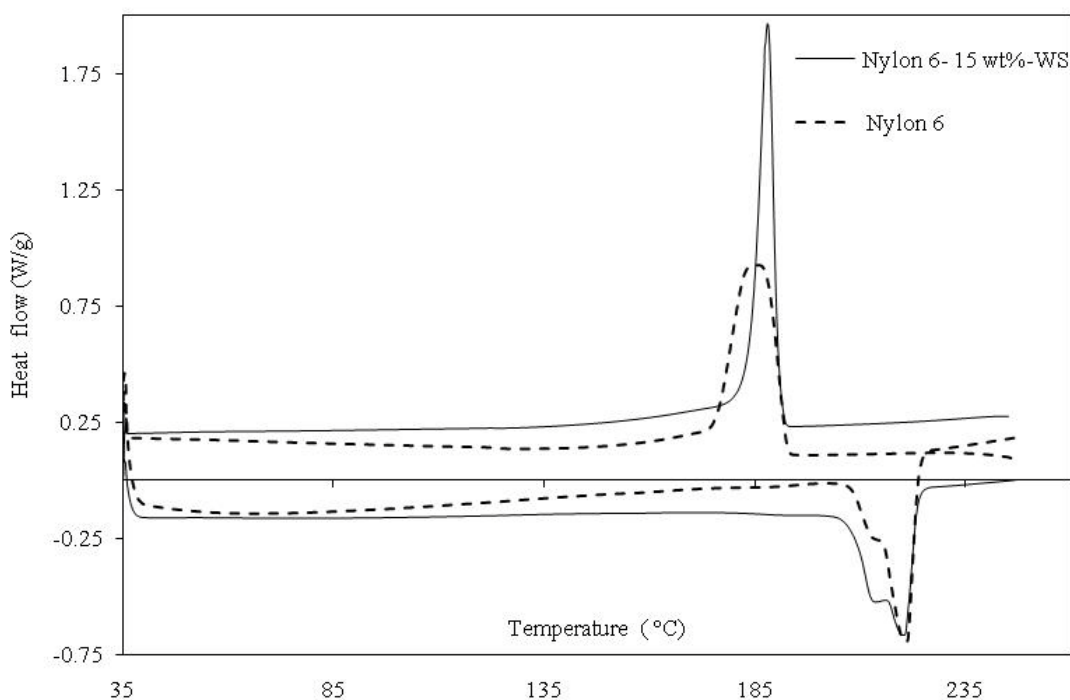
Figure 4-3: DSC thermograph of pure Nylon-6 and Nylon-6 with 15 wt-% WS (first cycle is erased)

The melting point is an indication for size (thickness) of crystalline region, while the degree of crystallinity shows the percentage of crystalline region (Schultz 2001). The narrow melting peak of Nylon-6 is an indication that most crystals are in the same size range.

Comparison between neat Nylon-6 and Nylon-6 after addition of 15 wt-% wheat straw showed that addition of filler did not make any change in crystals size but it changed the percentage of crystallinity. This is attributed to the nucleating effect of wheat straw which accelerates crystallization. If the rate of nucleation from the surface of the filler (WS) is

high, large number of nuclei will be made on the surface of the WS. Therefore, the nuclei are so packed that crystal growth is impossible in three dimensions (spherulites usually grow in three dimensions); the crystals growth is hindered in the plane of the filler direction. Thus, the only possible direction for crystal growth is normal to external nucleus surface. This type of morphology is called transcrystallization. It is known that when crystallization occurs at the presence of shear flow along with the polymer flow on the surface of the filler, there is more chance for transcrystallization (Schultz 2001). In this thesis, transferring Nylon-6/wheat straw compound in the mould induces transcrystallization due to shear forces that impose orientation on the polymer chains and encourage crystallinity. This not only can be concluded from an increase in percentage of crystallinity, but also it is apparent from the higher crystallization temperature of the sample with 15 wt-% WS compared to neat Nylon-6 (Table 4-1).

Salt was added to eliminate the crystalline structure of Nylon-6 to form a structure that is transferable at a lower processing temperature. Figure 4-4 represents the thermogram of Nylon-6 after addition of 4 wt-% salt. The melting and crystallization peaks of Nylon 6 were eliminated upon addition of salt, which is an indication of absence of crystalline structure.

It was observed that addition of salt at higher levels (higher than 4 wt-%) do not help with the processing because the compounding residence time increases drastically. In this case, the extruder and injection moulding machines could not maintain required shear and pressure for the material to be proceed. Therefore, it was decided to keep the level of salt at 4 wt-%.
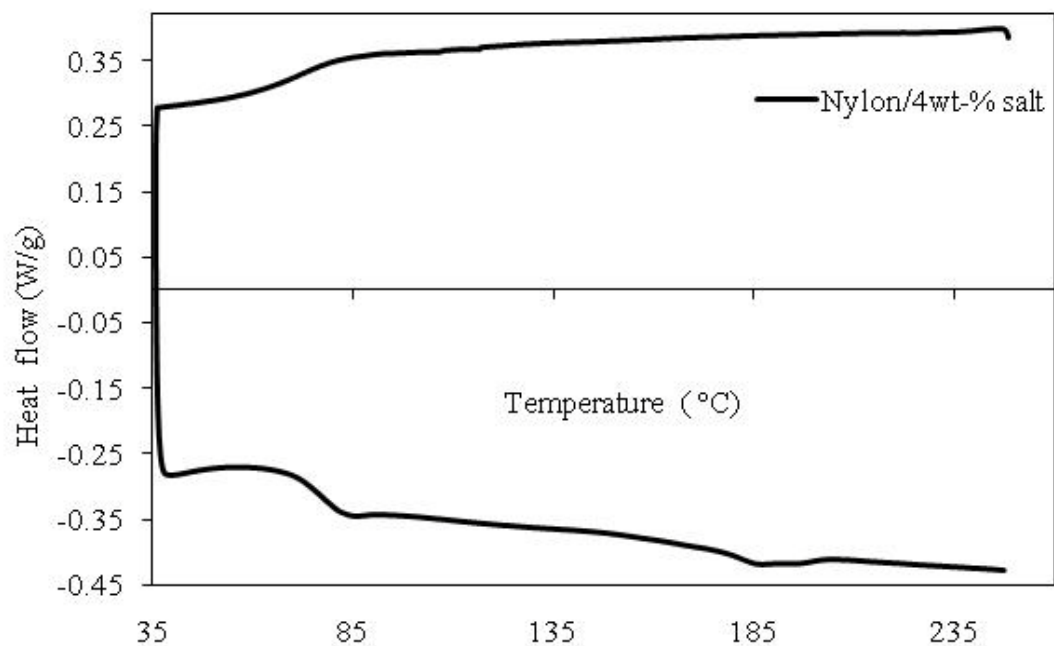
Figure 4-4: DSC thermogram of Nylon-6 with 4 wt-% of salt

On the other hand, addition of 4 wt-% plasticizer had no effect on the melting point and the degree of crystallinity as indicated by lower area under the melting peak (Figure 4-5).
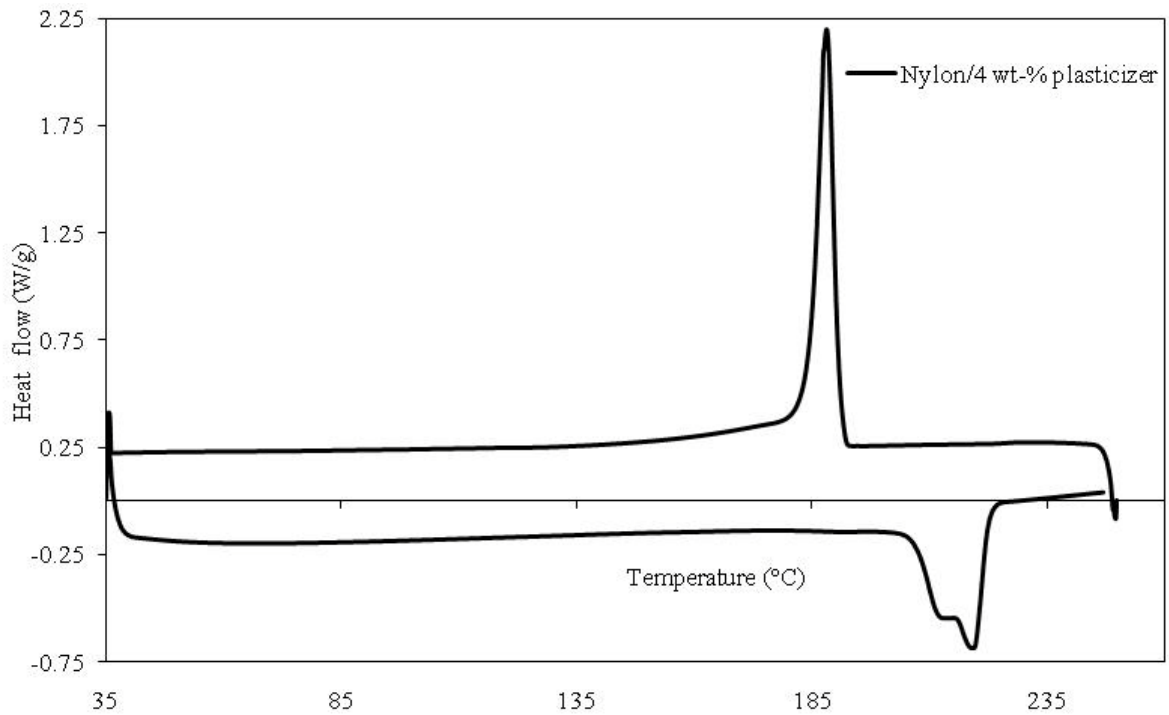
Figure 4-5: Nylon-6 with 4 wt-% plasticizer DSC curve

The effects of addition of different additives on melting point (T_m), crystallization temperature (T_c), and the degree of crystallinity (X_c) are summarized in Table 4-1.

Table 4-1: Crystallization behaviour of composite runs after extrusion

Run #	T_{m1}	T_{m2}	T_c	X_c
1	191.6	180.7	NA	10.6
2	201.4	185.4	155.6	14.3
3	206.7	193.0	167.4	19.6
4	213.2	202.6	178.2	17.2
5	219.2	212.9	188.4	16.8
6	219.5	213.4	187.9	21.8
Nylon-6	220.8	214.1	185.7	19.9

T_{m1} is the main melting peak temperature and T_{m2} is the temperature of the shoulder in lower temperatures. From Table 4-1, it can be seen that addition of salt and plasticizer at any level changed the crystallization temperature and decreased the percentage of

crystallinity. Moreover, the melting point was not affected by plasticizer and only changed according to the level of the salt. However, the percentage of crystallinity was affected the level of plasticizer as indicated from comparison in percentage of crystallinity of run 5 and run 6. The plasticizer affected the interface between the Nylon-6 and WS and decreased the shear stress during the processing. Therefore, the crystallization which was induced by shear on the surface of the fiber was lower in cases where plasticizer was added. Shear and interfacial interaction between fiber and matrix is known to be the most influential parameter in transcrystallization.

4.2.1 PROCESSABILITY AND RESIDENCE TIME

The quantification of flow behaviours is important because it shows how easy and fast a material can be processed. Therefore, the melt flow index (MFI) was measured on these samples. The results are shown in Table 4-2:

Table 4-2: MFI of runs before addition of WS

Run #	Salt (%)	Plasticizer (%)	MFI(g/10 min)	Normalized data
1	4	0	4.9	0.2
2	3	1	8.4	0.3
3	2	2	15.0	0.5
4	1	3	23.0	0.7
5	0	4	37.1	1.2
6	0	0	31.5	1.0

The last column (normalized data) indicates the ratio of MFI of each run to pure Nylon-6/ 15 wt-% WS composites. It can be seen from Table 4-2 that addition of 4 wt-% salt decreased the MFI. This increase in viscosity can be interpreted by the nature of interactions between the salt and Nylon-6 chains. Salt can interact with the polymer chains to cause a crosslinking effect. Lithium ions attack the carboxylic groups of the matrix and form junctions (similar to crosslinks) between the polymer chains (Xu 2008). Ionic interactions between the chains cause an increase in the viscosity of the matrix which consequently decrease the MFI.

On the other hand, the addition of plasticizer increased MFI of Nylon-6 due to an increase in the free volume between the polymer chains, which in return facilitates polymer chain motions (Nielsen 1994).

In runs with different level of salt and plasticizer, salt was responsible for the increase in viscosity and plasticizer was responsible for the increase in MFI. Thus, in runs 1 to 5, the effects of salt and plasticizer on viscosity were competing with each other as shown in Figure 4-6. From this Figure, it can be inferred that addition of salt affected the viscosity more than plasticizer. From this Figure, it can be inferred that addition of salt affected the viscosity more than plasticizer. Addition of 1 wt-% of salt affected the viscosity in such a way that even the addition of 3 wt-% plasticizer did not compensate for it. Thus, runs which contained any level of salt had higher viscosity in comparison to pure Nylon-6 (Figure 4-6).
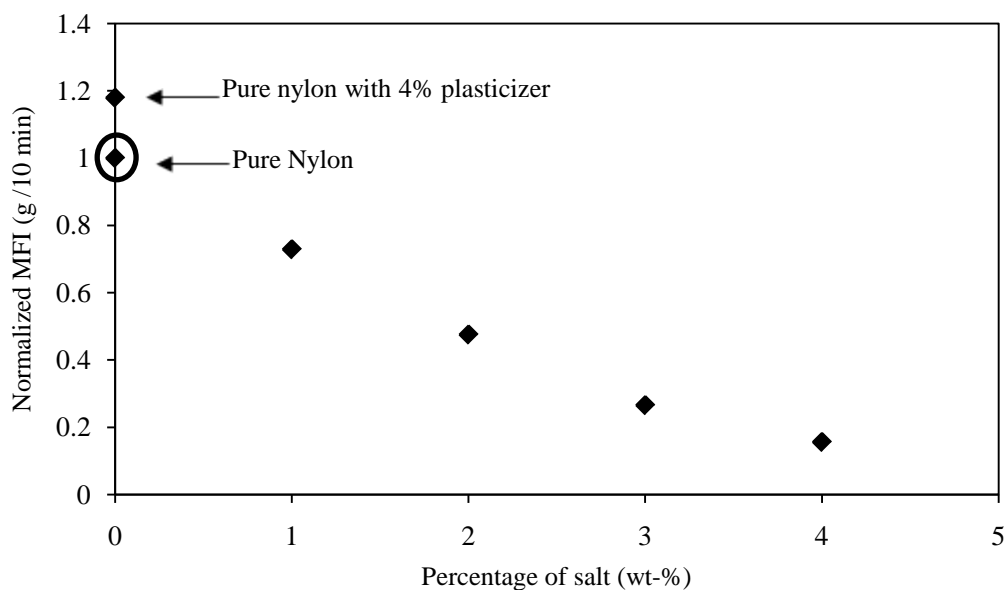
Figure 4-6: Trend of decrease in MFI of composite versus amount of salt

The viscosity is a critical flow property which dictates residence time of filled polymers in processing. Increase in MFI means decrease in melt viscosity which leads to a lower processing residence time. Lower residence time inhibits filler degradation due to lower exposure time to heat and shear.

The MFI of composites (after addition of wheat straw) was investigated and the results are shown in Table 4-3. It was found that there was no significant difference between runs as shown in the ANOVA Table 4-4. This is due to the fact that the addition of filler had a more significant effect on the MFI of the runs that addition of salt or plasticizer. It should be mentioned that MFI is mainly a method to identify the processability of the material; it is not a direct measure of a material viscosity. Therefore, more effective analyses are recommended to identify the effects of additives on the viscosity of the composite.

Table 4-3: MFI of composites

Sample #	Salt content (%)	Plasticizer content (%)	MFI(gr/10 min)	Normalized data
1	4	0	8.47	1.13
2	3	1	7.25	0.96
3	2	2	8.63	1.15
4	1	3	6.55	0.87
5	0	4	8.53	1.13
6	0	0	7.52	1.00

Table 4-4: Analysis of variance (ANOVA) table and F test which shows level of significance for difference between runs

Source	df	SS	MS	$F_{observed}$	$F_{crit.}$ 5,14.0.05
Between runs	5	0.0095	0.0019	0.02	3.34
Within runs	38	3.2518	0.0856		No significant difference between runs
Total	43	3.2613	0.0758		

df: Degree of freedom, SS: sum of squares, MS: mean square, $F_{observed} = \frac{Between\ group\ variability}{Within\ group\ variability}$,

F_{crit}; Critical number that the $F_{observed}$ must exceed to reject the hypothesis that the difference between runs is significant.

4.3 THERMAL PROPERTIES

Thermal degradation can happen during processing because the temperature required to processing Nylon-6 composites with wheat straw is above the temperature at which the thermal degradation of wheat straw starts. When Nylon-6 is used for automotive applications, it is usually filled with inorganic fillers or glass fiber to enhance its thermal

and mechanical properties and to lower cost. Thus, it is necessary to investigate thermal properties of Nylon-6 filled with wheat straw.

Thermal gravimetric analysis (TGA) was performed on extruded samples prior to injection moulding to determine the thermal properties of different formulation. Onset of degradation found at 1 % weight loss was obtained for each formulation as an indication of the point when thermal degradation starts. It was assumed that at 160 °C all bonded and unbounded molecules of water were evaporated (Sardashti 2009). Therefore, the weight loss up to 160 °C was attributed to water evaporation only. This temperature was well below the boiling point of plasticizer (314 °C) and onset lignin degradation (180 °C).

The temperature for onset of degradation and maximum rate of weight loss, T_{max}, are summarized in Figure 4-7 and Figure 4-8 respectively. The differential thermal analysis (DTG) plots the derivative of the curve obtained in the TGA, it is the rate of weight loss. The peak of curve is an indication for temperature at which the weight loss reaches its highest rate. This temperature is higher for samples with more thermal stability.

From Figure 4-7, one can conclude that all samples are degraded in the same temperature range except for run 6 which has no additives but WS. Therefore, it can be inferred that addition of salt and plasticizer at any level will enhance the tendency for degradation.

It can be seen in Figure 4-8 that run 6 has relatively higher T_{max} compared to all other runs except for run 5. This was attributed to the lower residence time of run 5 in the extruder which resulted in lower thermal degradation during extrusion. In other words, all runs have experienced higher thermal degradation compared to run 5 which make them to be more vulnerable to temperature. Note that although the residence time was not measured, the melt flow index (MFI) was measured. Samples with high MFI should have a low residence time because of their low viscosity. This is another indication that addition of salt had negative consequences on the thermal degradation of the composite.
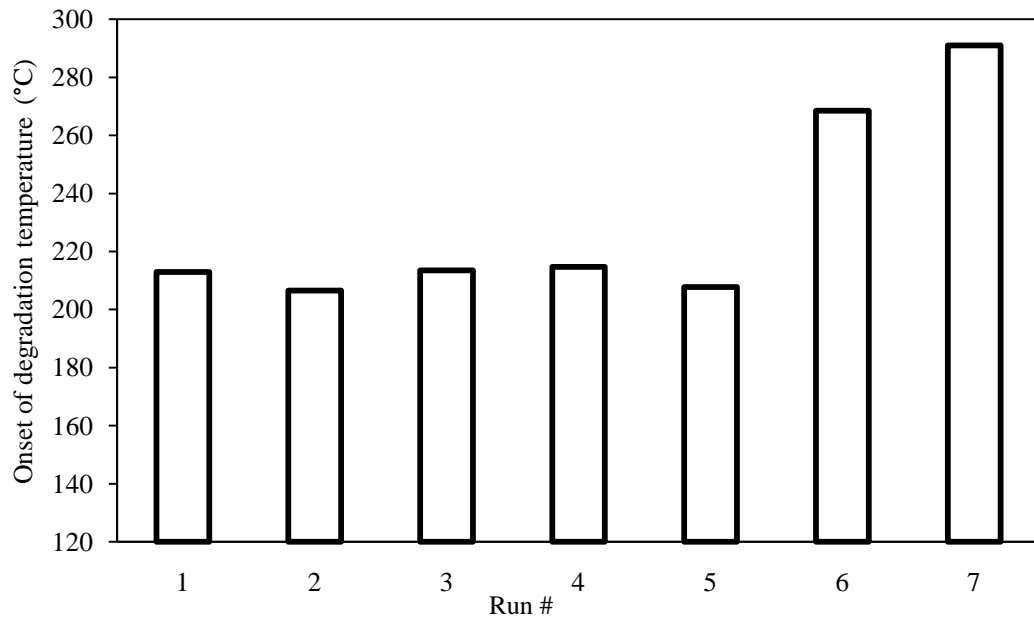
Figure 4-7: Onset of degradation temperature for different composite runs
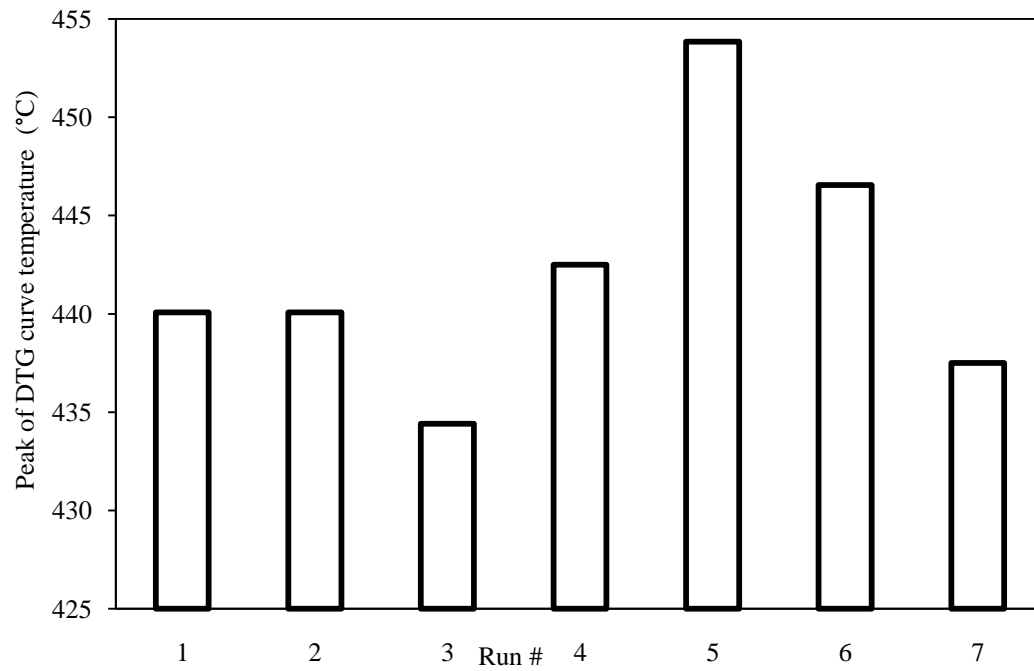
Figure 4-8: Temperature corresponding to peak of DTG curves

4.3.1 DEGRADATION KINETICS

In order to compare degradation kinetics of runs with different amount of additives, one needs to find the activation energy for degradation and the order of degradation reaction. For this purpose non-isothermal kinetic models are used. For non-isothermal single step reactions in solid state, Equation 4-1 can be written (Semsarzadeh, Poursorkhabi 2009):

$$rate = \frac{d\alpha}{dt} = f(\alpha)k(T) \qquad \text{Equation 4-1}$$

Where α is the reaction conversion and it can be defined by Equation 4-2:

$$\alpha = \frac{m_{i-m_t}}{m_i - m_f} \qquad \text{Equation 4-2}$$

In Equation 4-2 m_i and m_f are the initial and final mass of the samples taken from TGA and m_t is the instantaneous mass of sample in each time interval. f (α) in Equation 4-2 can be explained by kinetics of degradation models according to Equation 4-3 (Semsarzadeh, Poursorkhabi 2009):

$$f(\alpha) = \alpha^m(1-\alpha)^n[-\ln(1-\alpha)]^p \qquad \text{Equation 4-3}$$

Where m, n and p are determined based on nature of the reaction to make f (α) look like the equations presented in Table 4-5:

Table 4-5: Different forms of f(α) equation; copied from reference: (Semsarzadeh, Poursorkhabi 2009)

Mechanism	Symbol	F(α)
Reaction order model	F_n	$(1-\alpha)^n$
Random nucleation and growth of nuclei (Avrami-Erofeev equation)	An	$n(1-\alpha)[-\ln(1-\alpha)]^{1-1/n}$
2D diffusion (bidimensional particle shape)	D2	$1/(-\ln(1-\alpha))$
3D diffusion (tridimensional particle shape, Jander Equation)	D3	$3(1-\alpha)^{2/3}/2[1-(1-\alpha)^{1/3}]$
3D diffusion (Tridimensional particle shape, Ginstein-Brouhnstein Equation)	D4	$3/2[(1-\alpha)^{-1/3}-1]$

The rate constant of equation can be defined by an Arrhenius equation (Equation 4-4):

$$k(T) = Aexp(-\frac{E}{RT})$$

Equation 4-4

Where A is pre-exponential factor and E is the degradation activation energy.

E is an indication for the amount of energy that material should gain to overcome to energy barrier for degradation. In the Equation 4-1, for the case of degradation of polymer composites, correlation coefficient reaches its maximum when f (α) is in F_n form (Table 4-5). F_n for common reaction orders is presented in Table 4-6 (Genieva, Turmanova et al. 2008).

When the heating rate is constant ($\frac{dT}{dt} = q = const.$), by substituting Equation 4-3 and Equation 4-4, in Equation 4-1 , we can integrate Equation 4-1, and obtain Equation 4-5:

$$\frac{d\alpha}{dt} = Aexp\left(-\frac{E}{RT}\right)f(\alpha)$$

$$\xrightarrow{\int_0^\alpha d\alpha/f(\alpha)} \int_0^\alpha \frac{d\alpha}{\alpha^m(1-\alpha)[-\ln(1-\alpha)]^p}$$

Equation 4-5

$$= \frac{A}{q}\int_0^T \exp\left(-\frac{E}{RT}\right)dT$$

Analytical answer of the right hand side of Equation 4-5 is defined by g (α) and is presented in Table 4-6, as a function of degree of reaction.

Table 4-6: g(α) functions which corresponds to different f(α) functions for common reaction orders; copied from reference: (Genieva, Turmanova et al. 2008)

#	Mechanism	Name of function	$g(\alpha)$	$f(\alpha)$	Rate-determining mechanism
Chemical process or mechanism non-invoking equations					
1	$F_{1/3}$	one-third order	$1-(1-\alpha)^{2/3}$	$(3/2)(1-\alpha)^{1/3}$	Chemical reaction
2	$F_{3/4}$	Three-quarter order	$1-(1-\alpha)^{1/4}$	$4(1-\alpha)^{3/4}$	Chemical reaction
3	$F_{3/2}$	One and half order	$(1-\alpha)^{-1/2}-1$	$2(1-\alpha)^{3/2}$	Chemical reaction
4	F_2	Second order	$(1-\alpha)^{-1}-1$	$(1-\alpha)^2$	Chemical reaction
5	F_3	Third order	$(1-\alpha)^{-2}-1$	$(1/2)(1-\alpha)^3$	Chemical reaction

Using Equation 4-5, the maximum rate of degradation can be defined according to Equation 4-6:

$$-\frac{1}{\dfrac{df(\alpha)}{d\alpha}} = -\frac{1}{f'(\alpha_{max})} = \frac{A}{q}\frac{R\,T_{max}^2}{E}\exp\left(-\frac{E}{RT_{max}}\right) \qquad \text{Equation 4-6}$$

Combining Equation 4-5 with the Equation 4-6, the following equation can be obtained:

$$g(\alpha_{max}).f'(\alpha_{max}) = -h\left(\frac{E}{RT_{max}}\right) \qquad \text{Equation 4-7}$$

From Equation 4-7, it can be concluded that after finding the reaction order, the only parameter which can affect α_{max} is E/RT. The dependency of α_{max} on the reaction order can be defined based on Table 4-7. Thus, the amount of α_{max} from DTG can be used for identifying the order of decomposition reaction and selecting the correct F_n $F_n$function. Table 4-7 was used to determine reaction order from α_{max}that has been extracted from peak of DTG curve.

Table 4-7: Theoretical values for different reaction order corresponds to various α_{max} range; copied from reference: (Genieva, Turmanova et al. 2008)

α_{max}	n	α_{max}	n
0.913-0.920	0.1	0.569-0.604	1.1
0.850-0.862	0.2	0.551-0.587	1.2
0.799-0.816	0.3	0.534-0.571	1.3
0.756-0.777	0.4	0.519-0.557	1.4
0.719-0.743	0.5	0.504-0.543	1.5
0.687-0.713	0.6	0.491-0.531	1.6
0.659-0.687	0.7	0.478-0.519	1.7
0.633-0.663	0.8	0.466-0.507	1.8
0.610-0.642	0.9	0.455-0.496	1.9
0.588-0.622	1	0.444-0.486	2

After determining the reaction order from Table 4-7, the amount of g(α) can be found and substituted in Equation 4-5 to obtain Equation 4-8 (Genieva, Turmanova et al. 2008):

$$\ln \frac{g(\alpha)}{T^2} = \ln \frac{AR}{qE} - \frac{E}{RT}$$

Equation 4-8

Equation 4-8 is known as modified Coats and Redfern equation and the kinetic parameters can be inferred using this equation. For this reason, $\ln \left(\frac{g(\alpha)}{T^2}\right)$ should be plotted vs. 1/T for different formulations (Figure 4-9 for different formulations). g(α) is chosen from Table 4-6 after determining the reaction order from Table 4-7.
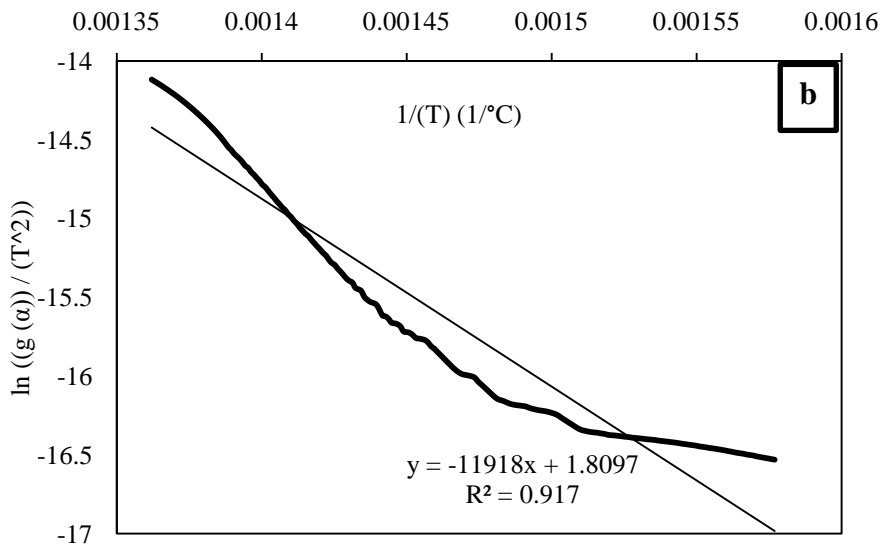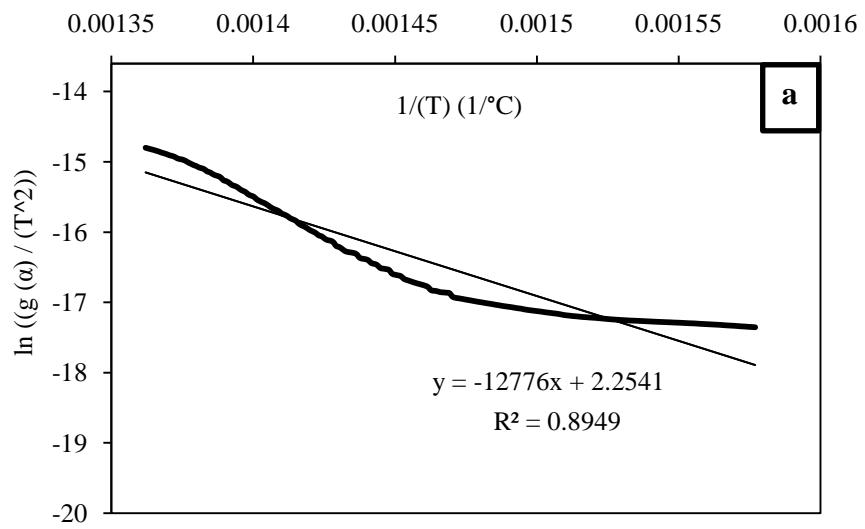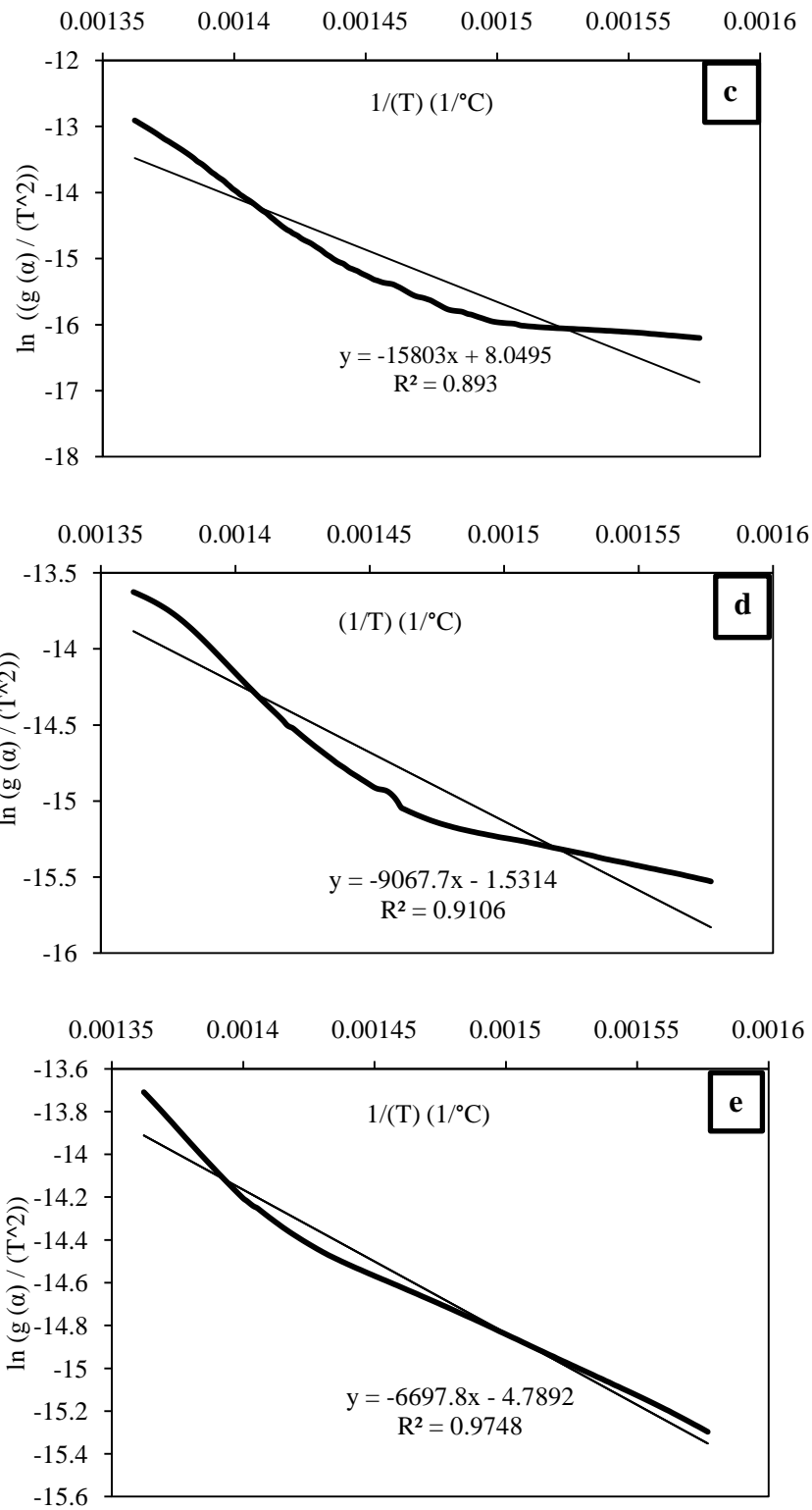
Figure 4-9: Plots of ln $(g(\alpha)/T^2)$ vs.(1/T) for different formulations a) run 1, b) run 2, c) run 3, d) run 4, e) run 5

The slope of the curves is -E/R. The term E can be used for comparison between runs which shows the tendency toward degradation during processing. The degradation kinetic parameters for different runs are summarized in Table 4-8. From Table 4-8 it can be seen that run 5 has the lowest energy barrier (E) for degradation as opposed to the case for T_{max}. This might be due to the simultaneous degradation of the low boiling point plasticizer and wheat straw. Hence, it is possible that the high evaporation rate of plasticizer is responsible for the low activation energy of run 5. A similar trend is observed for run 4 which has 3 wt-% plasticizer proving the mentioned statement.

In order to distinguish between the weight loss due to WS degradation and weight loss due to plasticizer evaporation, it is proposed to perform a TGA on Nylon-6 with 4 wt-% of plasticizer (without any WS). In this way, the extend of degradation due to plasticizer evaporation is obtained which consequently can be subtracted from the total composite weight loss to evaluate the degradation mainly from WS. From Table 4-8 it can be concluded that energy barrier (E) for degradation and amount of weight loss at T_{max} are positively correlated (Figure 4-10). This inference is reasonable since low energy barrier corresponds to more degradation and larger percentage of weight loss.

Table 4-8: Comparison between different runs activation energy and order of reaction

Run #	Run ID	n	E(J/mol)
1	15WS-4s-0p	0.9	106219.7
2	15WS-3s-1p	0.8	99086.3
3	15WS-2s-2p	1.3	131386.1
4	15WS-1s-3p	0.6	75388.9
5	15WS-0s-4p	0.5	55685.5
6	15WS-0s-0p	0.6	97356.9
7	Pure Nylon-6	0.8	201261.2
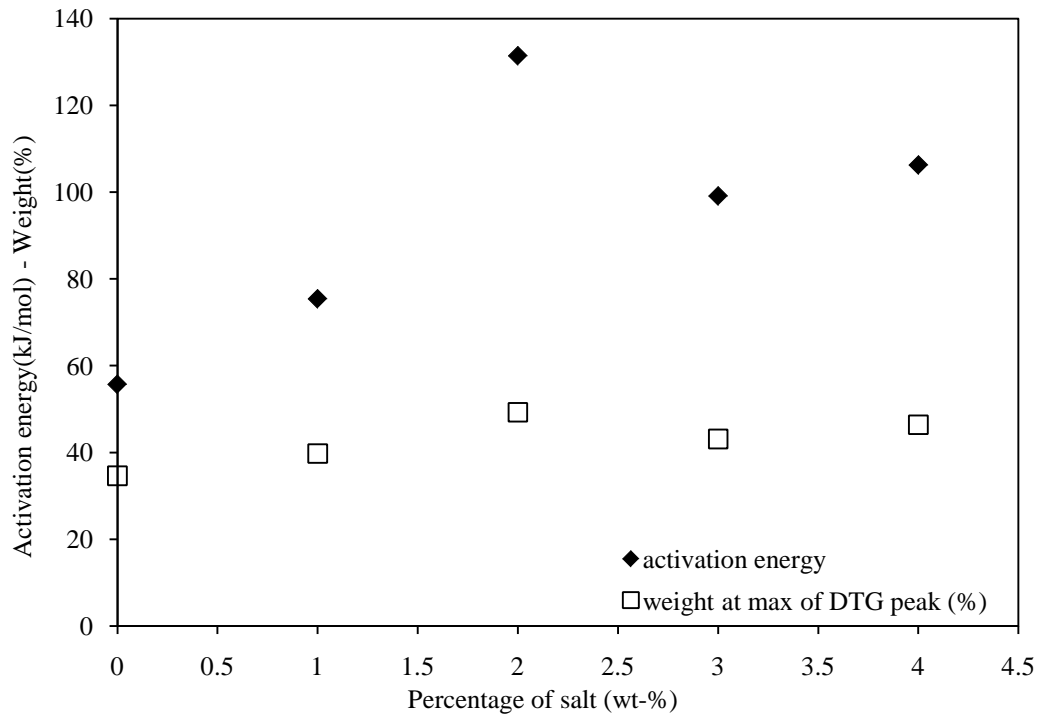
Figure 4-10: Agreement between energy barrier for degradation and percentage of weight loss

4.4 MECHANICAL PROPERTIES

Different methods were applied to measuring the mechanical properties of the composite samples. The data were used to distinguish the effect of the formulation on the mechanical properties of the composites. It should be noted in advance that the injection moulding process used here is not completely suitable for processing the composite, since this is a laboratory scale instrument and has very limited control on pressure and rate of filling the moulds. The specimen removal from the mould was done manually. This introduced variations in controlling the residence time during moulding. Therefore, inconsistency within each run of formulation was suspected. Also, color change in similar runs from sample to sample was observed. Therefore, in all mechanical property analysis, statistical significant tests were utilized to identify the possible significant error within formulation runs.

The other reason for performing statistical tests is that the difference between runs (treatments) might not seem pronounced in all tests, but statistical test shows that there is 95% confidence in the intervals that the difference between runs is significant (there is 5 % probability that there is no significant difference between the runs). The ANOVA table is presented for all of the mechanical tests.

4.4.1 IZOD IMPACT TEST

High impact resistance is an inherent characteristic expected from Nylon-6. For this reason, addition of different fibers and filler in Nylon-6 is not used to enhance the impact properties. In order to find the impact resistant associated with addition of WS, salt, and plasticizer, the Izod impact tests were conducted on injection moulded bars. It is known that is affected by microstructure of the composites like particle length distribution and its orientation with respect to applied load.

Addition of wheat straw without any additional treatments was found to decrease the impact properties. Decrease in impact resistance after addition of filler was also reported by Xu 2008 for Nylon-6/cellulose fiber composites and by Panthapulakkal et al. for propylene wheat straw composites (Xu 2008, Panthapulakkal, Sain 2006). Wu et al. also reported that addition of glass fiber decreased impact resistance in compare to pure Nylon-6. Wu et al. attributed this decrease in mechanical properties to stress concentration, voids and flaws which were formed at the end of the fibers or particles that contribute to crack initiation energy and facilitate crack propagation (Wu, Wang et al. 2001).

Figure 4-11 summarizes the impact properties of different formulated runs obtained from IZOD impact test.

Addition of any level of salt and plasticizer decreased the impact energy compared to run 6. Nylon-6 toughness is known to be due to crystalline structure and smooth crack growth (Wu, Wang et al. 2001, Lewis 2001, WRIGHT 2001). Both additives used here, salt and plasticizer, decreased the percentage of crystalline structure. In fact, addition of salt made Nylon-6 to behave like a brittle polymer. This behaviour is a result of decrease in the size

of plastic zone and the shear banding mechanisms which are responsible for energy dissipation. Consequently, the stress dissipation mechanisms are confined due to formation of rigid ionic bonding between polymer chains instead of hydrogen bonding between the polymer chains. As the energy cannot be dissipated in plastic (visco-elastic) deformation, it will be consumed during crack propagation via unstable crack growth mechanisms (Clemons 2000). On the other hand, the addition of plasticizer increases the polymer ability to undergo plastic (visco-elastic) deformation but it decreased the interfacial interaction between filler and matrix drastically. This can be the explanation why 4 wt-% plasticizer (run 5) not only acted as internal lubricant between Nylon-6 chains but also decreased the interfacial bonding and lead to deboning.
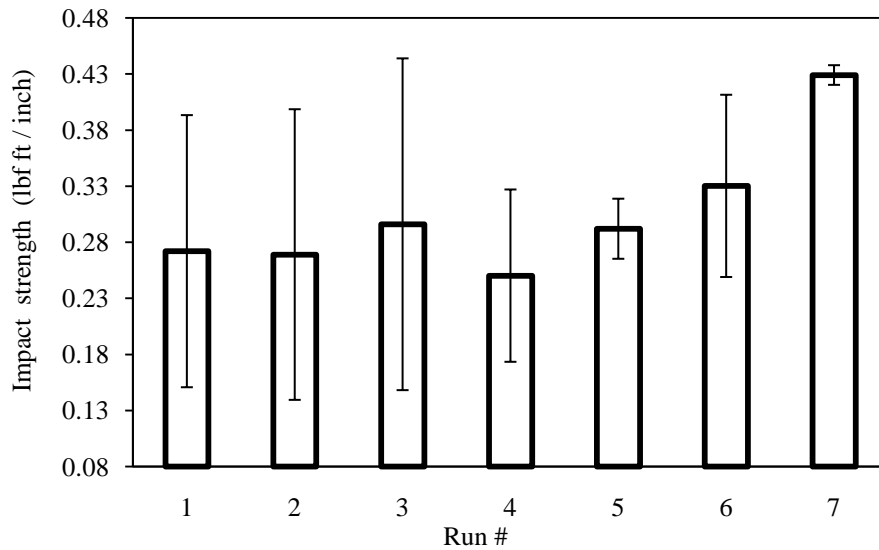
Figure 4-11: Impact resistance energy of different runs

Table 4-9: ANOVA table which proves that there is significant difference between impact strength of runs

Source	df	SS	MS	F $_{observed}$	F $_{crit.}$ 6,38,0.1
Between treatment	6	0.1253	0.0209	0.20	1.94
Within treatments	38	3.9807	0.1048		There is sig. difference between runs
Total	44	4.1060	0.0933		

Sig: significant

4.4.2 TENSILE TEST

Figure 4-12, Figure 4-13 and Figure 4-14 show the effect of different levels of salt and plasticizer on tensile strength, modulus and elongation of Nylon-6 with wheat straw (15 wt-%) compared to pure Nylon-6.

All runs have lower strength than pure Nylon-6. It is known that the composite strength depends largely on filler and matrix bonding (Clemons, Sanadi 2007). Thus, the low tensile strength of the composites might be because of the relatively weak bonding between filler and matrix. Despite the polar nature of Nylon-6, the interaction between wheat straw

69

particles and Nylon-6 was not good enough to enhance the strength of Nylon-6. This is believed to be consequence of the salt which may have promoted fiber degradation or the presence of plasticizer which may have contributed to deboning at the interface and consequently fibers pull out.

In runs 3 and 4, the low levels of salt decreased the melting point and the plasticizer decreased thermal degradation. Consequently, these runs had better tensile strength compared to the other runs except pure Nylon-6. These observations are in contrast with results reported by Xu in which the addition of fiber without any additives enhanced the strength of pure Nylon-6 (Xu 2008)(Xu 2008). On the other hand, Hristov et al. similarly observed the decrease in strength of Polypropylene/unmodified wood fiber composites (Hristov, Vasileva et al. 2004). They attributed lower yield strength of the composites to inadequate stress transfer from matrix to fiber through the weak interfacial boning. The lower tensile strength in Nylon-6/Wheat straw composites prepared here might also be due to the lower reinforcing capability of wheat straw acting mainly as filler rather than reinforcing fibers.

From results in Figure 4-13, it can also be inferred that addition of salt increased the tensile modulus significantly. This behaviour has also been reported by Acierno et al, the authors attributed this increase in modulus to higher orientation of polymer chains which leads to higher modulus and brittle behaviour of matrix (Acierno, La Mantia et al. 1979). After analysing modulus data in Figure 4-13, it can be observed that all runs had higher modulus than pure Nylon-6. Further, it was found that addition of salt and plasticizer increased the modulus. That means all treatments were effective.

The enhancement in modulus of the polymer with addition of salt is believed to be because of the formation of pseudo-cross-linking structure formed upon addition of salt. Higher modulus also was obtained when plasticizer was added and this is attributed to a lower extent of degradation during processing.

From result in Figure 4-14 it can be inferred that runs 3 and 4 not only had the highest strength among composites, but also they have the highest deformation prior to break. This indicated higher tendency for plastic (visco-elastic) deformation and energy dissipation.

Santos et al. also observed lower elongation at break of composite of Curaua fibers and Nylon-6 compared to neat polymer and attributed this to the physical interlocking of polymer chains, thus immobilizing the fiber, and to the orientation of matrix as a result of additional shear imposed by fibers (Santos, Spinace et al. 2007).

From the presented results, it can be inferred that the increase in one property often caused a decrease in other properties. For example, increase in modulus results in a decrease in elongation. Clemons mentioned that addition of fibers to plastic matrices usually increase the modulus but decreases the toughness. An increase in toughness usually causes a decrease in stiffness (Clemons 2000).
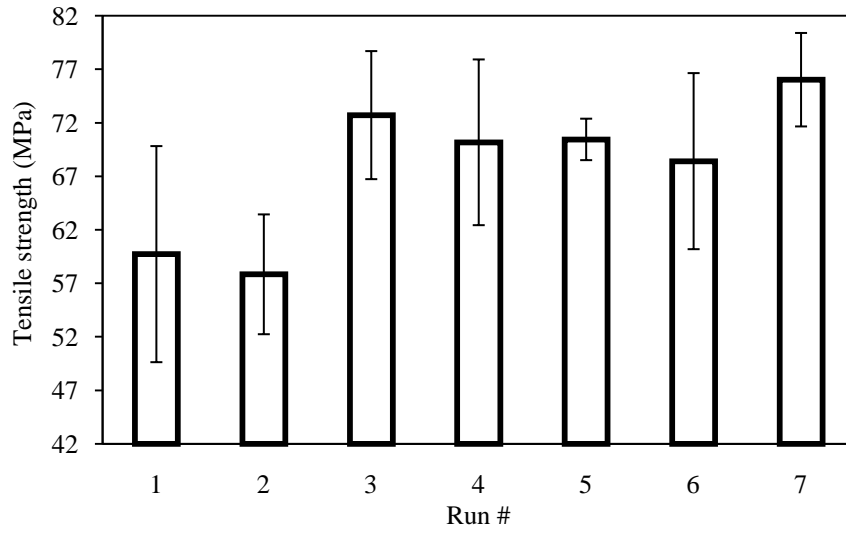
Figure 4-12: Maximum tensile strength of different runs
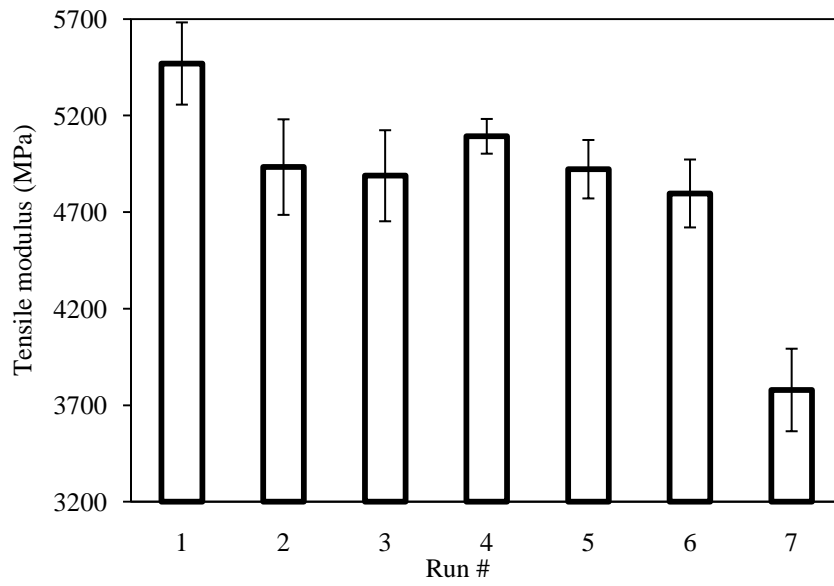
Figure 4-13: Tensile modulus of different runs
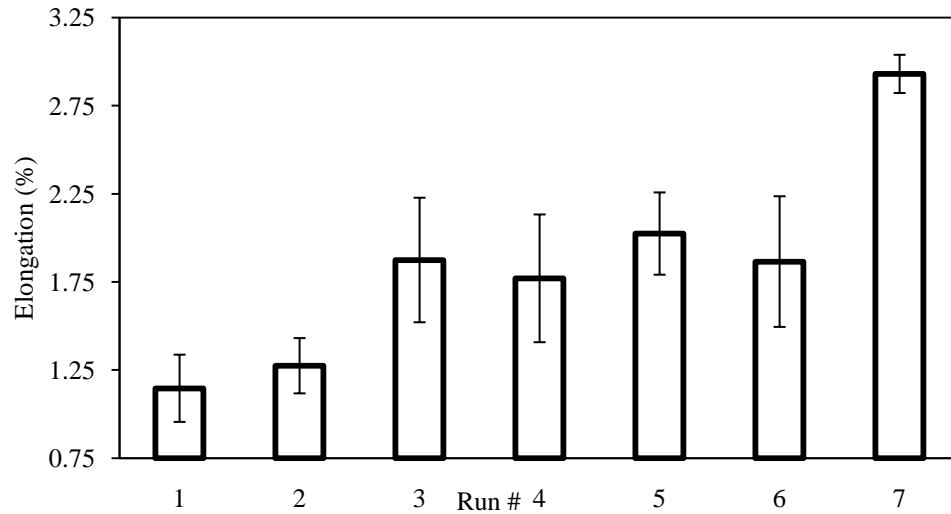
Figure 4-14: Elongation at break of different runs

ANOVA table confirms that there is significant difference between tensile properties of different runs (Table 4-10 and Table 4-11).

Table 4-10: ANOVA table which proves that there is significant difference between strength of runs

Source	df	SS	MS	$F_{observed}$	F_{crit}5,24,0.05
Between treatment	5	1482.62	296.52	4.80	2.62
Within Treatment	24	1481.67	61.74		There is sig. difference between runs
Total	29	2964.29	102.22		

Table 4-11: ANOVA table which proves that there is significant difference between modulus of the runs

Source	df	SS	MS	$F_{observed}$	F_{crit}5,24,0.05
Between treatment	5	1474475.52	294895.10	9.59	2.62
Within treatment	24	738276.86	30761.54		There is sig. difference between runs
Total	29	2212752.38	76301.81		

73

The stress-strain curves corresponding to run 7, run 6, run 1, and run 5 are shown in Figure 4-15, Figure 4-16, Figure 4-17, and Figure 4-18. It can be inferred from the comparison between Figure 4-15 with Figure 4-16 that addition of wheat straw changed mechanism of deformation of Nylon-6 from ductile (and tough) to brittle. The low elongation at break of all runs in comparison to pure Nylon-6 is another evidence of changing the mechanisms of deformation. The reduction in the amount of elongation at break of run 6 compared to pure Nylon-6 can also be attributed to the addition of fillers, which have significantly higher modulus and less ductility compared to matrix.

Therefore, it can be concluded that the addition of salt makes pseudo crosslinked structure, thus contributes to increase the modulus. However, this molecular structure formed by addition of salt also prohibits molecular motions which are responsible for high elongation at break, so a brittle material is be formed (Figure 4-17).
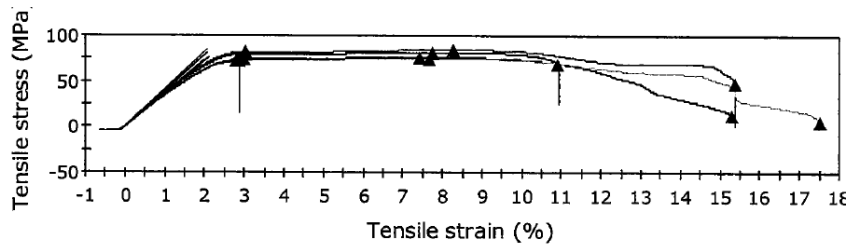
Figure 4-15: Tensile stress-strain curve for pure Nylon-6 (5 specimen measured)
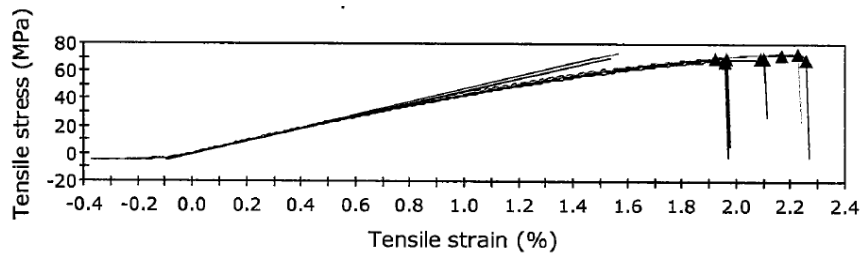
Figure 4-16 : Tensile stress-strain curve for tensile test of run 6(5 specimen measured)
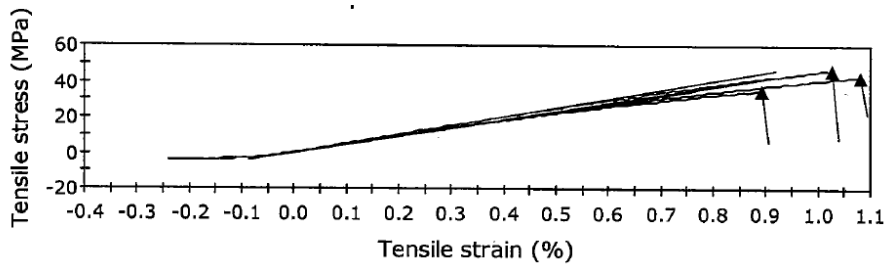
Figure 4-17: Tensile stress-strain curve for tensile test of run 1(5 specimen measured)
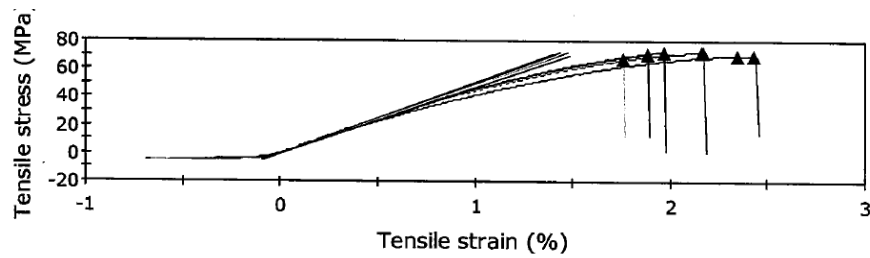
Figure 4-18: Tensile stress-strain curve for tensile test of run 5(5 specimen measured)

4.4.3 FLEXURAL TEST RESULTS

The flexural properties are important parameters for a range of applications in the automotive field. Flexural analyses on different formulation were found to be significantly different from each other. (Table 4-12 and Table 4-13).

Table 4-12: ANOVA table which proves that there is significant difference between flexural modulus of runs

Source	df	SS	MS	$F_{observed}$	$F_{crit.}$5,14.0.05
Between treatments	5	4748.12	949.62	5.79	2.96
Within treatments	14	2294.63	163.90		
Total	19	7042.75	370.67		There is a sig. difference

Table 4-13: ANOVA table which proves that there is significant difference between flexural strength of runs

Source	df	SS	MS	$F_{observed}$	$F_{crit.}$5,14.0.05
Between treatments	5	123179	246359	3.02	2.96
Within treatments	14	114027	81447.6		
Total	19	237206	124845		There is a sig. difference

The effect of addition of salt and plasticizer on flexural properties was investigated and the results are shown in Figure 4-19 and Figure 4-20. It can be seen that addition of salt increased the flexural modulus significantly; this is attributed to formation of ionic coordination between salt and chains of Nylon-6. However, addition of 4 wt-% plasticizer decreased the flexural modulus; this is attributed to a change in free volume. Plasticizer contributed to increasing the free volume and mobility of chains. The flexural modulus and strength were both in agreement with tensile modulus and tensile strength results.

Interestingly, the highest flexural strength was measured in run 3, which also had the highest activation energy for thermal degradation (Figure 4-10).
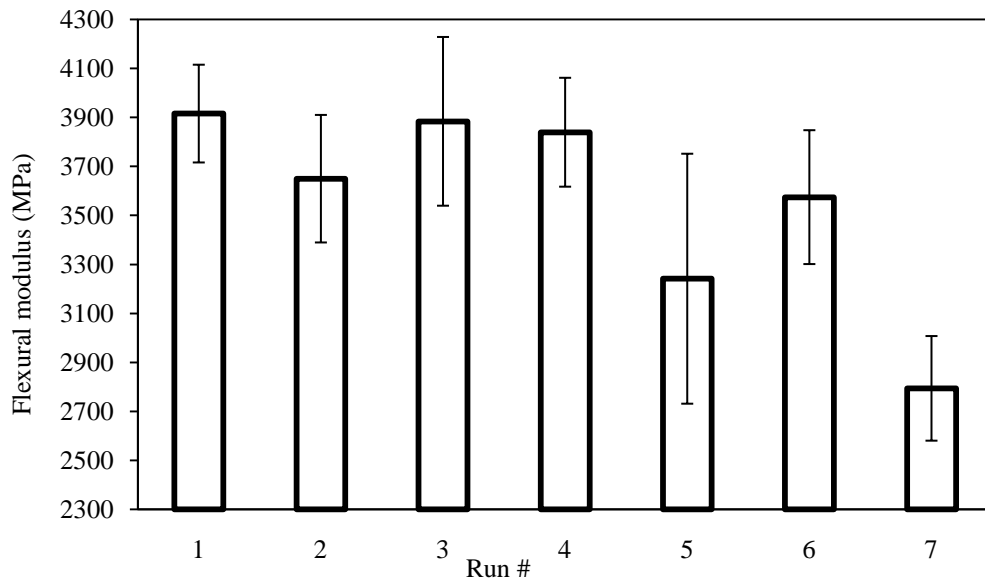
Figure 4-19: Flexural modulus of different runs
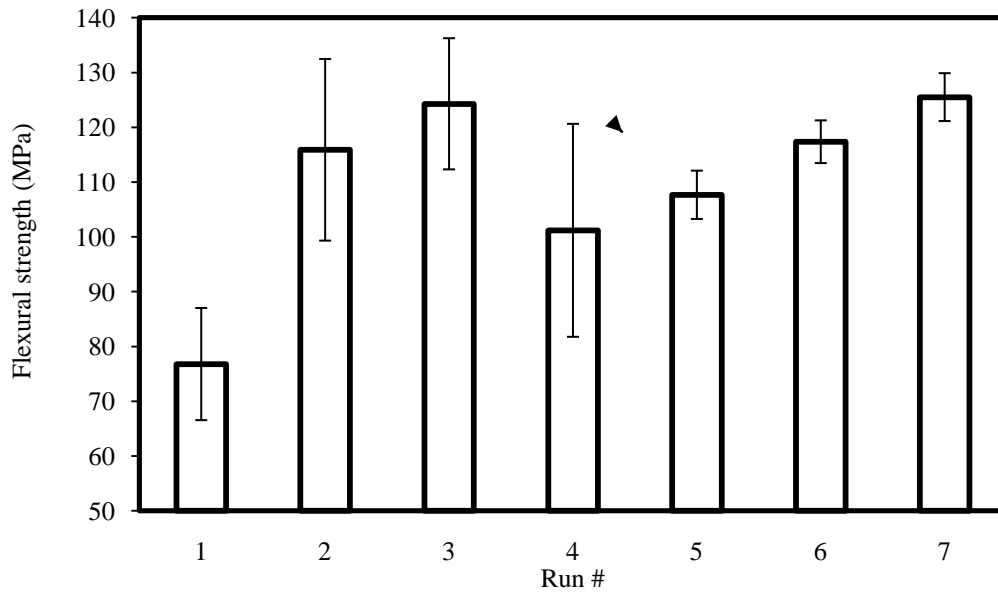
Figure 4-20: Flexural strength of different runs

4.5 MORPHOLOGY

The morphology of the composites was investigated with field emission scanning electron microscopy (FESEM) was used. The images are used to compare interfacial bonding between wheat straw and Nylon-6 in different runs and in the presence of different levels of salt and plasticizer. The surface of the composites were analysed after cold fracture. The images were taken in high and low magnification. In low magnification, the overall dispersion, wetting and spots indicating deboning can be seen. In high magnification, observations were made on the interface of filler and matrix to provide information about crack growths on the interface and the mechanism of load transfer between filler and matrix.

Figure 4-21 shows the cross section (obtained by cold fracture) of run 1 composites. It can be seen that there is good wetting and bonding between Nylon-6 and wheat straw. It can also be speculated that salt increased the surface energy and polarity of Nylon-6 and improved the interfacial bonding. The hole in the same figure at low magnification represents no fiber pull out (the residue of the wheat straw particle was inside the matrix). These aforementioned properties are features of a brittle fractured surface.
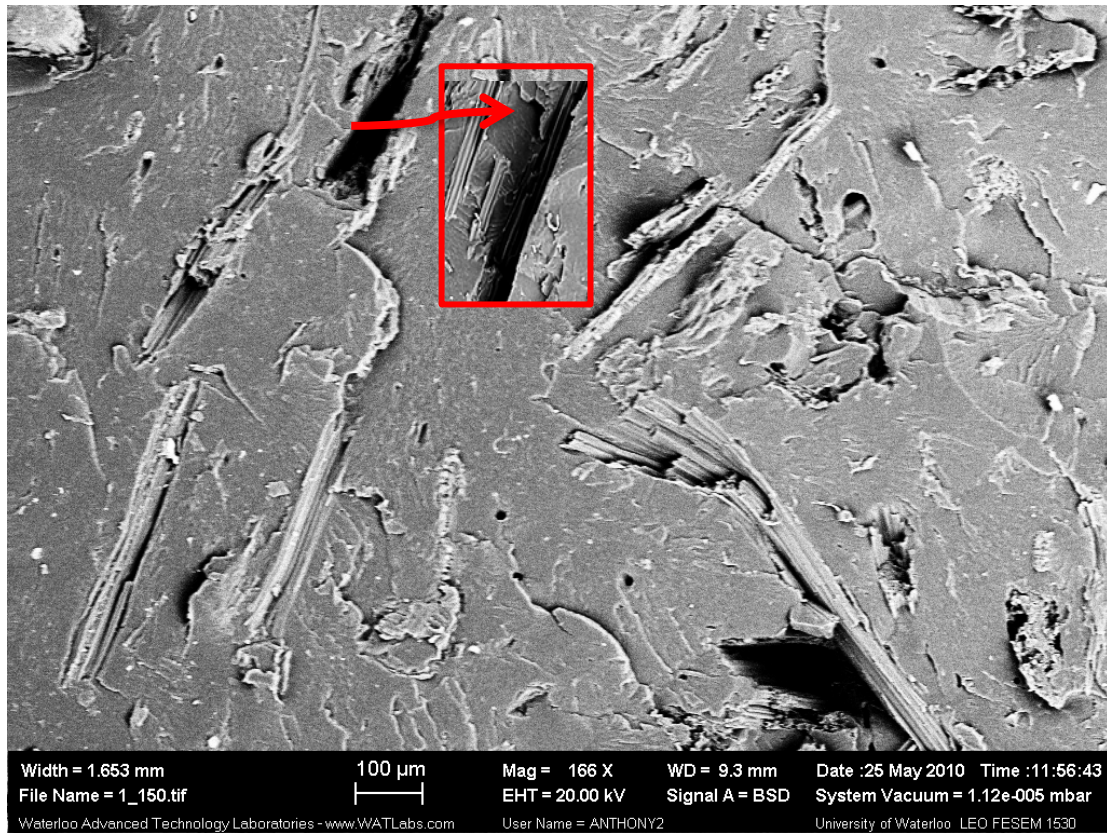
Figure 4-21: Surface of Nylon-6/ 4 wt-% salt/15 wt-% WS composites (run 1). The hole on the surface is zoomed and shown by red arrow and frame.

Figure 4-22 shows the crack propagation initiated in the matrix and propagated through the fiber causing filler breakage. The perfect bonding limited the energy dissipation mechanism and promoted a brittle failure. This can show why a relatively low impact resistance was obtained for this run (run 1).
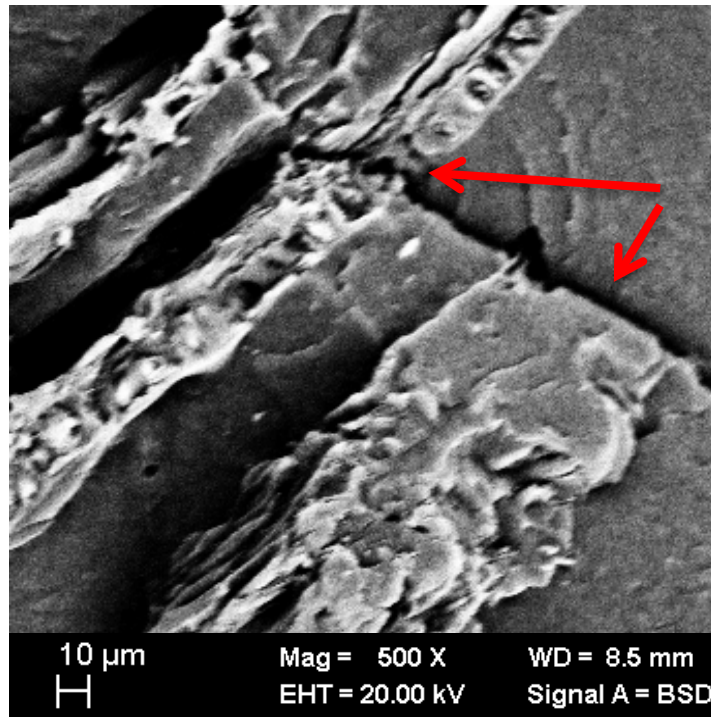
Figure 4-22: Evidence for good interfacial bonding in Nylon-6/ 4 wt- % salt/15 wt- % WS composites (run 1)

Figure 4-23 shows cross section of the specimen bars which were made according to run 5. The weak interface between fiber and the matrix can be observed in the figure. Propagation of the cracks mainly around the interface is both an indication of weak interfacial bonding and the presence of plastic (visco-elastic) deformation mechanisms for better energy dissipation than run 1.
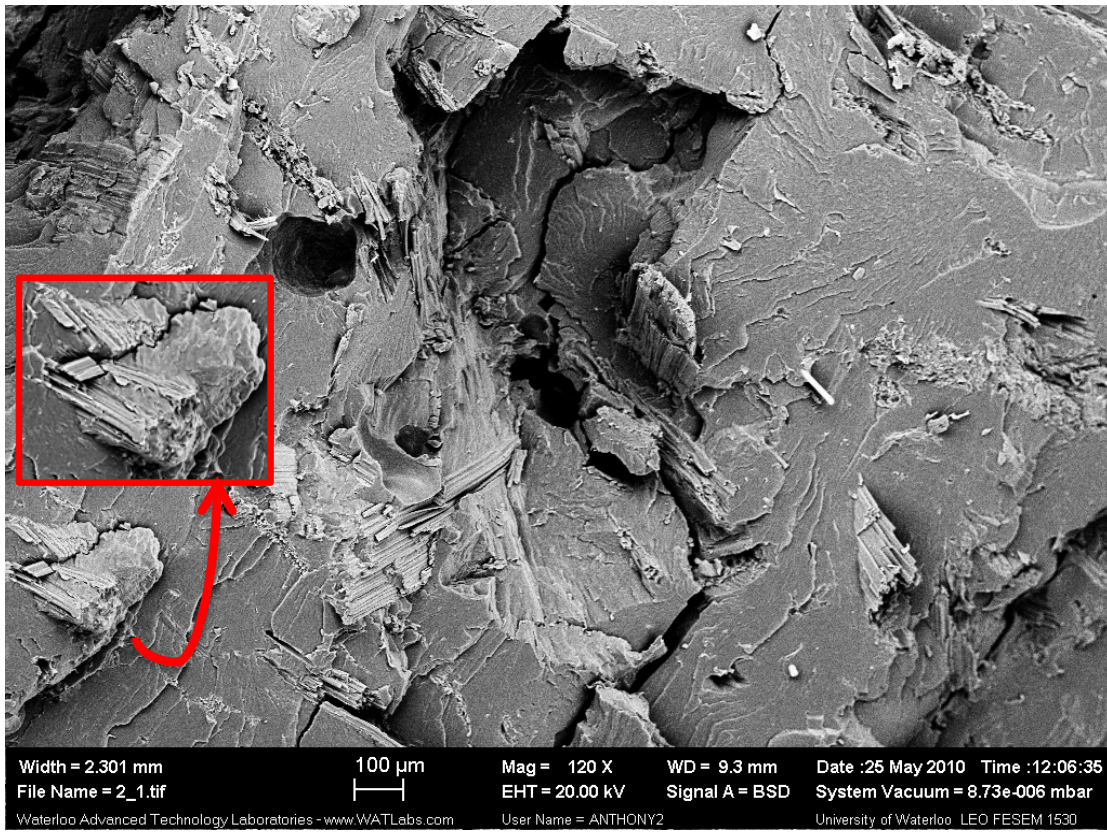
Figure 4-23: Surface of Nylon-6/4 wt-% plasticizer/15 wt-% WS composites (run 5). The interface between wheat straw particle is zoomed and shown by an arrow and red frame

Figure 4-24 represents the cross section of the specimens made from run 3. Good wetting of the filler by the matrix can be observed in this figure. It should be noted that the tensile strength, elongation, and impact properties of this run was found to be the highest among all runs. This indicated that the interfacial bonding was strong enough to transfer the energy from the matrix to the filler and at the same time the interface was flexible enough to allow for energy dissipation.
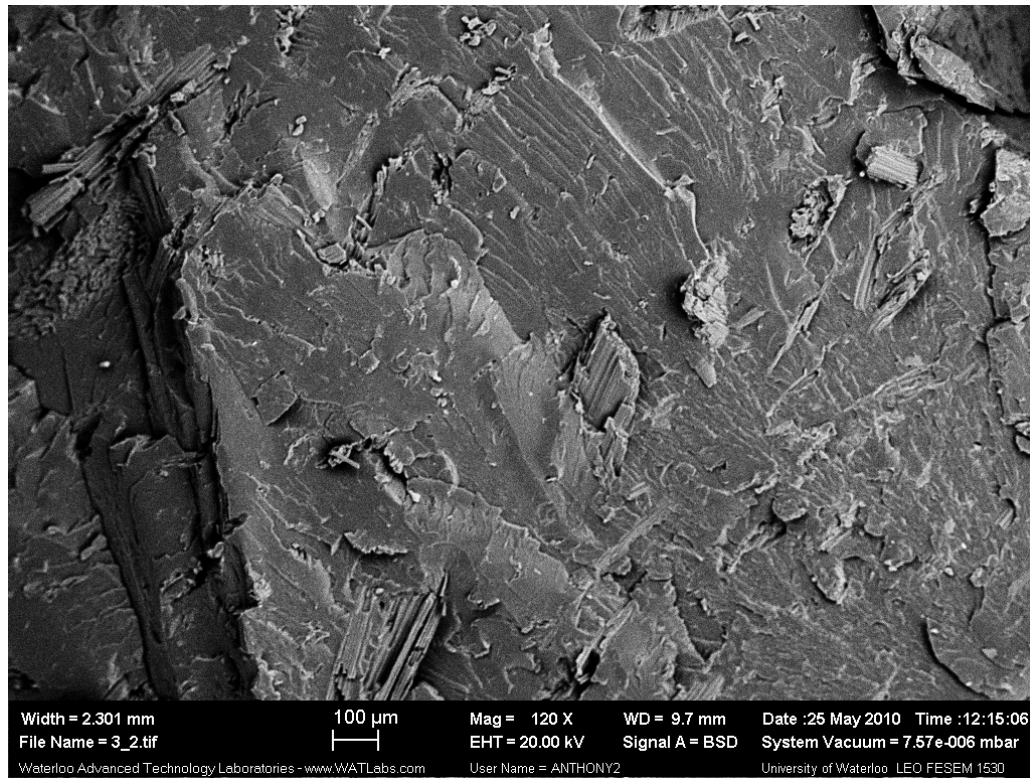
Figure 4-24: Surface of Nylon-6/ 2 wt-% salt-2 wt-% plasticizer/15 wt-% WS composites (run 3)

Figure 4-25 and Figure 4-26 represent the interfacial bonding of run 6 specimens. From Figure 4-26, the crack pinning mechanisms are clearly observed. Crack is initiated in the matrix, propagated around the interface of the filler, and then bow out to the next filler. This energy dissipation mechanism is believed to be the reason for high impact properties.
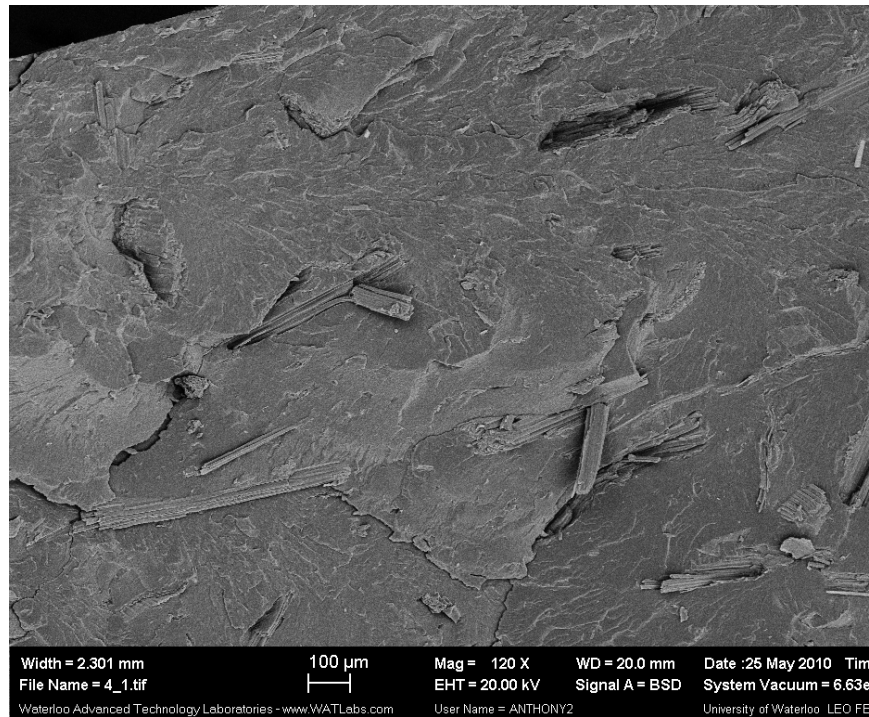
Figure 4-25: Cross section of Nylon-6/15 wt-% WS composite

From Figure 4-26, toughening mechanisms in polymer composites (crack pinning and crack bow out) can be evidenced. It can also be seen that deboning changes crack propagation direction, leads to the crack growth on the interface of fiber and matrix and stops the crack propagation.

The interaction on the interface between Nylon-6 and wheat straw should be studied in more detail to find if there is a need for coupling agent or if the interaction between fiber and matrix is high enough.
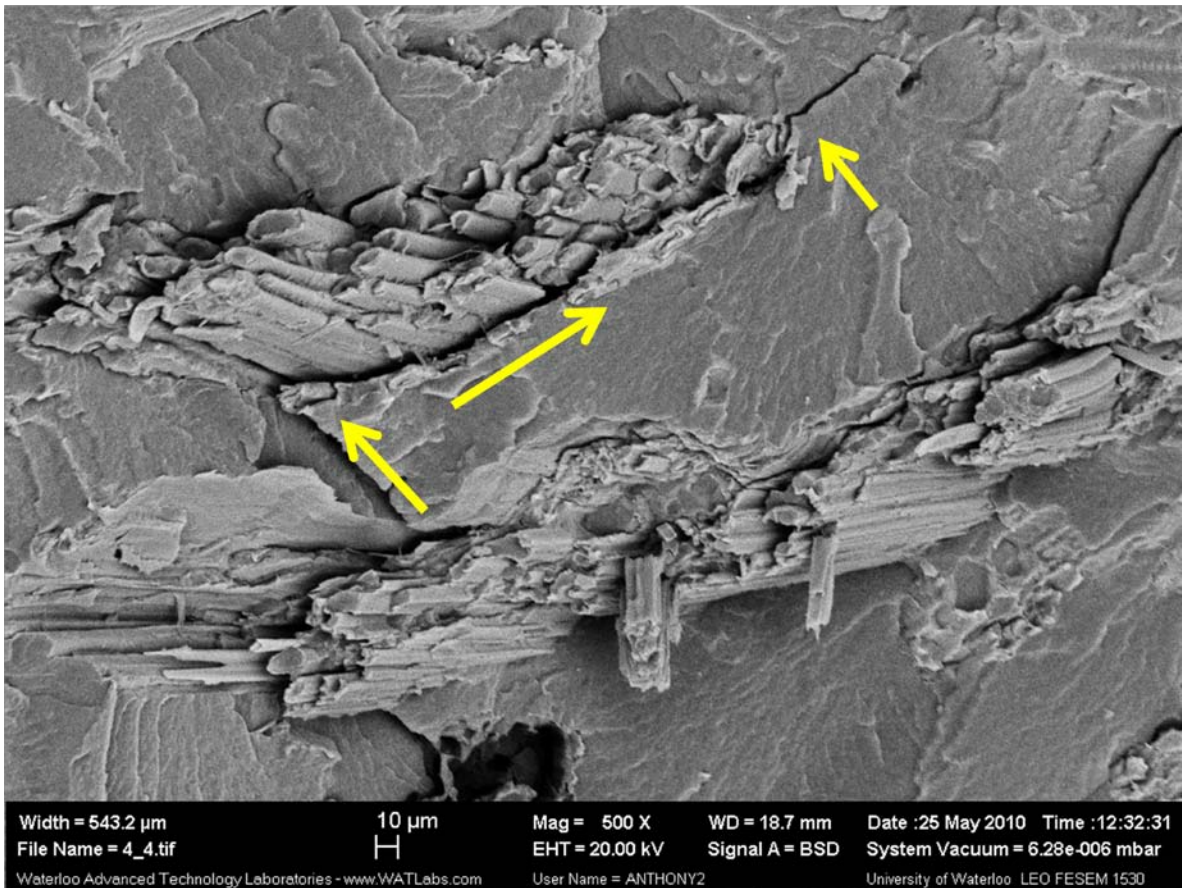
Figure 4-26 : High magnification pictures taken from interfacial bonding between Nylon-6/ 15 wt-% WS composites (run 6)

It can stated that in order to better understanding the role of interfacial bonding on the mechanical properties, additional investigation on the interfacial bonding between the filler and matrix should be performed. In general, there should exist a balance between the energy transfer mechanisms and the energy dissipation mechanisms from the matrix to the filler. Both mechanisms are affected by interfacial properties. Knowledge in this matter will justify if addition of other additives such as coupling agent or lubricant are necessary to enhance the properties.

4.6 CRYSTALLIZATION KINETICS

The most important phase transition for processing semicrystalline polymers is crystallization. The crystallization kinetics of neat Nylon-6 and the effect of additives and filler on crystallization behaviour are studied by using the Avrami equation. Crystallization kinetics can be analysed by both isothermal and non-isothermal methods (Patel, Spruiell 1991, Di Lorenzo, Silvestre 1999, Li, Zhang et al. 2003).

Crystal morphology, orientation, percentage and distribution are parameters that affect mechanical properties (Zhang, Zhou et al. 2008). Further, the crystal solidification rate and the crystal formation rate can affect crystal morphology and the size of crystallites (Schultz 2001). Moreover, the crystallization rate is dictated by the cooling rate and the packing pressure during processing steps. In this study, the rate of polymer crystallization and nucleation were found using isothermal methods. Samples of pure Nylon-6, Nylon-6/4 wt-% plasticizer, Nylon-6/4 wt-% salt, Nylon-6/2 wt-% salt and 2 wt-% plasticizer, and Nylon-6/15 wt-% WS were chosen for this analysis to observe the effect of additives on crystallization kinetics.

4.6.1 ISOTHERMAL ANALYSIS

To analyse crystallization rate, samples were heated to 240 °C, held isothermal for 10 min to ensure that the thermal history of the specimens were removed. Samples were then cooled to the onset temperature of crystallization at a rate of 50 °C per min. The samples were kept in the isothermal condition for 20 min for crystallization. Then they were heated to 230 °C at a rate of 10 °C per min again to obtain the melting peak of crystals from the isothermal conditions.

The areas under the melting peaks varied due to a) different isothermal temperature (cooling) and b) formulation. For pure Nylon-6, the crystallization peak started at 192 °C (onset of crystallization). This temperature was found from previous DSC analysis with the non-isothermal and ramp method. For the isothermal studies on Nylon-6, isothermal temperatures of 192 °C 190 °C, 188 °C, 186 °C, 184 °C and 178 °C were chosen. Similar

isothermal temperatures were chosen for samples with 4 wt-% plasticizer and samples with 15 wt-% wheat straw. This was done because the addition of plasticizer or wheat straw did not change the crystallization temperature and the location of the melting and crystallization peak (Table 4-1).

For samples with 2 wt-% salt and 2 wt-% plasticizer, the onset crystallization temperature shifted to 176 °C, hence, 174 °C, 172 °C, 170 °C, and 168 °C were selected for isothermal temperatures (Table 4-1).

No crystallization peak was observed in the DSC thermogram of sample with 4 wt-% salt as shown in Figure 4-4. Therefore, the baseline fluctuation (step-like pattern) observed at 140 °C was chosen for isothermal temperature followed by 138 °C, 136 °C, 134 °C, 132 °C and 121 °C.

It should be noted that nucleation mechanisms are due to the attraction between nucleating molecules and neighbours to decrease the surface energy of the crystal nucleus. Polymer chains need to go through conformation changes to reach a stable structure with a minimum level of energy. It can be concluded that cooling conditions have significant effects on crystal formations. In lower isothermal temperatures, the driving force for attraction of chains to the nucleus is rather high. However, high melt viscosity confines conformation adjustments and introduces imperfections to crystal structure.

The Avrami equation (Equation 4-9) was used to model isothermal crystallization of samples:

$$1 - X(t) = \exp(-kt^n) \qquad \text{Equation 4-9}$$

Where n is the Avrami exponent and K is the crystallization rate constant. Applying double logarithmic operations on this equations result in a linear equation:

$$\log(-\ln(1 - X(t))) = \log K + n \log t \qquad \text{Equation 4-10}$$

Crystallization might consist of three stages: 1) nucleation that appears as a delay in the signal (the period which X(t) or heat flow VS. t curves is flat before curves suddenly increase) (Albano, Papa et al. 2003);

2) primary growth of crystallites; and

3) secondary crystallization that is indicated as a change in the slope of the log(-ln(1-X(t)) vs. t curves.

Avrami plots showed good linearity during the first stage; n and K can be obtained by plotting $\log(-\ln(1 - X(t)))$ VS. $\log t$. It might be the case that each curve consist of two linear sections with different slopes as mentioned above. This behaviour is called secondary crystallization. According to Rybnikar et al., this stage occurs at the end of a primary isothermal condition when spherulites are already made and the amorphous region between lamellae is rearranged inside the crystalline structure (Rybnika 1960). As a result of this behaviour, a sudden increase in the curves as an indication of increase in density occurs.

The amount for "n" in the Avrami equation can be attributed to nucleation mechanisms and dimension of growth. For example the amount of n between 2 to 4 is expected for crystallization from a molten state. The Avrami exponent is defined as $n = \gamma + \lambda$ where γ is 0 for constant nucleation rate and 1 for nucleation with irregular intervals. The parameter λ corresponds to the growth stage, and for rod-like crystals and linear growth of the crystals, it is equal to 1; for two dimensional and disc growth, it is equal to 2; and for three dimensional and spherical growth of the crystals, it is equal to three (Albano, Papa et al. 2003).

In Equation 4-10, when X=0.5 and t=$t_{1/2}$, Equation 4-11 will result (Zhang, Zhou et al. 2008):

$$t_{1/2} = (\ln 2 / K)^{1/n}$$

Equation 4-11

It is expected that $t_{1/2}$ increases with an increase in the temperature due to lower nucleation rates in higher temperatures, which delay crystal formation at the beginning of the isothermal condition.

$\tau_{1/2}$ is an indication of the rate of crystallization, and it is defined by Equation 4-12:

$$\tau_{1/2} = (t_{1/2})^{-1}$$

<div align="right">Equation 4-12</div>

The other parameter that gives the notion for the rate of crystallization is t_{max}, which corresponds to the time required to reach the maximum rate of crystallization, and it is equal to the time when the graph of heat fusion versus time slope changes (moving to slower kinetics). This point will be acquired by solving the equation of $\dfrac{dH(t)}{dt} = 0$, where H(t) is the heat flow rate. Using the Avrami equation, t_{max} can be extracted as a function of n and K (Equation 4-13):

$$t_{max} = (\frac{n-1}{nk})^{1/n}$$

<div align="right">Equation 4-13</div>

It is also worth noting that Avrami parameter K depends on the temperature at which isothermal conditioning of the sample was conducted. The Arrhenius equation (Equation 4-14) is used to describe this dependency:

$$K^{1/n} = K_0 \exp(-\Delta E / RT_c)$$
$$(1/n)\ln K = \ln K_0 - (\Delta E / RT_c)$$

<div align="right">Equation 4-14</div>

In the Equation 4-14, K_0 is the temperature independent pre-exponential factor; R is the gas constant, and ΔE is the activation energy, which is needed for crystallization (Cebe, Hong 1986). By Plotting $(1/n)\ln K$ versus $1/(RT_c)$, ΔE can be obtained from the slope of the resulted line. This free energy (ΔE) is consist of two terms ΔE^* and ΔF, which ΔE^* corresponds to activation energy needed for movement of the chains from amorphous

boundaries to the crystalline regions, and ΔF is the nucleation activation energy (Lin, Chen et al. 2009).

4.6.1.1 CRYSTALLIZATION KINETICS OF PURE NYLON-6, NYLON-6 BLENDS, AND THEIR COMPOSITES

Nylon-6 isothermal thermograms for different cooling temperatures are presented in Figure 4-27. It can be seen that there is no time lag during the first stages of crystallization time. This indicated that no induction time is needed for formation of the nuclei, the nucleation is almost instantaneous, and the nuclei are already present in the Nylon-6 prior to the isothermal temperature. This behaviour can be either due to the presence of impurities which act as nucleating agent during cooling (heterogeneous nucleation) or due to the differences between melting and isothermal temperature (supercooling) which causes formation of nuclei before reaching the isothermal temperature.

Moreover, from the graphs in Figure 4-27 and Figure 4-28, it is apparent that a decrease in the isothermal crystallization temperature resulted a shift towards lower temperatures are narrower graphs. This behaviour is due to the increase in crystallization rate in the lower temperatures (higher supercoolings) indicated by the increase in the slope of the curves in Figure 4-31. Narrow curves (Figure 4-27) and high rates of crystallization are indication of lower time for the chain arrangement (Table 4-14).
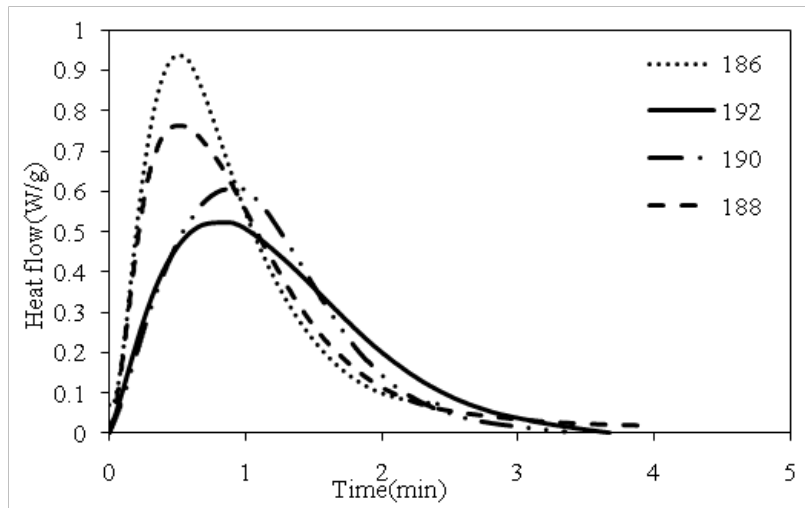
Figure 4-27: DSC thermogram of pure Nylon-6 in different cooling temperatures
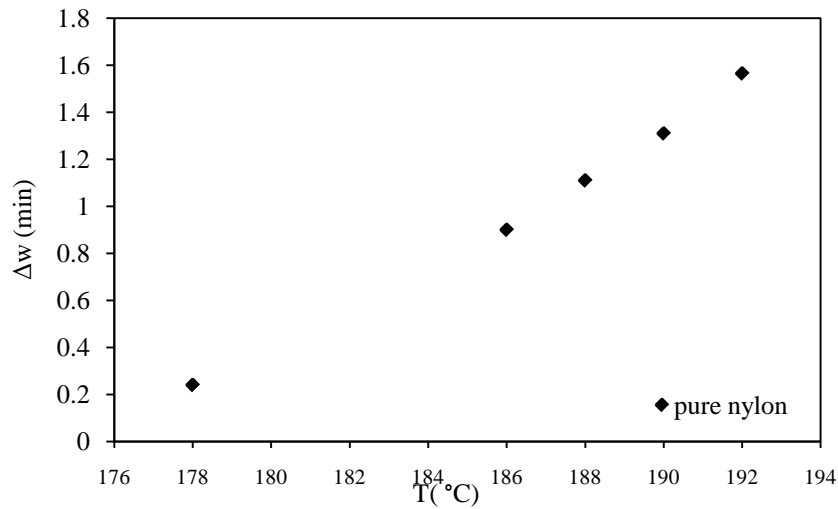
Figure 4-28: Width at half height of crystallization peak

Table 4-14: Crystallization duration time for different isothermal temperatures of Nylon-6

Isothermal temperature (°C)	Δt(min)
192	3.67
190	3.35
188	13.58
186	2.45
178	0.38

Two distinctive melting peaks (from 210$^{\mathrm{o}}$C to 225$^{\mathrm{o}}$C) were found during the heating stage of Nylon-6 as it was mentioned before in this document (section 6 4.2) and indicated in Figure 4-29 (Li, Zhang et al. 2003).

The first melting peak is observed as a shoulder in the lower temperatures which corresponds to the gamma crystalline structure. This peak shifted to lower temperatures in higher supercoolings. The cooling temperature did not affect the alpha crystalline structures (indicated by T$_2$) significantly as the temperature of the second peak did not change considerably (Table 4-15).

The area under the endothermic melting peak (ΔH_m) was higher for the crystals that were made at higher nucleation rates (lower temperatures). This can be due to the higher nucleation rate at lower temperatures. Higher number of nuclei represents more perfect crystallites (narrower peak), thus the heat for melting of these crystals is higher. This is in agreement with the observations that Albano et al. and Li et al. reported for the talc filled Polypropylene composites and Nylon-1012 (Li, Zhang et al. 2003, Albano, Papa et al. 2003).
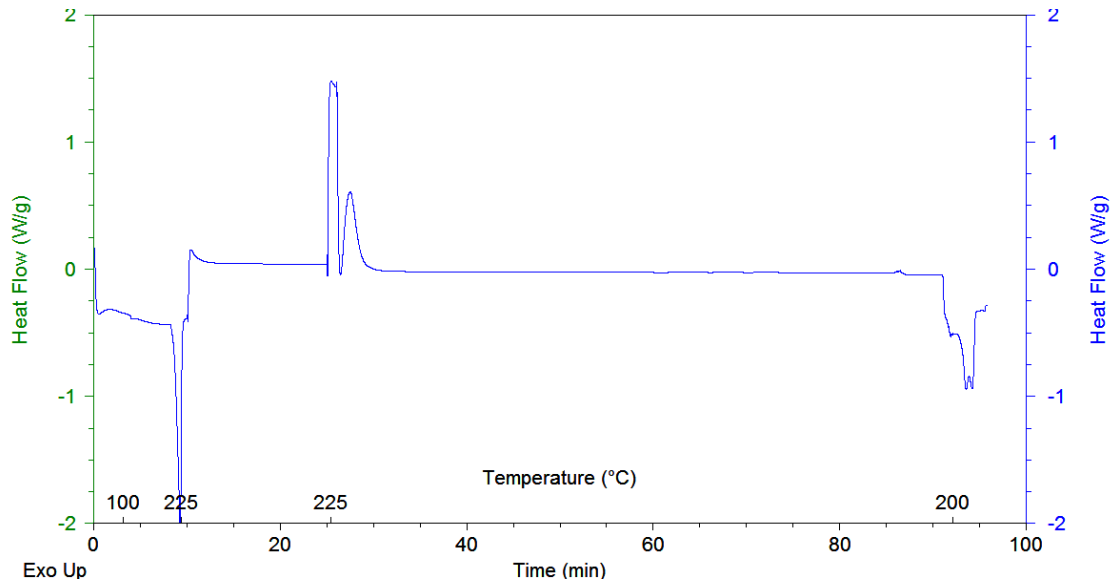
Figure 4-29: Presence of two peaks from 210 °C to 225 °C are due to melting of two type of crystals which were made isothermally

Table 4-15: Area under melting curves after isothermal cooling, first and second peak location for neat Nylon-6

Isothermal temperature (°C)	ΔH_m (W/g)	T_{m1} (°C)	T_{m2} (°C)
192	38.07	214.3	220
190	35.3	214	221
188	39.22	212.2	220
186	41.4	211.2	221
178	44.13	207	220.6

Figure 4-30 shows the Avrami plots at different isothermal temperatures. From the slope and intercept of the curves, n and K constant were obtained and the results are summarized in Table 4-16.

Parameter $t_{1/2\ theo}$ and $t_{max\ theo}$ were calculated using Equation 4-11 and Equation 4-13. $t_{max\ exp}$ and $t_{1/2exp}$ were found by extracting the time which corresponds to X=0.5 and the time at which the maximum heat of fusion occurs respectively.

The theoretical and the experimental amounts of t_{max} and $t_{1/2}$ were in agreement with each other in higher cooling temperatures compared to lower cooling temperatures. These values

can be used to identify the crystallization rate. It was further concluded that the mentioned values are inversely correlated with the slope of the X (t) vs. t curves. As the isothermal temperature decreases, the $t_{1/2}$ decreases as well.

Comparing the Avrami plots at different isothermal temperatures (Figure 4-29), it can be seen that the decrease in the cooling temperature from 192 °C to 186 °C caused a secondary crystallization (Figure 4-31). However, further increase in the supercooling temperature decreases secondary crystallization indicated by the change in the slope. Gradual increase in X (t) with time in 188 °C and change in slope of log (-ln (1-x)) versus log(t) graphs in 186 °C (Figure 4-31) are an indication of secondary crystallization (Albano, Papa et al. 2003).

The reduction in secondary crystallization at low temperatures was because of the crystallization kinetics favouring nucleation rather than growth. As the growth of the crystals are hindered, larger number of nuclei are made, and hence spherulites with smaller sizes are produced. A smaller spherulite results a lower secondary crystallization as was the case in this analysis.

For samples which were isothermally cooled at 188 °C, the Avrami indices were acquired from the first part of the curve (primary stage of crystallization, Figure 4-31), hence the equation of the line is not represented on the corresponding curve.

y = 1.8645x − 0.241
R² = 0.9983

y = 2.0278x − 0.1935
R² = 0.9987
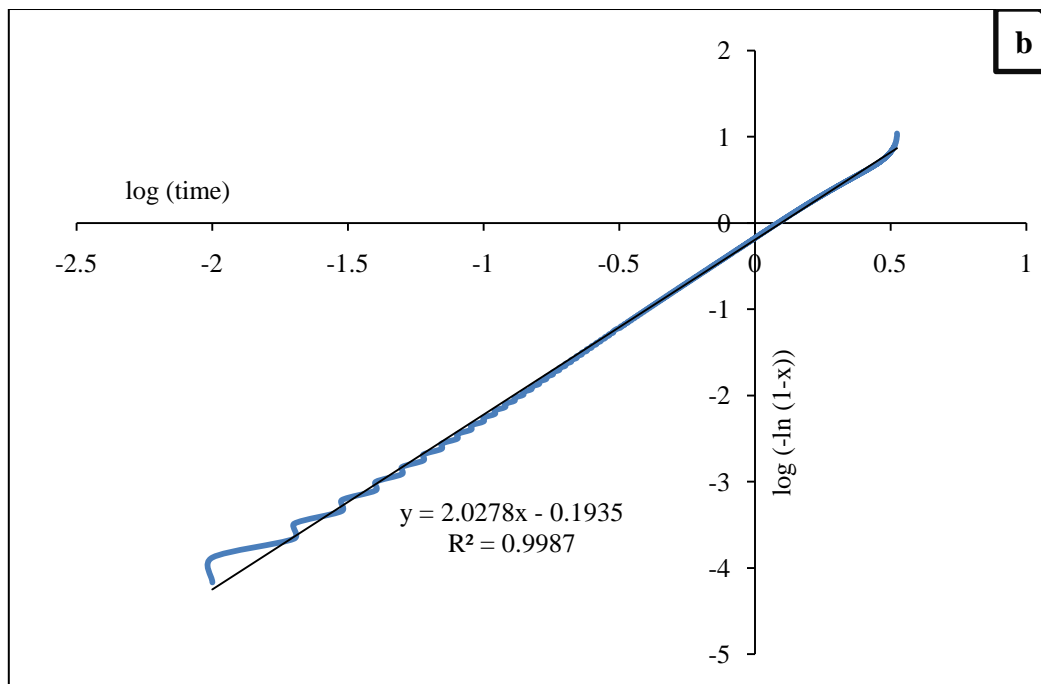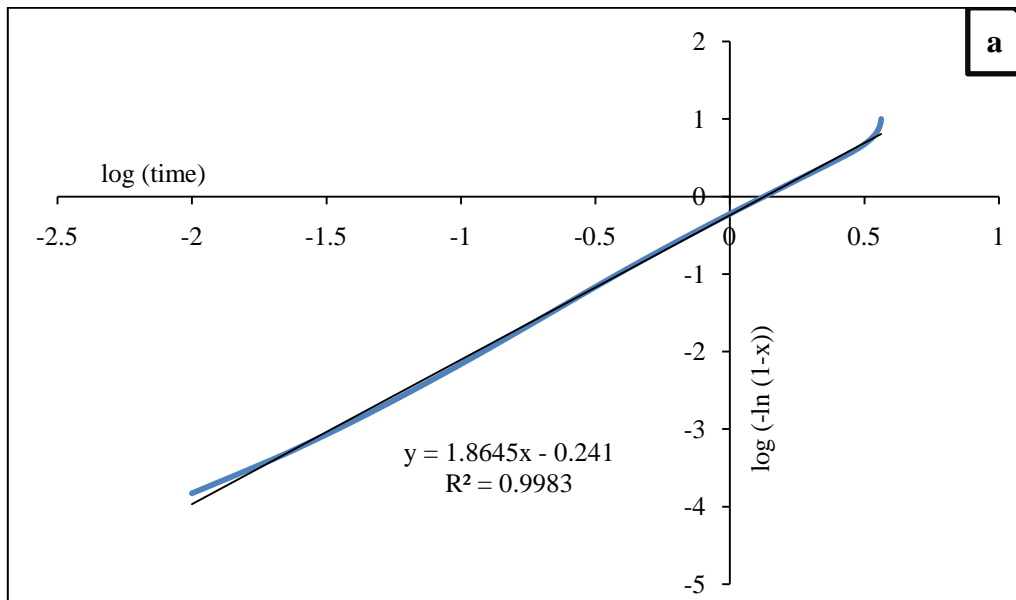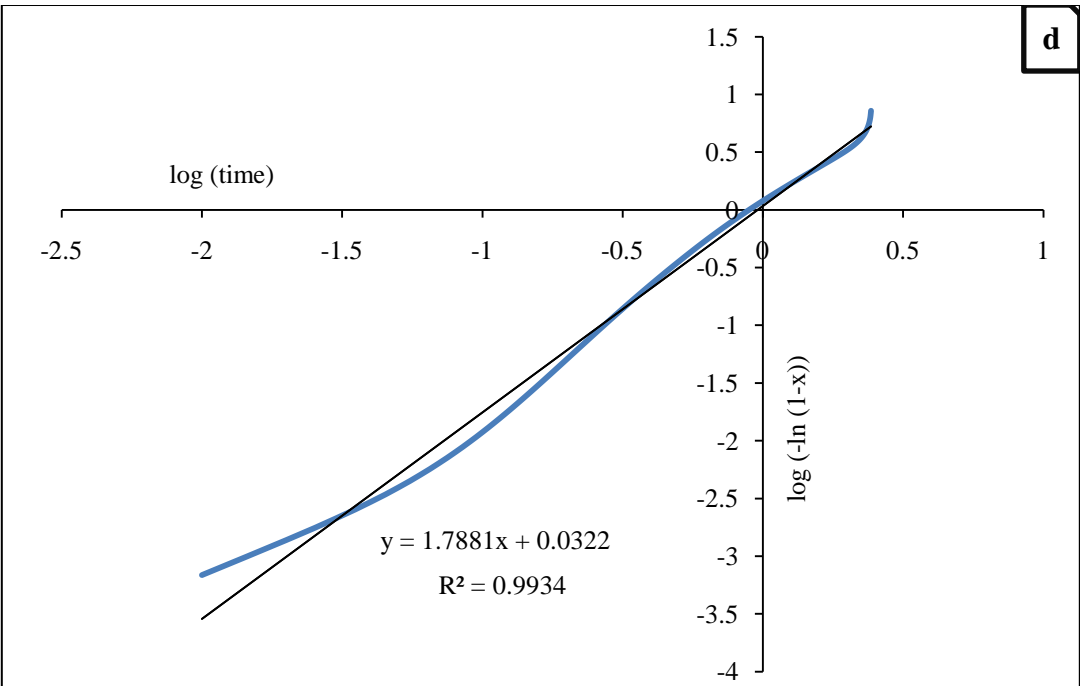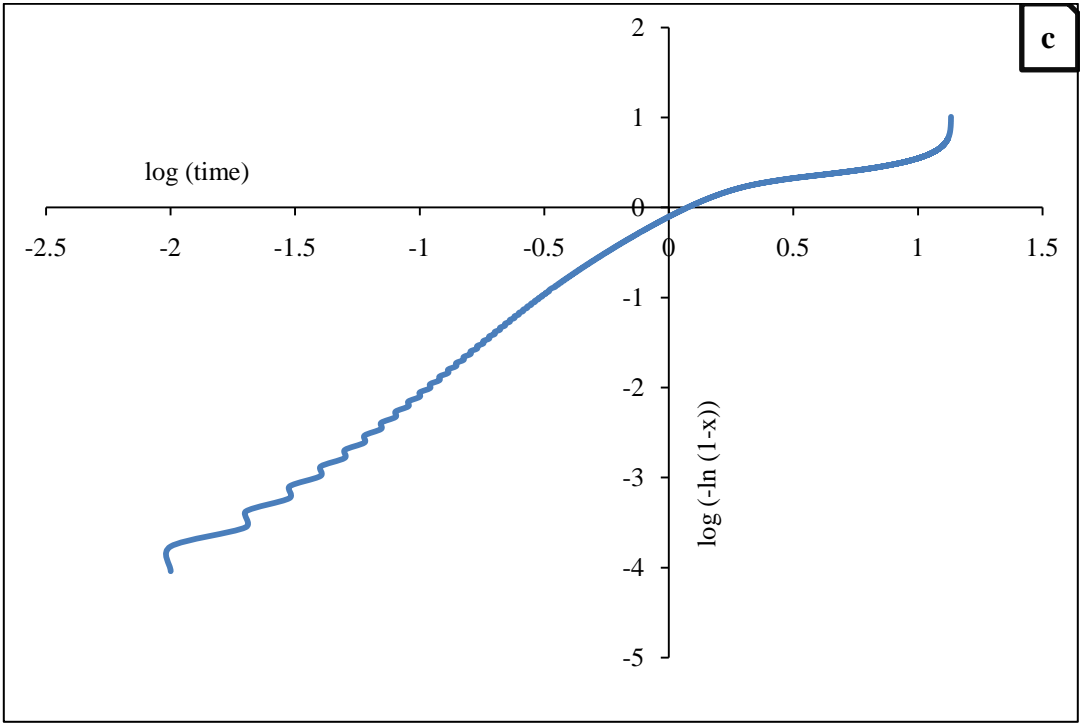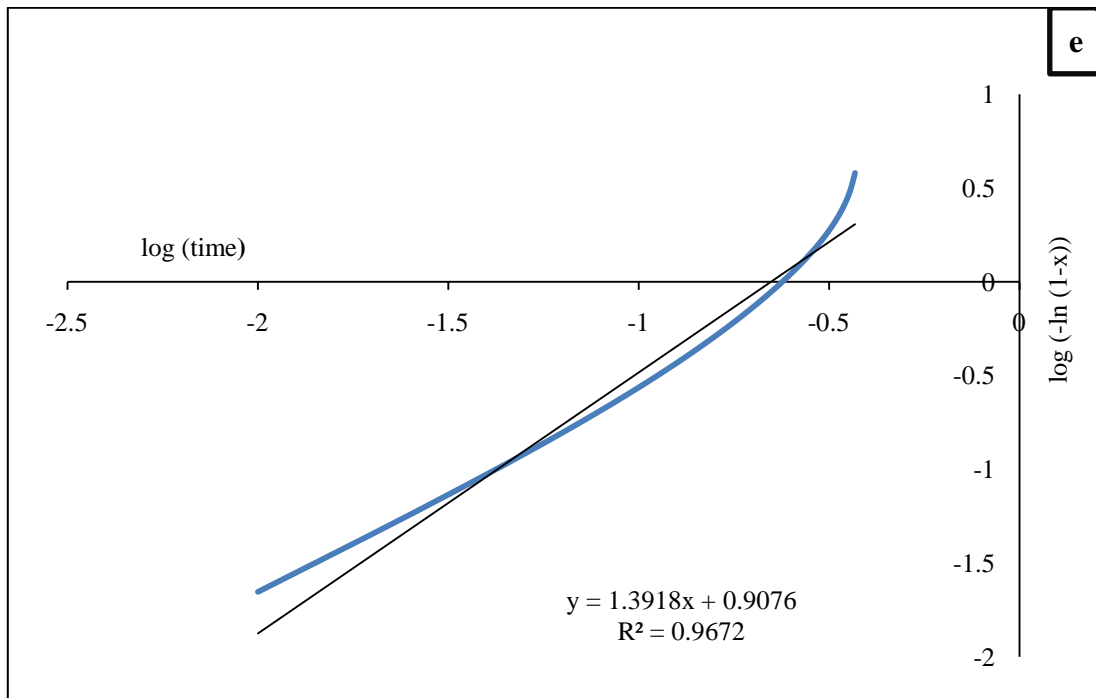
Figure 4-30: Avrami plots of pure Nylon-6 cooled at differnt temperature a) 192 °C, b)190 °C, c) 188 °C, d) 186 °C, e) 178 °C

Table 4-16: Summary of experimental and theoretical values for $t_{1/2}$, t_{max} and Avrami indices in different

Isothermal Nylon-6	$t_{1/2exp}$ (min)	$\tau_{1/2exp}$ (min^{-1})	$t_{1/2theo}$ (min)	$\tau_{1/2theo}$ (min^{-1})	$t_{max-exp}$ (min)	$t_{max-theo}$ (min)	n_{plot}	K_{plot}
192	1.09	0.92	1.11	0.90	0.83	0.89	1.86	0.57
190	1.02	0.98	1.04	0.96	0.92	0.89	2.03	0.64
188	0.92	1.09	0.94	1.06	0.52	0.76	1.85	0.77
186	0.72	1.39	0.78	1.28	0.51	0.61	1.79	1.08
178	0.19	5.26	0.17	5.84	0.21	0.09	1.39	8.08
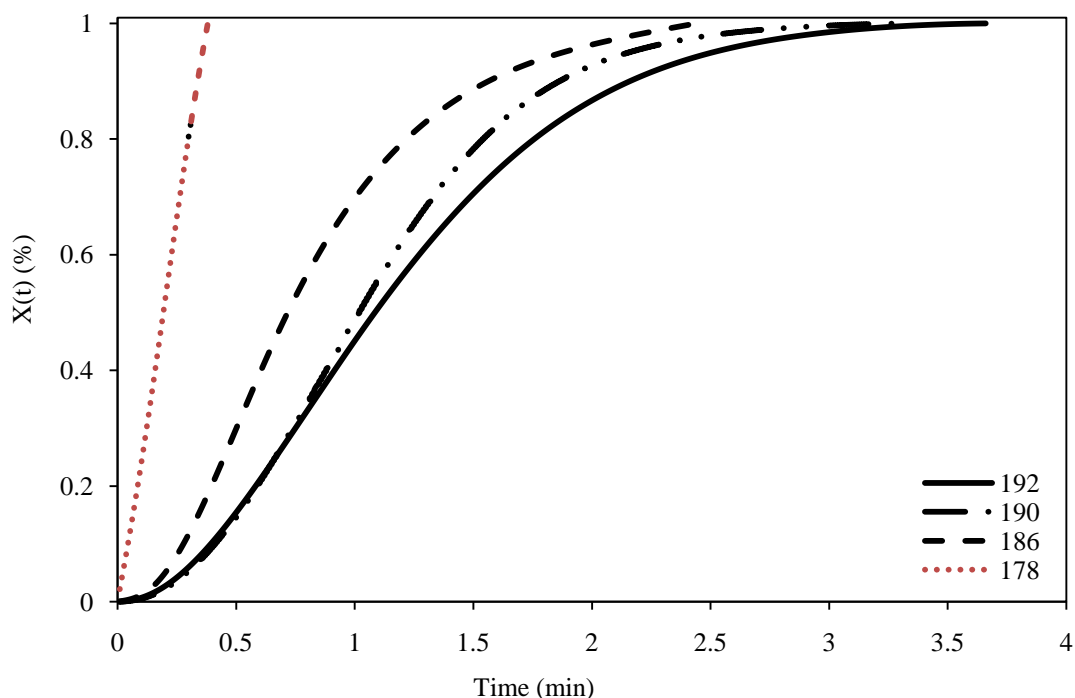
Figure 4-31 : Increase in X (t) with time in different isothermal temperature

The same procedure was applied to samples with 4 wt-% of plasticizer, 2 wt-% salt and 2 wt-% of plasticizer, 4 wt-% of salt and composite sample with 15 wt-% WS. The aim was to monitor the effect of presence of salt and plasticizer individually, and in combination with Nylon-6. The effect of filler on the crystallization kinetics was studied by doing the same analysis on the sample with 15 wt-%WS and no additives. For these samples the DSC thermograms are shown in Figure 4-32, Figure 4-33 and Figure 4-34.

Nylon-6 with 4 wt-% salt did not show any crystallization or melting peaks (Figure 4-2), either during or after the isothermal mode (Figure 4-35). Figure 4-35 for the same samples shows the heat flow at the isothermal temperatures of 140 °C and higher temperature (melting section) versus time. Since no crystalline peak was obtained for this run, no crystallization kinetic studies were performed.

The effect of isothermal temperature on crystallization behaviour was found to be similar for all samples as shown in Figure 4-32, Figure 4-33 and Figure 4-34. The decrease in the crystallization isothermal temperature (higher supercooling) resulted in narrower peaks and

a shift towards lower temperature. From these patterns the decrease in crystallization rate as a result of slower spherulite growth can be concluded. This can be confirmed by studying the X (t) versus time graphs which show that as supercooling increased, the maximum degree of crystallinity was reached faster (Figure 4-36 and Figure 4-37 and Figure 4-38).
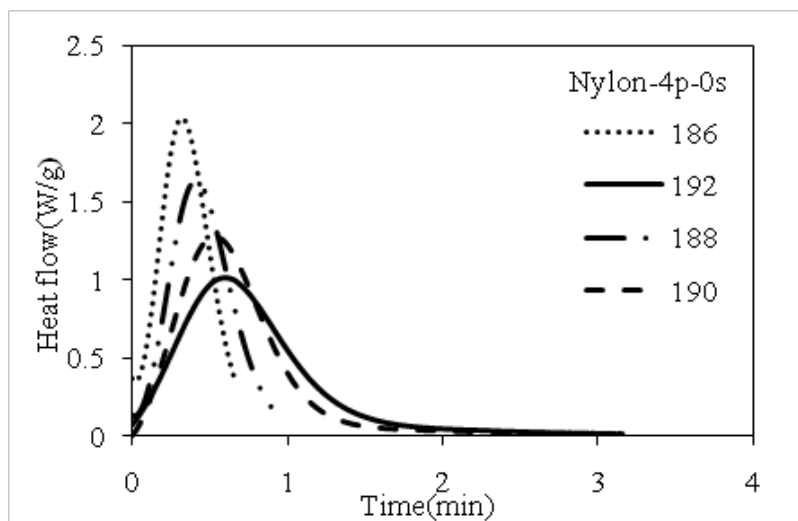
Figure 4-32: DSC thermograms of Nylon-6 with -4 wt-% plasticizer in different cooling temperatures
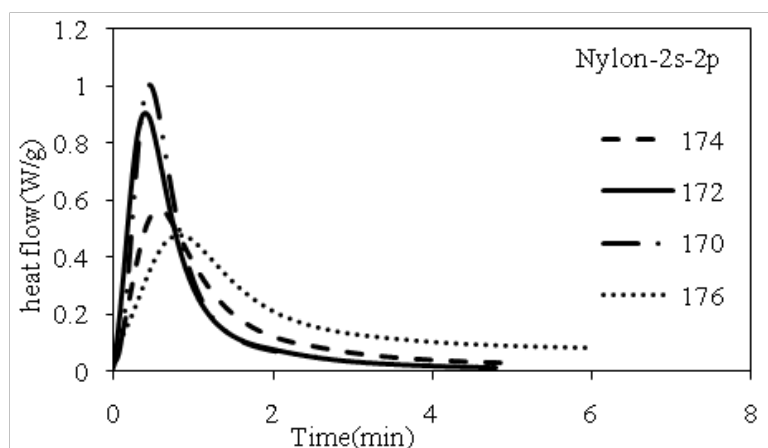
Figure 4-33: DSC thermograms of Nylon-6 with 2s-2p in different cooling temperatures
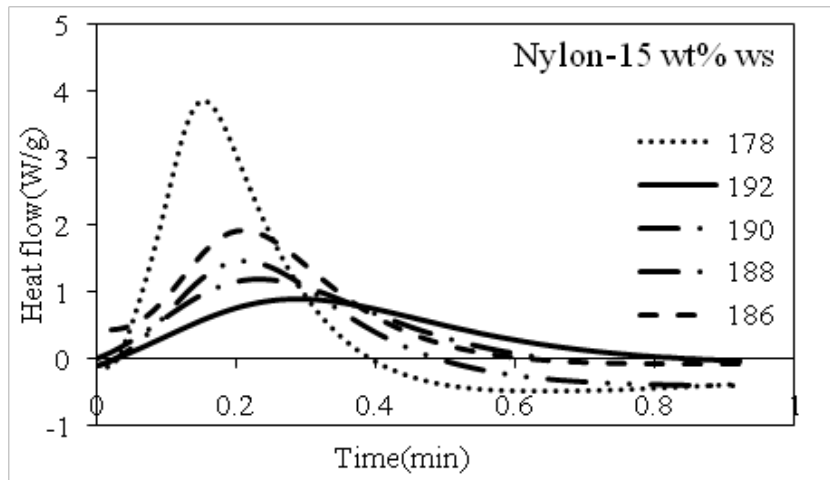
Figure 4-34: DSC thermograms of Nylon-6 with 15 wt-% WS in different cooling temperatures
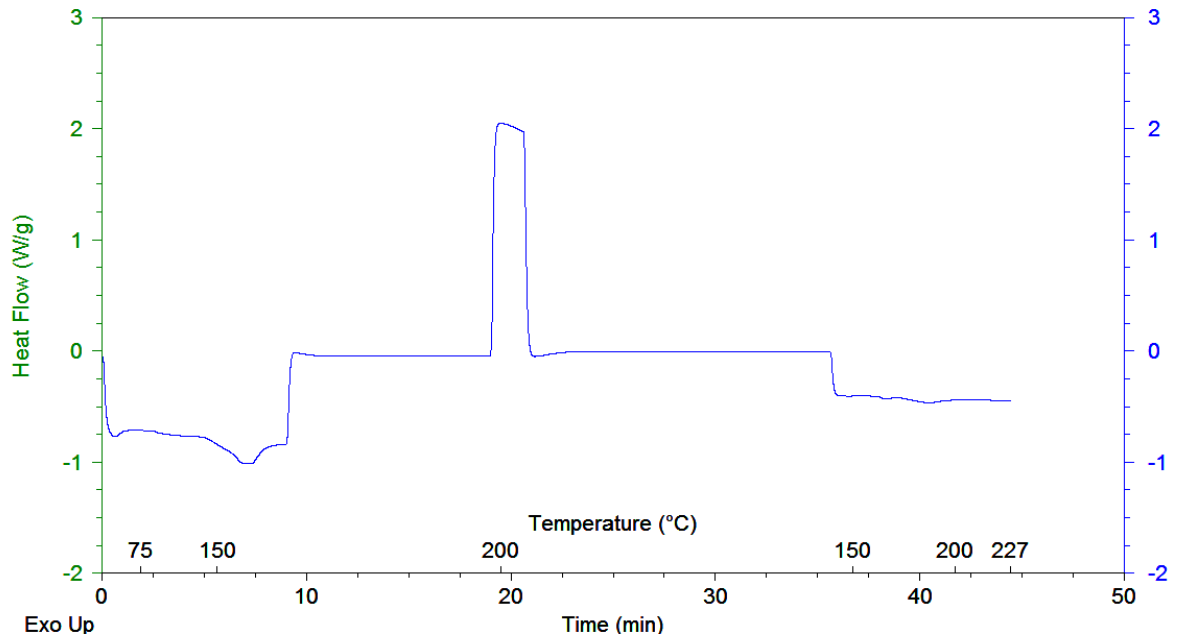
Figure 4-35: DSC thermogram during isothermal and after isothermal conditioning of Nylon-6 with 4 wt-% LiCl
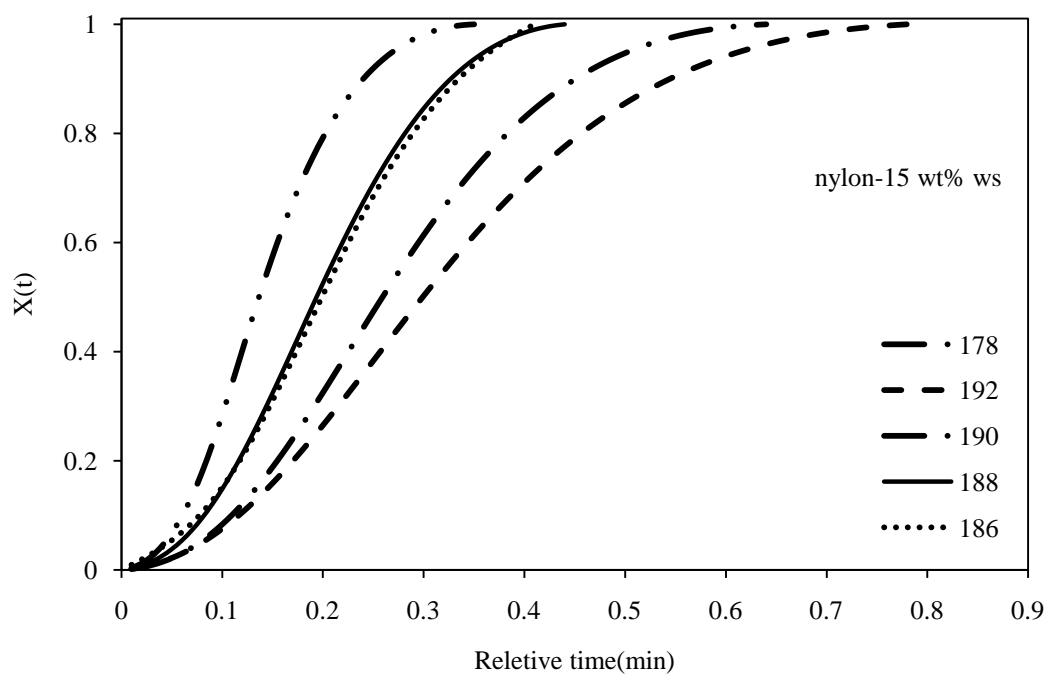
Figure 4-36: Increase in X (t) with time in different isothermal temperature for Nylon-6 with 15 wt-% WS
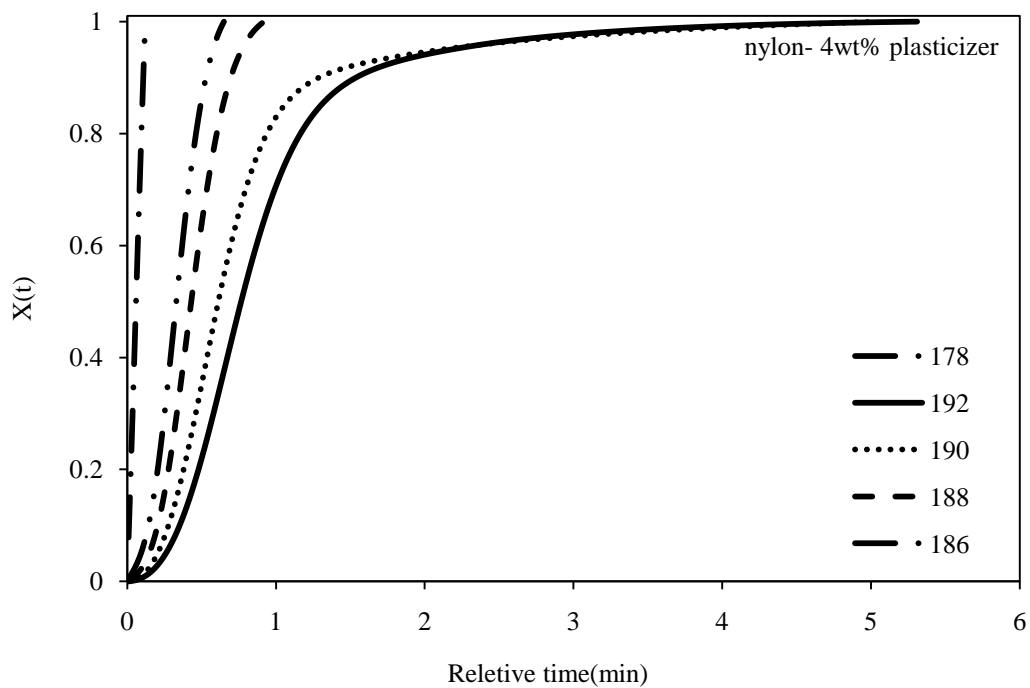
Figure 4-37 :Increase in X (t) with time in different isothermal temperature Nylon-6 with 4 wt-% plasticizer
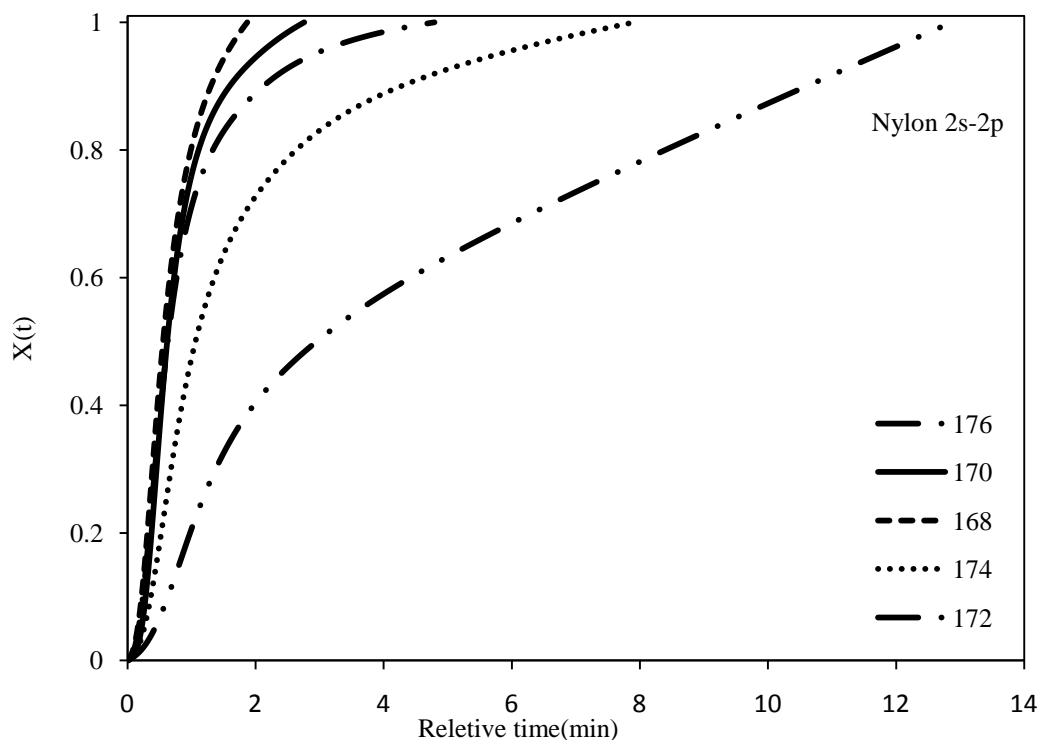
Figure 4-38: Increase in X (t) with time in different isothermal temperature Nylon-6 with salt (2 wt-%) and plasticizer (2 wt%)

The width at half the height of the DSC peaks were measured and plotted in Figure 4-39 to identify the duration of crystallization. Table 4-17, Table 4-18 and Table 4-19 summarize the duration of crystallization period for samples in different isothermal temperatures.

From Figure 4-39 it can be seen that Nylon-6/4 wt-% plasticizer had a lower width than neat Nylon-6. Albano et Al. mentioned that narrower peaks can be due to narrower crystal distribution (Albano, Papa et al. 2003). Consequently, the crystal size in the sample with 4 wt-% plasticizer was more uniform than in neat Nylon-6. In another word, the nuclei which were present in the sample prior to the isothermal conditions were growing during the isothermal time, and the formation of nuclei during growth was decreased due to high chain motion. The higher chain motion was also seen by comparison between total crystallization time of pure Nylon-6 and Nylon-6 with 4 wt-% plasticizer (Table 4-18 and Table 4-14).

101

Sample with 15 wt-% WS had the narrowest peaks (Figure 4-34) and the smallest Δw (Figure 4-38). It can be concluded that the crystal size distribution was more homogeneous. This is because the wheat straw particles can act as nucleating agent. Similar to previous cases, most nuclei are made prior to isothermal condition and they all grow at the same time. Hence, crystallites with same size are made. Moreover, as the number of nuclei is higher compared to neat Nylon-6, smaller crystals are formed. Smaller crystals offer faster spherulite collision which can result in a shorter first stage crystallization time.

The second stage of crystallization (if present) is short because spherulites are small. In this case, it does not take much time for chains to modify their position inside the crystalline structure. As a result, the rate of crystallinity was higher in Nylon-6/15 wt-% wheat straw sample. This increase in rate can also be concluded from Table 4-17 and lower duration of crystallization period. On the other hand, sample with 2 wt-% salt and plasticizer had the lowest homogeneity in crystal size due to highest Δw amounts. As it was expected, the total time which is needed for reaching maximum percentage of crystallinity increased (Table 4-21 and Figure 4-37). This was due to the presence of salt and elimination of hydrogen bonds which are responsible for crystallinity.
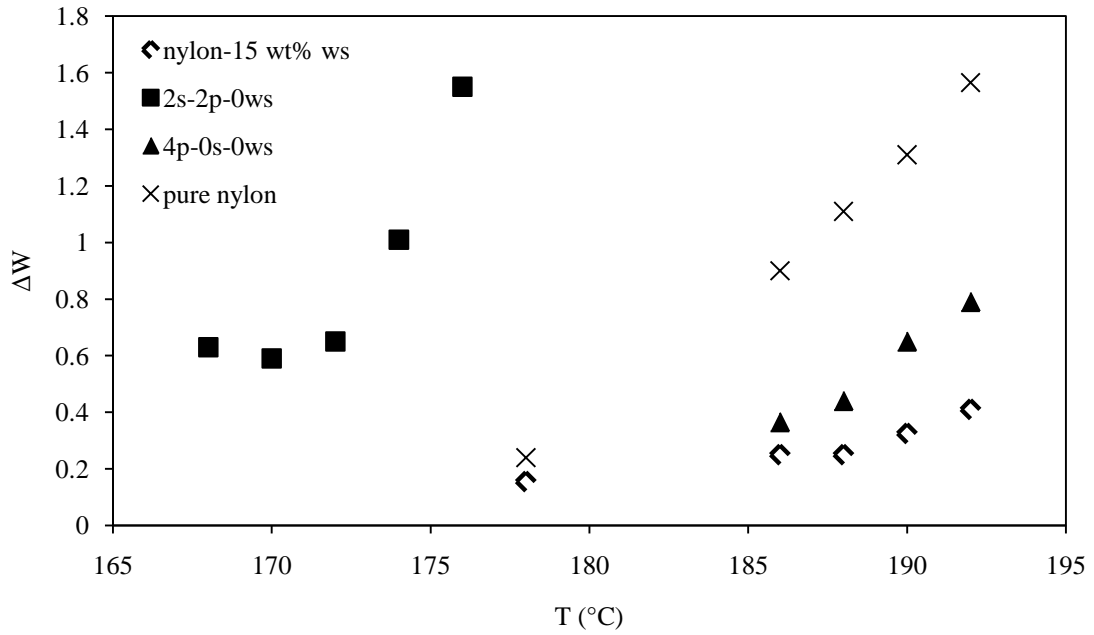
Figure 4-39: Width in half hight of DSC peak for all samples in diffrent isothermal temperatures

Table 4-17: Crystallization duration in different temperatures for Nylon-6/15 wt-% WS composites

Isothermal temperature (°C)	Δt(min)
192	0.78
190	0.64
188	0.44
186	0.41
178	0.35

Table 4-18: Crystallization duration in different temperatures for Nylon-6/4 wt-% plasticizer

Isothermal temperature (°C)	Δt(min)
192	5.32
190	5.05
188	0.93
186	0.65
178	0.12

Table 4-19: Crystallization duration in different temperatures for Nylon-6/2 wt-% salt-2 wt-% plasticizer

Isothermal temperature (°C)	Δt(min)
176	12.87
174	7.91
172	4.79
170	2.77
168	2.77

Table 4-20, Table 4-21 and Table 4-22 summarize data that were obtained from the Avrami plots. Sample with 4 wt-% of plasticizer and sample with 15 wt-% of WS had faster crystallization kinetics and lower t_{max} than pure Nylon-6. Increase in crystals growth rate for the sample with 15 wt-% of WS compared to pure Nylon-6 was more dramatic than sample with 4 wt-% plasticizer. This can be due to the fact that the density of nuclei are larger in sample with 15 wt-% of wheat straw and that influence the rate more than the chain motions in sample with 4 wt-% of plasticizer.

In addition, the dependency of crystallization rate on isothermal temperature in samples with 4 wt-% plasticizer and 2 wt-% salt/2 wt-% plasticizer samples was more significant than in sample with 15 wt-% WS. Also, the crystallization rate of the sample with 2 wt-% salt / 2 wt-% plasticizer was affected by temperature more severely than for the sample with 4 wt-% plasticizer.

In general, two nucleation modes are suggested for polymers. In one case, the nucleation happens through heterogeneous nuclei which are made prior to isothermal conditions; in this mode the growth of nuclei are simultaneous and the growth rate is constant with time. In another possible case, homogenous nucleation can also take place during the growth step of heterogeneous crystallites in untransformed regions (amorphous regions) between spherulites; consequently the activation energy of nucleation is the summation of thermal and athermal nucleation stages (Albano, Papa et al. 2003).

The second possibility for nucleation mode is the simultaneous growing nuclei with inconsistent growth rate (Albano, Papa et al. 2003). Homogeneous nucleation is known to

be responsible for increase in rate of crystallization in lower isothermal temperature. As mentioned previously, crystallization rate increases with increase in supercooling temperature. This increase for sample with 2 wt-% salt/2 wt-% plasticizer was higher than for sample with 4 wt-% plasticizer. This difference can be attributed, possibly, to the presence of different nucleation modes. Lower homogeneous nucleation in the sample with 4 wt-% plasticizer might be the reason for lower sensitivity to temperature. This sample had higher chain motion because of the addition of plasticizer. High chain motion could have hindered the thermal homogeneous nucleation.

In the comparison between $t_{1/2}$ and t_{max} of the sample with 2 wt-% salt/2 wt-% plasticizer with other samples, it is inferred that the addition of salt not only decreased the percentage of crystallinity (section 4.2) but also decreased the crystallization rate. This drop in rate due to the presence of salt was so severe that even the addition of the same amount of plasticizer could not compensate for its effect. This is in agreement with Δt data (Figure 4-20) and width DSC thermograms (Figure 4-33).

It is worth to note that $t_{1/2exp}$ and $t_{1/2theo}$ have better agreement with each other than $t_{max\ exp}$ and $t_{max\ theo}$.

Comparisons were made on another Avrami index (n) for different samples. It can be seen that for pure Nylon-6 the Avrami index (n) varied in the range of 1.39-2.03. For Nylon-6 with 4 wt-% plasticizers and Nylon-6 with 15 wt-% WS, the Avrami index (n) changed in the range of 1.39 to 2.23 and 1.79 to 2.15, respectively. For the sample with 2 wt-% salt / 2 wt-% plasticizer it changed between 1.334 and 1.78. Assuming that crystallization was instantaneous, nucleation was constant and γ was zero; therefore the range of Avrami index (n) indicates both one and two dimensional growth of spherulites. Similar behaviour has been reported in the literature (Lin, Chen et al. 2009).

In Table 4-20, Table 4-21, and Table 4-22 the different values of the index n are an indication of different nucleation mechanisms. Further, comparison between K constants (crystallization rate constant) of different samples showed that the sample with 15 wt-% WS and sample with 2 wt-% salt / 2 wt-% had the highest and lowest tendency for crystallinity, respectively; see (Figure 4-26).

Table 4-20: Summery of experimental and theoretical, and Avrami indices in different cooling times for Nylon-6 with 4 wt-% plasticizer

Isothermal temperature (°C)	$t_{1/2exp}$ (min)	$\tau_{1/2exp}$ (min^{-1})	$t_{1/2theo}$ (min)	$\tau_{1/2theo}$ (min^{-1})	$t_{max-exp}$ (min)	$t_{max-theo}$ (min)	n_{plot}	K_{plot}
192	0.77	1.30	0.79	1.27	0.67	0.71	2.23	1.17
190	0.62	1.61	0.63	1.58	0.53	0.57	2.21	1.92
188	0.43	2.32	0.42	2.40	0.36	0.41	2.08	4.28
186	0.33	3.03	0.31	3.21	0.32	0.25	1.87	6.17
178	0.06	16.67	0.05	18.61	0.05	0.03	1.39	40.75

Table 4-21: Summery of experimental and theoretical, and Avrami indices in different cooling times for Nylon-6 with 2wt-% salt and 2wt-% plasticizer

Isothermal temperature (°C)	$t_{1/2exp}$ (min)	$\tau_{1/2exp}$ (min^{-1})	$t_{1/2theo}$ (min)	$\tau_{1/2theo}$ (min^{-1})	$t_{max-exp}$ (min)	$t_{max-theo}$ (min)	n_{plot}	K_{plot}
176	2.96	0.34	3.44	0.29	0.84	0.75	1.14	0.17
174	1.06	0.94	1.52	0.66	0.58	0.55	1.24	0.41
172	0.63	1.58	0.88	1.13	0.4	0.41	1.33	0.82
170	0.62	1.61	0.80	1.26	0.45	0.61	1.78	1.04
168	0.56	1.79	0.61	1.63	0.38	0.45	1.71	1.61

Table 4-22: Summery of experimental and theoretical, and Avrami indices in different cooling times for Nylon-6 with 15 wt-% WS

Isothermal temperature (°C)	$t_{1/2exp}$ (min)	$\tau_{1/2exp}$ (min^{-1})	$t_{1/2theo}$ (min)	$\tau_{1/2theo}$ (min^{-1})	$t_{max-exp}$ (min)	$t_{max-theo}$ (min)	n_{plot}	K_{plot}
192	0.30	3.33	0.29	3.44	0.26	0.24	1.93	7.57
190	0.26	3.85	0.25	3.96	0.23	0.22	2.09	12.30
188	0.195	5.13	0.19	5.37	0.18	0.16	2.10	23.74
186	0.20	5.00	0.19	5.36	0.19	0.15	1.79	14.06
178	0.14	7.14	0.14	7.37	0.12	0.12	2.16	51.55
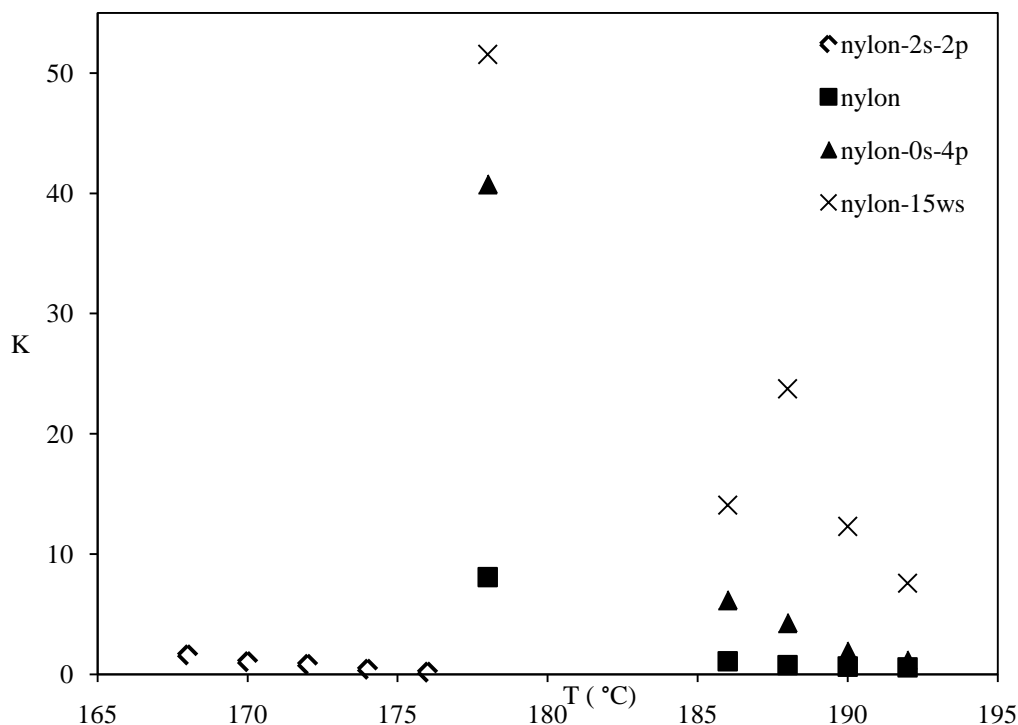
Figure 4-40: Comparison between crystallization rate constant of different samples in different isothermal temp.

The increase in K and decrease in $t_{1/2}$ and t_{max} showed that addition of wheat straw and plasticizer increased the rate of crystallization but the addition of salt decreased the crystallization rate.

By applying linear regression on the (lnK) VS (1/T) data, activation energy (ΔE) for crystallization was obtained. The amounts for ΔE of different samples are summarized in Table 4-23. It can be seen that addition of WS decreased the activation energy for crystallization; however, the presence of salt and plasticizer decreased the crystallization activation energy.

Table 4-24, Table 4-25, and Table 4-26 summarize the location and area of double melting peaks. In all cases (except for 2 wt-%salt/2 wt-% plasticizer from temperature 170°C to

168°C) any increase in supercooling, increased the area under the melting peak. This observation was consistent with observations in pure Nylon-6.

From these tables, is it also found that sample with 2 wt-% salt / 2 wt-% plasticizers and sample with 4 wt-% plasticizer the melting peak location was not affected by temperature. However for sample with 15 wt-% WS the second melting peak location shifted to lower temperatures with a decrease in isothermal temperatures. This might be due to the formation of smaller crystallites as a result of higher nucleation rate at lower temperatures.

Table 4-23: Activation energy for crystallization

Sample	ΔE (KJ/mol)
pure Nylon-6	234.671
Nylon-6/4p-0WS	328.67
Nylon-6/2p-2s-0WS	361.601
Nylon-6/15 WS-0s-0p	91.587

Table 4-24: area under melting curves after isothermal cooling, first and second peak location for the Nylon-6 with 2s-2p

Isothermal temperature (°C)	ΔH_m (W/g)	T_{m1} (°C)	T_{m2} (°C)
176	24.58	-	206.22
174	26.41	197.54	207.72
172	28.96	196.42	208.08
170	32.03	195.76	207.87
168	28.8	195.11	207.26

Table 4-25: Area under melting curves after isothermal cooling, first and second peak location for the Nylon-6 with 4p

Isothermal temperature (°C)	ΔH_m (W/g)	T_{m1} (°C)	T_{m2} (°C)
192	36.42	214	220.00
190	41.25	212.8	219.40
188	40	212.5	220.59
186	41.46	211.6	220.43
178	46.09	-	220.51

Table 4-26: Area under melting curves after isothermal cooling, first and second peak location for the Nylon-6 with 15 wt-% WS

Isothermal temperature (°C)	ΔH_m (W/g)	T_{m1} (°C)	T_{m2} (°C)
192	35.36	219.62	213.50
190	36.88	219.16	212.49
188	39.106	219.58	211.75
186	36.012	219.66	210.52
178	40.023	219.74	208.08

4.7 CORRELATION BETWEEN FORMULATION AND MECHANICAL AND PHYSICAL PROPERTIES

The aim of this section is to present possible models that predict physical and mechanical properties of Nylon-6/wheat straws composites with different level of salt and plasticizer. For this reason expert design software was utilized. Using this program, the experiments were designed to acquire a linear model for different level of salt and plasticizer.

The mixture design was developed based on the percentages of the additives salt and plasticizer. The low and high level of each additive was set between 0 and 4 wt-%. The summation of additives mixture was also set to 4 wt-%.

Based on the experimental design the percentages of other components (filler, polymer and antioxidant level) were kept constant. Five experiments were suggested for a linear model and simplex lattice. Run 1 to 5 shown in Table 3-3 were proposed by expert design for modeling composite properties based on different level of salt and plasticizer. Tensile modulus, strength, elongation at yield, flexural modulus and strength, and percentage of crystallinity were chosen as response variables. The software analyzed the response data and suggested suitable models for each of these responses versus percentage of salt and plasticizer. The suggested models were analyzed for the significance with ANOVA tables.

4.7.1 TENSILE MODULUS

Table 4-27 shows standard deviation and R square values for the suggested tensile modulus equation. From this table we can conclude that cubic model had the closest fit on tensile modulus data.

Table 4-27: Different models order and R-squares for each model

Model Summary Statistics			
Source	Std. Deviation	R-Squared	
Linear	220.4599	0.374831	
Quadratic	196.3066	0.669542	
Cubic	45.55494	0.991102	Suggested

STD: Standard deviation

Figure 4-41 also shows graphically how the curve is fitted on our data. Equation 4-15 represents the equation obtained from the statistical analysis.

$Tensile\ Modulus$

$$= 1368.7562142857 \times salt + 1231.9562142857$$
$$\times plastisizer - 70.06892857143 \times salt$$
$$\times plastisizer - 36.0835 \times salt \times plastisizer \times (salt$$
$$- plastisizer)$$

Equation 4-15
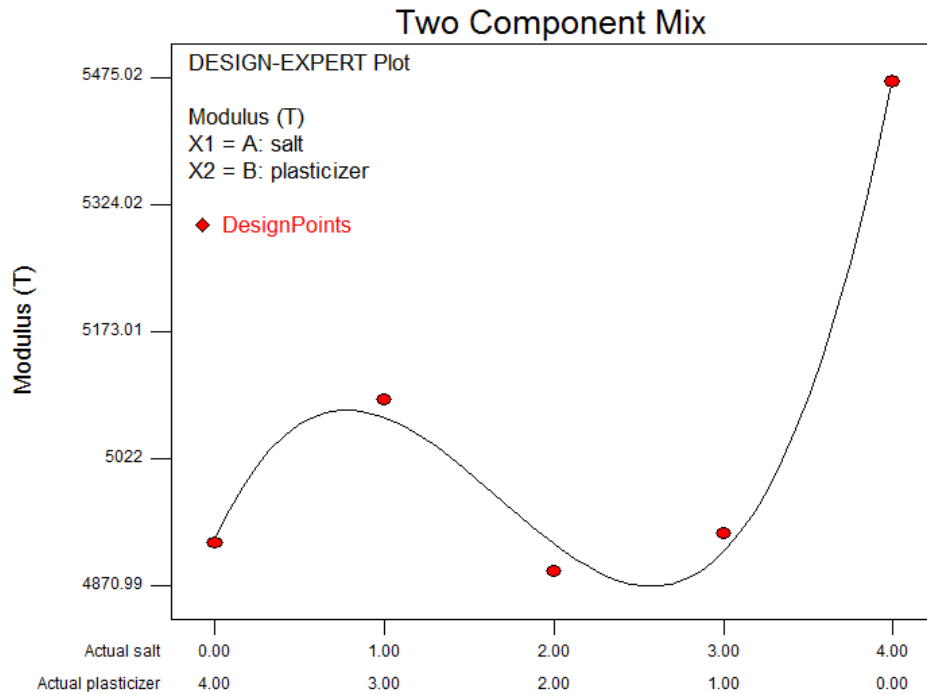
Figure 4-41: Modulus versus salt percentage data and fitted model

ANOVA table were developed from expert design program to analyze level of significance of the suggested cubic model (Table 4-28). From the last column it could be inferred that there is 27.24 % possibility that model is insignificant based on a 90 % confidence interval.

Table 4-28: ANOVA table for determining significance of suggested third order statistical model for module

Source	SS	df	MS	$F_{observed}$	$Prob > F_{crit.}$	Comment
Model	87421.57	1	87421.57	1.8	0.27	The model is not sig.
Residual	145807.80	3	48602.58			
Total	233229.30	4				

4.7.2   STATISTICAL MODELS FOR OTHER MECHANICAL AND PHYSICAL PROPERTIES

The same procedure applied to the tensile modulus was applied for other mechanical and physical properties (response variables). The order of models was selected using the expert

design software based on the correlation coefficient. Significance of the models was determined by ANOVA tables. The model with highest correlation coefficient is presented in Table 4-29. The degree of the model and probability of its insignificance are also reported in Table 4-29. The last column defines the probability of which models become insignificance due to large noise or error. We choose models based on a 90 % confidence interval. With this confidence in intervals, the elongation at break and the percentage of crystallinity are properties that can be modeled significantly with different levels of salt and plasticizer.

Figure 4-42 shows the linear model which fits elongation and Figure 4-43 shows the non-linear model for percentage of crystallinity.

Table 4-29: Suggested model order, significance and confidence in interval for each mechanical property

Response variable	Order of suggested model	Model	Significance	Probability
Tensile modulus(MPa)	3	1368.756*S+1231.956*P-70.06892857143*S *P-36.08375*S*P(S-P)	NO	11.99
Tensile strength(MPa)	1	14.855*S+18.233*P	NO	12.07
Elongation at break (%)	3	0.29180*S+0.51700*P	YES	2.51
Flexural Modulus (MPa)	3	976.99064*S + 808.53164*P +67.32621*S*P - 43.87458S*P*(S-P)	NO	13.69
Flexural Strength (MPa)	3	18.973*S+26.697*P+6.91*S*P+2.512 S*P*(S-P)	NO	25.84
Percentage of crystallization (%)	2	2.59241* S+4.13107* P+1.12968* S*P	YES	10
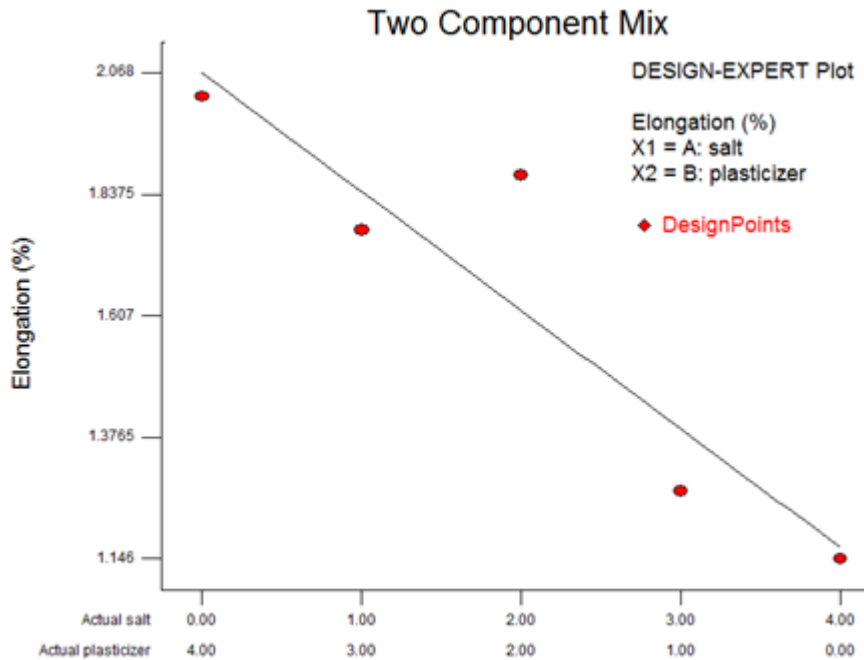
Figure 4-42: Elongation at break VS. percentage of sallt
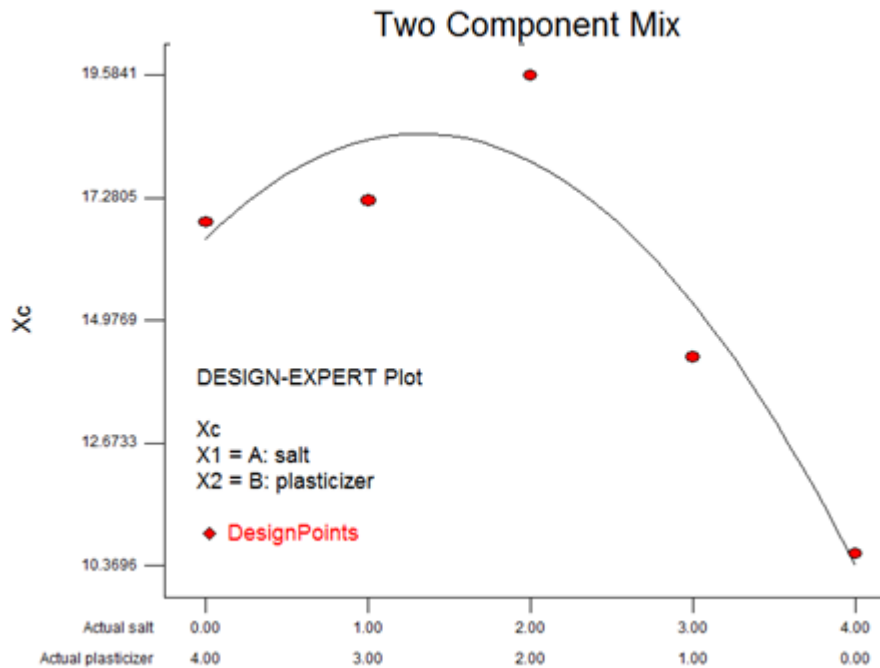
Figure 4-43: Percentage of crystallinity VS. Percentage of salt

It worth to note that the tensile strength, tensile modulus, and flexural modulus are relatively good models since the insignificance probabilities are relatively low.

An attempt was made to correlate the composite mechanical properties to physical properties of matrix and fiber. The mechanical properties were correlated to X_c (percentage of crystallinity) and activation energy for degradation.

In this thesis the activation energy was used as a critical variable for mechanical properties. Wheat straw loses its consistency during degradation and its modulus and mechanical properties depend on the level of degradation. Moreover, as the particles degrade, the interfacial bonding between particle and matrix reduces and strength of the composite decreases. The models presented in the Appendix for modulus and strength of the composite. In these models the modulus of the composite depends largely on the modulus of the fiber and the modulus of the matrix, and the strength of the composite depends on the interfacial properties.

In order to investigate correlation between the mechanical properties and the physical properties, the percentage of crystallinity and the activation energy for thermal degradation were correlated to mechanical properties by linear regression method. The level of significance of the linear models and each of the regression coefficients were investigated by F test and plotting ANOVA tables.

The percentage of crystallinity of matrix (X_c) is known as a physical parameter that changes modulus and strength of matrix; as a result, it affects the composite modulus and strength. The activation energy for the thermal degradation of the fiber was chosen because it is a parameter that is associated with bonding strength on the surface of the wheat straw fiber.

Table 4-30 presents the linear models and indicates the significance of the effect of physical properties on mechanical properties. From the data summarized in Table 4-30, it can be inferred that the mathematical strength (either flexural or tensile) can be correlated to activation energy for thermal degradation rather than to crystallinity X_c. This is due to the fact that strength depends on interface and interfacial bonding changes with fiber thermal degradation.

From Table 4-30, one can also infer that both high activation energy and X_c have negative effects on the modulus. This was expected as the main factor dictating the behaviour of the modulus is the percentage of salt.

The decision for significance of the linear model and each of coefficients were made based of F-test with 90 % confidence in intervals.

Table 4-30: Statistical models for correlating mechanical properties to activation energy for degradation and percentage of crystallinity

Response variable	Model	Model overall significance	Significance	Activation energy significance
Tensile modulus(MPa)	6638.629-7.03E-3*(E)-59.8541*(Xc)	YES	Significant	Insignificant
Tensile strength(MPa)	35.492+1.63E-5*(E)+1.734*(Xc)	YES	Insignificant	Significant
Elongation at break (%)	0.967-4.2371E-06*(E)+0.06598*(Xc)	YES	Significant	Significant
Flexural modulus (MPa)	4552.54 -3.61E-3*(E)-34.319*(Xc)	NO	Insignificant	Insignificant
Flexural Strength (MPa)	35.492+1.63E-5*(E)+1.734*(Xc)	YES	Insignificant	Significant
Impact (lb ft/inch)	0.11119+9.25E-07(E)+5.37E-3*(Xc)	YES	Insignificant	Significant

5   CONCLUSIONS AND RECOMMENDATIONS

1) Addition of 4 wt-% salt to Nylon-6/wheat straw composites decreased the melting temperature, crystallization temperature and crystallinity (X_c) of the composite. On the other hand, addition of 4 wt-% plasticizer did not affect melting and crystallization temperature, but decreased the X_c of the composites.

2) Addition of 4 wt-% of the salt to Nylon-6 decreased its MFI; however addition of 4 wt-% of the plasticizer increased the MFI and facilitated processing by extrusion and injection molding.

3) The activation energy for thermal degradation was measure and it was found for all runs; Nylon-6/2 wt-% salt/2 wt-% and Nylon-6/1 wt-% salt/3 wt-% plasticizer had the highest and lowest degradation energy compare to other runs, respectively.

4) Nylon-6/wheat straw (15 wt-%) had higher modulus and lower strength compared to neat Nylon-6. Different levels of salt and plasticizer were mixed to improve mechanical properties of Nylon-6/ 15 wt-% WS composites by decreasing its processing temperature and facilitating processing by extrusion and injection moulding. All runs with any level of salt and plasticizer had higher tensile and flexural modulus compared to Nylon-6/ 15 wt-%WS composites. In addition, most of the runs had higher tensile strength compared to composites with no additives. However, the treatment did not cause any enhancement in strength and elongation of the composite. It was found that run 3 (2 wt-% of salt/2 wt-% of plasticizer) had the highest mechanical properties and relatively easier processing.

5) Addition of salt to Nylon-6 reduced the rate of crystallization. In contrast, addition of wheat straw to Nylon-6 increased the percentage of crystallinity, the crystallization rate and the tendency for crystallization. Addition of 4 wt-% plasticizer to Nylon-6 increased crystallization rate. Addition of WS increased the tendency for crystallization.

6) Elongation at break and percentage of crystallinity were the only properties that could be modeled statically with 90 % confidence interval.

7) It was found that the strength was a function of interfacial bonding between filler and matrix and it was affected by thermal degradation, while the modulus was correlated to crystallinity X_c.

Recommendations

1) In terms of processing, using low temperature processing methods is suggested.

2) The effect of processing parameters on properties is recommended to be investigated as the processing parameters affect the wetting, degradation and consequently mechanical properties of the composites. Thus, it is recommended that processing parameters also be optimized based of mechanical properties.

3) Experiments in this thesis were designed for linear correlation between property and composition of composites. Therefore, for other properties with nonlinear dependency on level of salt and plasticizer, the data points were not enough to result a significant model.

There was a need for further experimental data. The following experiments are suggested by expert design for the properties which this program suggested fitting a cubic model on them (Table 5-1).

Table 5-1: The suggested mechanical tests for fitting a nonlinear model on data

Run #	Irganox	Salt	Plasticizer	Wheat straw
	(% wt)	(% wt)	(% wt)	(% wt)
6	0.1	1.33	2.67	15
7	0.1	2.67	1.33	15

4) It is recommended that a set of experiments be done in different level of wheat straw filler. Hence, the models which were presented in the Appendix can be used to fit the experimental data. In this way agreement between these theoretical models and experimental data can be evaluated. After evaluating models, the modulus and strength of wheat straw particles can be determine theoretically by a backward procedure (Sánchez, Alvarez 1999).

5) It is suggested that the mechanical tests that are critical for automotive applications like heat distortion temperature (HDT) be conducted on the composite. HDT along with water absorption properties of composite bars can give insight to the performance of these pieces. Dynamic mechanical thermal analysis (DMTA is another test which can give information about dispersion and wetting of wheat straw in the matrix. By sweeping different frequencies and temperatures, long term performance of the composites can be investigated with time-temperature superposition. The glass transition temperature (T_g) can be measured with DMTA.

6) In this study only additives were used that were suggested in the literature for manufacturing Nylon natural filler composites (Misra M., K. et al. 2004, Xu 2008). There are other methods and other additives that are suggested for decreasing processing temperature and easing the process. Blending Nylon-6 with Nylon-11 is one of these ideas for decreasing the melting point. It is stated in the literature that blending of Nylon-6 with Nylon-11 can lead to chemical copolymerization due to interchange exchange reactions and the melting point of the Nylon-6 decreases (Kohan. 1995). As the properties of Nylon-11 is not quite lower than Nylon-6, blending the two at a proper ratio will lower processing temperature. There are other additives suggested in the literature that eliminate hydrogen bonding and might be able to lower the melting point. polyvinylpyrrolidone, Polyethylene glycol are two additive that might not be as strong as LiCl in reducing the melting point but they do not increase the viscosity and may even be able to decrease the viscosity due to their plasticizing effect (Zhang, Huang et al. 2007). Reactive polymers with anhydride functional group might also be able to decrease processing temperature and ease the polymer melts transfer during processing (Gardner, West et al. 2009).

REFERENCES

ACIERNO, D., LA MANTIA, F.P., POLIZZOTTI, G. and CIFERRI, A., 1979. Bulk properties of synthetic polymer-inorganic salt systems. V. Mechanical properties of oriented poly(caproamide). *Journal of Polymer Science: Polymer Physics Edition,* **17**(11), 1903-1912.

ALBANO, C., PAPA, J., ICHAZO, M., GONZÁLEZ, J. and USTARIZ, C., 2003. Application of different macrokinetic models to the isothermal crystallization of PP/talc blends. *Composite Structures,* **62**(3-4), 291-302.

ASTM INTERNATIONAL, 2008a. ASTM D 1238 - 04c Standard Test Method for Melt Flow Rates of Thermoplastics by Extrusion Plastometer.

ASTM INTERNATIONAL, 2008b. ASTM D 256 - 06a Standard Test Methods for Determining the Izod Pendulum Impact Resistance of Plastics.

ASTM INTERNATIONAL, 2008. ASTM D 618-08 Standard Practice for Conditioning Plastics for Testing.

ASTM INTERNATIONAL, 2008a. ASTM D 790 - 03 Standard Test Methods for Flexural Properties of Unreinforced and Reinforced Plastics and Electrical Insulating Materials.

ASTM INTERNATIONAL, 2008b. ASTM D 790 - 07 Standard Test Method for Flexural Properties of Unreinforced and Reinforced Plastics and Electrical Insulating Materials.

ASTM INTERNATIONAL, 2008c. ASTM Standard D 638 - 10 Standard Test Method for Tensile Properties of Plastics.

BALASUBRAMANIAN, D. and SHAIKH, R., 1973. On the interaction of lithium salts with model amides. *Biopolymers,* **12**(7), 1639-1650.

CARLSON, E. and NELSON, K., Nylon under the hood: a history of innovation [Homepage of http://plastics.dupont.com/plastics/pdflit/americas/markets/nylon_under_hood.pdf], [Online] [09/01, 2010].

CEBE, P. and HONG, S., 1986. Crystallization behaviour of poly(ether-ether-ketone). *Polymer,* **27**(8), 1183-1192.

CHEMICALLAND21, N-BUTYL-BENZENESULFONAMIDE [Homepage of http://chemicalland21.com/industrialchem/plasticizer/N-BUTYL-BENZENESULFONAMIDE.htm], [Online] [09/01, 2010].

CHEN, J. and GARDNER, D.J., 2008. Dynamic mechanical properties of extruded nylon–wood composites. *Polymer Composites,* **29**(4), 372-379.

CIBA SPECIALTY CHEMICALS INC., Ciba IRGAFOS 168 processing stabiliser [Homepage of http://www.bjmytimes.com/ciba/ciba/IRGAFOS168.pdf], [Online] [09/01, 2010].

CLEMONS, C. and SANADI, A., 2007. Instrumented impact testing of kenaf fiber reinforced polypropylene composites: effects of temperature and composition. *Journal of Reinforced Plastics and Composites,* **26**(15), 1587-1602.

CLEMONS, C.M., 2000. *Microstructural effects on the dynamic fracture toughness of cellulose-fiber-reinforced polypropylene*, PHD thesis: University of Wisconsin.

CLEVELAND, J., SPIEGELHALTER, T., SCHIERLE, G. and SCHILER, M.A.D.,J., The potential application of natural fiber reinforced bio-Polymer (NFRbP) composites in architecture [Homepage of http://www.creativepultrusions.com/NewsArchives/Cleveland-NFRbP_CPI-graphic.pdf], [Online] [09/01, 2010].

DAGLI, S., 1994. Kinetic studies and process analysis of the reactive compatibilization of nylon 6/polypropylene blends. *Polymer Engineering and Science,* **34**(23), 1720.

DI LORENZO, M.L. and SILVESTRE, C., 1999. Non-isothermal crystallization of polymers. *Progress in Polymer Science,* **24**(6), 917-950.

DWEIRI, R. and AZHARI, C.H., 2004. Thermal and flow property–morphology relationship of sugarcane bagasse fiber-filled polyamide 6 blends. *Journal of Applied Polymer Science,* **92**(6), 3744-3754.

GARDNER, D., WEST, C.H. and HAN, Y.S., 2009. Thermoplastic composites containing lignocellulosic materials and methods of making the same, Patent Docs. 20090036575.

GENIEVA, S.D., TURMANOVA, S.C., DIMITROVA, A.S. and VLAEV, L.T., 2008. Characterization of rice husks and the products of its thermal degradation in air or nitrogen atmosphere. *Journal of Thermal Analysis and Calorimetry,* **93**(2), 387-396.

GOLBABAIE, M., 2008. *Characterization of Ontario crop fibers for use in biocomposites (wheat and soy)*, M.Sc. thesis: University of Guelph.

HO, J. and WEI, K., 2000. Induced $\gamma \rightarrow \alpha$ crystal transformation in blends of polyamide 6 and liquid crystalline copolyester. *Macromolecules,* **33**(14), 5181-5186.

HRISTOV, V.N., VASILEVA, S.T., KRUMOVA, M., LACH, R. and MICHLER, G.H., 2004. Deformation mechanisms and mechanical properties of modified polypropylene/wood fiber composites. *Polymer Composites,* **25**(5), 521-526.

JACOBSON, R., CAULFIELD, D. and SEARS, K. AND UNDERWOOD, J., 2001. Low temperature processing of ultra-pure cellulose fibers into nylon 6 and other thermoplastics, 2001, The Sixth International Conference on Woodfiber-Plastic Composites: Madison, USA.

JACOBSON, M., FERRANTE, L., BRIENS, C. and BERRUTI, F., 2009. Hydrodynamic study of vertical lift tubes: Determination of flow regime by signal analysis. *Powder Technology,* **196**(1), 74-79.

JIANGSU KANGXIANG GROUP COMPANY, N-BUTYL-BENZENESULFONAMIDE [Homepage of http://www.kangxiang.com/images/3-pro-303-1.gif], [Online] [09/01, 2010].

JOSHI, S.V., DRZAL, L.T., MOHANTY, A.K. and ARORA, S., 2004. Are natural fiber composites environmentally superior to glass fiber reinforced composites? *Composites Part A,* **35**(3), 371-376.

KEATING, M., GARDNER, K., NG, H., MARKS, D., YUNG, W., AVAKIAN, P. and STARKWEATHER, H., 1999. Polymorphism in polyamide of DytekÂ®-A and dodecanedioic Acid. *Journal of Thermal Analysis and Calorimetry,* **56**(3), 1133-1140.

KOHAN, M.I., 1921, Nylon plastics. Edited by Melvin I. Kohan. New York: Wiley.

LEWIS, P.R., 2001. Failure of plastics and rubber products: causes, effects and case studies involving degradation. *Polymer Testing,* **20**(8), 945-945.

LI, Y., ZHANG, G., ZHU, X. and YAN, D., 2003. Isothermal and nonisothermal crystallization kinetics of partially melting nylon 10 12. *Journal of Applied Polymer Science,* **88**(5), 1311-1319.

LIN, S., CHEN, E., LIU, K. and WU, T., 2009. Isothermal crystallization behavior of polyamide 6,6/multiwalled carbon nanotube nanocomposites. *Polymer Engineering & Science,* **49**(12), 2447-2453.

LINCOLN, D.M., VAIA, R.A., WANG, Z., HSIAO, B.S. and KRISHNAMOORTI, R., 2001. Temperature dependence of polymer crystalline morphology in nylon 6/montmorillonite nanocomposites. *Polymer,* **42**(25), 9975-9985.

LIU, H., WU, Q. and ZHANG, Q., 2009. Preparation and properties of banana fiber-reinforced composites based on high density polyethylene (HDPE)/Nylon-6 blends. *Bioresource Technology,* **100**(23), 6088-6097.

LOOKCHEM, Irganox 1098 [Homepage of
http://www.lookchem.com/300w/201001/img/23128-74-7.jpg], [Online] [09/01, 2010].

LOZANO-GONZÁLEZ, M.J., RODRIGUEZ-HERNANDEZ, M.T., GONZALEZ-DE LOS SANTOS, E.A. and VILLALPANDO-OLMOS, J., 2000. Physical–mechanical properties and morphological study on nylon-6 recycling by injection molding. *Journal of Applied Polymer Science,* **76**(6), 851-858.

MCHENRY, E. and STACHURSKI, Z.H., 2003. Composite materials based on wood and nylon fibre. *Composites Part A: Applied Science and Manufacturing (Incorporating Composites and Composites Manufacturing),* **34**(2), 171-181.

MISHRA, S. and SAIN, M., 2009. Commercialization of wheat straw as reinforcing filler for commodity thermoplastics. *Journal of Natural Fibers,* **6**(1), 83.

MISRA M., K., M., TUMMALA P. and T., D., 2004. Injection molded biocomposites from natural fibers and modified polyamide. Brookfield, CT, ETATS-UNIS: Society of Plastics Engineers.

NIELSEN, L.E., 1994. Mechanical properties of polymers and composites. New York: M. Dekker.

PANTHAPULAKKAL, S., ZERESHKIAN, A. and SAIN, M., 2006. Preparation and characterization of wheat straw fibers for reinforcing application in injection molded thermoplastic composites. *Bioresource technology,* **97**(2), 265-272.

PANTHAPULAKKAL, S. and SAIN, M., 2006. Injection Molded Wheat Straw and Corn Stem Filled Polypropylene Composites. *Journal of Polymers and the Environment,* **14**(3), 265-272.

PATEL, R.M. and SPRUIELL, J.E., 1991. Crystallization kinetics during polymer processing - Analysis of available approaches for process modeling. *Polymer Engineering & Science,* **31**(10), 730-738.

PLASTIC TECHNOLOGY, Keeping-up with NPE nylon compounds with novel natural fiber from Brazil [Homepage of http://www.ptonline.com/articles/kuw/34715.html], [Online] [09/01, 2010].

RAMAZANI S.A, A. and MOUSAVI S, S.A., 2005. Investigation of vacuum annealing effects on physical–mechanical properties of thermoplastic parts. *Materials and Design,* **26**(1), 89-93.

RAUWENDAAL, C., 2001. Polymer extrusion. Cincinnati, Ohio: Hanser Gardner Publications.

RHD POLYMER AND CHEMICAL LLC, Plastics process aids INTEC technology from ITPS (International Technical Polymer Systems) [Homepage of http://www.rhdpolymerandchemical.com/custom.asp?id=182525&page=2&shopperid=], [Online] [09/01, 2010].

RUSSELL, D.P. and BEAUMONT, P.W.R., 1980. Structure and properties of injection-moulded nylon-6. *Journal of Materials Science,* **15**(1), 197-207.

RYBNIKA, F., 1960. Secondary crystallization of polymers. *Journal of Polymer Science,* **44**(144), 517-522.

SÁNCHEZ, C.G. and ALVAREZ, L.A.E., 1999. Micromechanics of lignin/polypropylene composites suitable for industrial applications. *Die Angewandte Makromolekulare Chemie,* **272**(1), 65-70.

SANTOS, P.A., SPINACE, M.A.S., FERMOSELLI, K.K.G. and DE PAOLI, M.A., 2007. Polyamide-6/vegetal fiber composite prepared by extrusion and injection molding. *Composites Part A,* **38**(12), 2404-2411.

SARDASHTI, A., 2009. *Wheat straw-clay-polypropylene hybrid composites*, M.A.Sc. thesis: University of Waterloo.

SCHULTZ, J.M., 2001. Polymer crystallization: the development of crystalline order in thermoplastic polymers. Washington, D.C.: American Chemical Society.

SEARS, K., JACOBSON, R., CAULFIELD, D. and UNDERWOOD, J., 2001. Reinforcement of engineering thermoplastics with high purity wood cellulose fibers, 2001, The Sixth International Conference on Woodfiber- Plastic Composites: Madison, USA.

SEMSARZADEH, M.A. and POURSORKHABI, V., 2009. Synthesis and kinetics of non-isothermal degradation of amide grafted high density polyethylene. *Polymer Degradation and Stability,* **94**(10), 1860-1866.

VALENZA, A., SPADARO, G., CALDERARO, E. and ACIERNO, D., 1993. Structure and properties of nylon 6 modified by γ-irradiated linear low density polyethylene. *Polymer Engineering and Science,* **33**(13), 845-850.

WEI, M., DAVIS, W., URBAN, B., SONG, Y., PORBENI, F.E., WANG, X., WHITE, J.L., BALIK, C.M., RUSA, C.C., FOX, J. and TONELLI, A.E., 2002. Manipulation of Nylon-6 crystal structures with its α-cyclodextrin inclusion complex. *Macromolecules,* **35**(21), 8039-8044.

WRIGHTHT, D., 2001. Failure of plastics and rubber products: cause, effects and case studies involving degradation. Smithers Rapra Press.

WU, S., WANG, F., MA, C.M., CHANG, W., KUO, C., KUAN, H. and CHEN, W., 2001. Mechanical, thermal and morphological properties of glass fiber and carbon fiber reinforced polyamide-6 and polyamide-6/clay nanocomposites. *Materials Letters,* **49**(6), 327-333.

WU, T. and LIAO, C., 2000. Polymorphism in nylon 6/clay nanocomposites. *Macromolecular Chemistry and Physics,* **201**(18), 2820-2825.

XIE, S., ZHANG, S., WANG, F., LIU, H. and YANG, M., 2005. Influence of annealing treatment on the heat distortion temperature of nylon-6/montmorillonite nanocomposites. *Polymer Engineering & Science,* **45**(9), 1247-1253.

XU, X., 2008. *Cellulose fiber reinforced nylon 6 or nylon 66 composites*, PHD thesis: Georgia Institute of Technology.

XU, Y., SUN, W., LI, W., HU, X., ZHOU, H., WENG, S., ZHANG, F., ZHANG, X., WU, J., XU, D. and XU, G., 2000. Investigation on the interaction between polyamide and lithium salts. *Journal of Applied Polymer Science,* **77**(12), 2685-2690.

ZHANG, F., ZHOU, L., XIONG, Y. and XU, W., 2008. Investigation on nonisothermal crystallization kinetics of the high-flow nylon 6 by differential scanning calorimetry. *Journal of Polymer Science Part B: Polymer Physics,* **46**(20), 2201-2211.

ZHANG, S., HUANG, X., ZHANG, M. and ZHAO, J., 2007. Effect of intermolecular interactions and cooling rates on crystallization behaviors of polyamide 6 Blends. *Journal of Thermoplastic Composite Materials,* **20**(1), 93-109.

ZHAO, Z., ZHENG, W., YU, W., TIAN, H. and LI, H., 2004. Unusual crystallization behavior in Nylon-6 and Nylon-6/montmorillonite nanocomposite films. *Macromolecular Rapid Communications,* **25**(14), 1340-1344.

ZHOU, Q., WANG, K. and LOO, L.S., 2009. Abrasion studies of nylon 6/montmorillonite nanocomposites using scanning electron microscopy, fourier transform infrared spectroscopy, and X-ray photoelectron spectroscopy. *Journal of Applied Polymer Science,* **113**(5),3286-3293

APPENDIX

1.1 THEORETICAL MODEL

Factors affecting the polymer composites properties are: size, shape, distribution, aspect ratio, orientation, volume fraction of the filler and ratio of filler to polymer modulus.

As composites were developed during the time, mathematical models were used to describe composites mechanical properties. In this section, some of the models which were introduced in the literature for modulus, strength and elongation of the composites, based on properties of matrix and particles, are explained

1.1.1 MODELS FOR MODULUS OF COMPOSITES

Models are developed under either constant stress or strain conditions. The upper bound is the longitudinal module of the composite where the strain is uniform on particles and matrix. The lower bound is the transverse module of the composite where the stress is uniform.

The simplest model is based on mixture law. This method is simplified the composite to two phase models (Particle and Matrix).

This model is known as series model when strain is uniform and it is also known as parallel model when stress is uniform (transverse modulus).

Series and Parallel models:

In the case of longitudinal stress where strain is the same in both phases and Poisson Ratio is equal to 0.5, the composite modulus can be written based on modulus and volume fraction of particle and matrix.
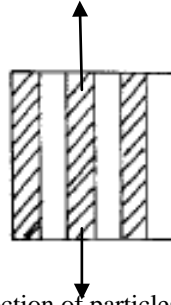
Figure 1 : Direction of the load is parallel to direction of particles and matrix orientation

$$E_c = E_p V_p + E_m V_m$$

Equation 1

Ec, Ep and Em are longitudinal modulus of composite, particle and matrix in the direction of the load which is the direction which they are oriented. Vp and Vm are particle and matrix volume fraction. In the case of transverse stress (Figure 2) where stress is the same in both phases, Poison Ratio and transverse modulus of composites can be defined by Equation 2 and Equation 3, respectively:

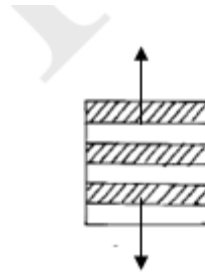$$v_c = \frac{v_p E_m V_P + v_m E_P V_m}{E_m V_P + E_P V_m}$$

Equation 2

Figure 2: Direction of the load is perpendicular to direction of particles and matrix orientation

$$E_c = \frac{E_P E_m}{E_m V_P + E_P V_m}$$

Equation 3

It is proven by experimental data that isostrain and isostress assumptions are not sufficiently describe modulus of the composite with randomly oriented particles.

For randomly oriented composites Equation 4 can be used to describe overall modulus of the composites:

$$E_{random} = (3/8)E_L + (5/8)E_T$$

<div align="right">Equation 4</div>

In Equation 4, E_L and E_T are modules in longitudinal and transverse directions for unidirectional short fiber composites. For perfect anisotropic composite with random orientation in all three directions Equation 4 changes to Equation 5:

$$E_{random} = 0.184E_L + 0.816E_T$$

<div align="right">Equation 5</div>

Takayanagi model

According to Takayanagi model (Equation 6) estimate the modulus between the upper and the lower boundaries. Introduction of the landa parameter is in good agreement with experimental data in the range of 0-30 % of fillers. λ was found to be 4.5 by adjusting the model using the curve fitting technique:

$$E_{c(T)} = (1-\lambda)E_m + \frac{\lambda}{\dfrac{1-V_P}{E_m} + \dfrac{V_P}{E_P}}$$

<div align="right">Equation 6</div>

Halpin and Tsai model

Halpin Tsai is a model for describing randomly oriented short fibers (Equation 7):

$$\frac{E_C}{E_P} = \frac{1 + 2(l/d)\eta_L V_f}{1 - \eta_L V_f} \qquad \frac{E_C}{E_P} = \frac{1 + 2\eta_T V_f}{1 - \eta_T V_f}$$

<div align="right">Equation 7</div>

$$\eta_L = \frac{(\dfrac{E_f}{E_m}) - 1}{(\dfrac{E_f}{E_m}) + (\dfrac{2l}{d})} \qquad \eta_T = \frac{(\dfrac{E_f}{E_m}) - 1}{(\dfrac{E_f}{E_m}) + 2}$$

<div align="right">Equation 8</div>

This model has been used by Gonzales et al. for modeling modulus of Polypropylene/lignocellulosic composites (Sánchez, Alvarez 1999). Liu et al. also evaluated predictability of this model for HDPE/ Nylon-6 banana fiber reinforced composites. They find good agreement between experimental and theoretical modulus values except in high percentages of fibers that deviation from theoretical model occurs due to fibber-fibber interactions (Liu, Wu et al. 2009). Halpin-Tsai model fitted the experimental values of composite modulus in different volume fraction of the filler pretty well and was used to calculate the lignin's tensile modulus.

1.1.2   MODELS FOR STRENGTH OF THE COMPOSITES

The theories on the strength of the composites are not as well developed as the modulus theories. The main theories are based on: failure of elements, effective available area, and interfacial adhesion between fiber and matrix. These models can be categorized based on the assumptions which were made, during developing them:

1) Theories which are based on failure of the composite after failure of particulate phase:

Sahu- Broutman Model

The assumption is that the composite will fail after the fracture of one element. In this theory addition of small amount of the filler will decrease the strength to a point where further addition of filler doesn't change the strength. The theory is not valid due to neglecting the particle-particle interactions and because composite does not necessarily fail after the failure of a particular phase.

2) Theories which based on matrix available area and dispersion level (Power law):

Power Law

The power law model is based on the assumption that the strength directly depends on the available area of the matrix (the area which is not filled with the particles). Depend on the interaction between filler and matrix; the model can have different constants.

Cases A:

Poor Interface and no stress concentration:

$$\sigma_{cu} = \sigma_{mu}(1 - aV_p^n)$$

<div align="right">Equation 9</div>

Where σ_{cu} and σ_{mu} are maximum tensile strengths of the composite and the matrix, respectively, V_p is the volume fraction of the filler and a and n are constants depending on the particle shape and its arrangement inside the modeled composite.

Case B:

Poor Interface and stress concentration (Nielson model):

$$\sigma_{cu} = \sigma_{mu}(1 - V_p^{2/3})K$$

<div align="right">Equation 10</div>

This model (Equation 10) can be simplified more by the assumption that the stress concentration factor is negligible and equal to 1 (K= 1). The model did not predict good estimates of the strength values for the case of lignocellulosic fillers in polypropylene matrix.

Pukansky model

Pukansky model (Equation 11) was used by Sanchez and Alvarez for fitting the maximum tensile strength of composites and determine lignocellulosic fibers strength (Sánchez, Alvarez 1999):

$$\sigma_{tc} = \sigma_{tP} \frac{1 - V_f}{1 + 2.5V_f} \exp(BV_f)$$

<div align="right">Equation 11</div>

B is interface property factor and it takes account for both the strength and size of the interface between filler and matrix. The value of variable B (interfacial property factor) was found by plugging the experimental values of the composite strength in Equation 11 versus volume fraction of fiber to get the best fit (Sánchez, Alvarez 1999).

1.1.3 MODELS FOR ELONGATION AT BREAK OF THE COMPOSITES

Nielson model was used to find the elongation at maximum strength point. Elongation at maximum tensile strength was tried to model by using Equation 12:

$$\frac{e_{tm}}{e_{tc}} = \frac{1}{1 - V_p^{1/3}}$$

Equation 12

In Equation 12, e_{tm} and e_{tc} are elongation at break of matrix and composite.

The assumptions for Equation 12 are:

1) Perfect interfacial bonding.

2) Matrix carries the load which is forced on the composite.

3) Changes in the nature due to addition of the fillers are negligible.

The last assumption is not true in the cases that transcrystallization is present.

The models introduced above cannot be used to model wheat straw composites properties in this project. That is because the modulus of the wheat straw filler is not known. Theoretical modulus can be found for wheat straw by fitting curve on composite modulus or strength data in different volume fractions of wheat straw and extract wheat straw modulus.